

Acta Biochimica et Biophysica Hungarica

VOLUME 26, NUMBERS 1-4, 1991/92

From 1993 becoming **Neurobiology**

EDITOR

J. TIGYI

ADVISORY BOARD

**S. DAMJANOVICH, E. HIDVÉGI, L. KESZTHELYI,
Georgina RONTÓ, F. SOLYMOSY, F. B. STRAUB,
Gertrude SZABOLCSI, P. VENETIANER**



Akadémiai Kiadó, Budapest

ABBPAP 26 (1-4) 1-164 (1991/92) HU ISSN 0237-6261

Acta Biochimica et Biophysica Hungarica

a Quarterly of the Hungarian Academy of Sciences

Editor

J. TIGYI

Managing editors

N. HALÁSZ and A. NIEDETZKY

Technical editor

E. KÓMÁR

Acta Biochimica et Biophysica Hungarica is published in yearly volumes of four issues by

AKADÉMIAI KIADÓ

Publishing House of the Hungarian Academy of Sciences

H-1117 Budapest, Prielle K. u. 19-35

Subscription information

Orders should be addressed to

AKADÉMIAI KIADÓ

H-1519 Budapest, P.O. Box 245

Acta Biochimica et Biophysica Hungarica is abstracted/indexed in Biological Abstracts, Chemical Abstracts, Chemie-Information, Current Contents-Life Sciences, Excerpta Medica database (EMBASE), Helminthological Abstracts, Index Medicus, International Abstracts of Biological Sciences, Nutrition Abstracts and Reviews

© Akadémiai Kiadó, Budapest

INSTRUCTION TO AUTHORS

Acta Biochimica et Biophysica Hungarica will primarily publish original and significant papers from Hungarian research institutes, universities and other laboratories. Original papers written in English in diverse fields of modern experimental biology will be considered for publication. Novel aspects of the information described in the paper should be clearly emphasized.

Manuscripts (one original and two copies) should be submitted to

Dr. Cs. Csontos, Department of Medical Chemistry, University Medical School, 4012 Debrecen, POB 7, Hungary (*Biochemistry*)

or

Dr. A. Nidetzky, Department of Biophysics, University Medical School, 7624 Pécs, POB 99, Hungary (*Biophysics*).

To ensure rapid and accurate publication, the author(s) are invited to follow the instructions described below. Manuscripts which do not conform these rules will be returned.

Preparation of manuscript

Full-length papers should not exceed 10 typewritten pages on A4 size high quality paper. The complete manuscript including the space occupied by figures, tables, references, acknowledgement etc. should not exceed 15 pages.

Short communications of total length of 5 pages will also be accepted.

PUBLISHER'S NOTE

The journal Acta Biochimica et Biophysica Hungarica has been published by Akadémiai Kiadó, the Publishing House of the Hungarian Academy of Sciences, for twenty-six years.

In 1993 it will be relaunched under the new title **"Neurobiology"**. The aim of this change has been to adjust the scope of the journal to the challenges of this dynamic field. The journal will be supplied to all subscribers of Acta Biochimica et Biophysica Hungarica.

PROTEIN KINASE C SUBTYPES IN HUMAN T LYMPHOCYTES

N.O. Christiansen and C.S. Larsen

Department of Medicine and Infectious Diseases, Marselisborg Hospital,
University of Aarhus, DK-8000 Aarhus C, Denmark

Summary: As contradictory results have previously been published on protein kinase C subtypes in human T lymphocytes, we made comparable studies on protein kinase C subtypes in human lymphocytes and in rat brain. In accordance with results published by Shearman et al. [16] we found that human T lymphocytes only contain type II = β and type III = α protein kinase C.

INTRODUCTION

In vivo activation of protein kinase C is proposed to involve a receptor-induced hydrolysis of polyphosphoinositides. The subsequent production of diacylglycerols causes an association of protein kinase C with the cell membrane and thereby activation of the enzyme [13].

Substantial evidence indicates that protein kinase C is implicated in the activation of T lymphocytes. Thus, phorbol esters and calcium ionophores have a synergistic effect on T lymphocyte proliferation [6, 17]. In addition, triggering of the T cell antigen receptor/CD3 complex by the antigen, monoclonal antibodies, or mitogenic lectins induce translocation of protein kinase C [11, 12]. Furthermore, interleukin-2 (IL-2) release and IL-2 receptor expression are associated with the activation of protein kinase C [4, 5, 8, 9].

Recently, rat brain has been reported to contain three isotypes of protein kinase C named type I = γ , Type II = β , and type III = α [14, 15]. Different protein kinase C subtypes have also been detected in human T lymphocytes. However, quite contradictory results have been published [1, 16]. We therefore compared the

chromatographic elution profiles of protein kinase C obtained from rat brain and human T lymphocytes.

MATERIALS AND METHODS

PD-10 gelfiltration columns were obtained from Pharmacia, Sweden. HPLC hydroxylapatite columns (0.5x7 cm) were from Pentax, Germany. Other materials were obtained as described [2, 3].

Buffer solutions

Buffer A is 20 mM Tris-HCl (pH 7.5), 10 mM EGTA, 4 mM EDTA, 1 mg/ml soybean trypsin inhibitor and 1 mM dithiothreitol. Buffer B is 20 mM Tris-HCl (pH 7.5), 0.5 mM EGTA, 0.5 mM EDTA, 20 μ g/ml soybean trypsin inhibitor and 1 mM dithiothreitol. Buffer C is 20 mM KH_2PO_4 (pH 7.5).

Human T lymphocytes were isolated as described [10]. Protein kinase C activity was assayed in the presence or absence of phosphatidylserine and diolein as described [2].

Semipurification of human T lymphocyte protein kinase C

$2\text{-}6 \times 10^8$ lymphocytes were resuspended in 5 ml of buffer A. The lymphocytes were ultrasonically disrupted and centrifugated at 20,000 g for 30 min. The supernatant was loaded on a DEAE cellulose column (5.5x1.5 cm) equilibrated in buffer B. The column was washed with 50 ml of the same buffer and eluted by buffer B containing 100 mM NaCl. The fractions containing protein kinase C was desalted on a PD-10 gelfiltration column.

Semipurification of rat brain protein kinase C

Cytosol (20,000 g supernatant) was prepared from four rat brains homogenized in 10 volumes of buffer A and loaded onto a DEAE cellulose column (3.5x7 cm) equilibrated in buffer B and washed with 100 ml of the same buffer. Protein kinase C was eluted by a linear gradient of NaCl (0-0.4 M). Fractions of 10 ml were collected, and the fractions containing protein kinase C activity were pooled and concentrated to about 10 ml using an Amicon ultrafiltration cell equipped with a PM-10 filter membrane. Prior to HPLC chromatography 1 ml of this concentrated enzyme was desalted on a PD-10 column.

HPLC hydroxylapatite chromatography of rat brain and human T lymphocyte protein kinase C

Cytosol protein kinase C from $1\text{-}3 \times 10^8$ human T lymphocytes or rat brain was loaded onto a HPLC hydroxylapatite column connected to a Waters HPLC-controlling system. The column was equilibrated using buffer C, and the enzyme was loaded at a flow rate of 1 ml/min. and washed for 20 minutes with the same buffer. Protein kinase C was eluted with a gradient of potassium phosphate as indicated in Fig. 1.

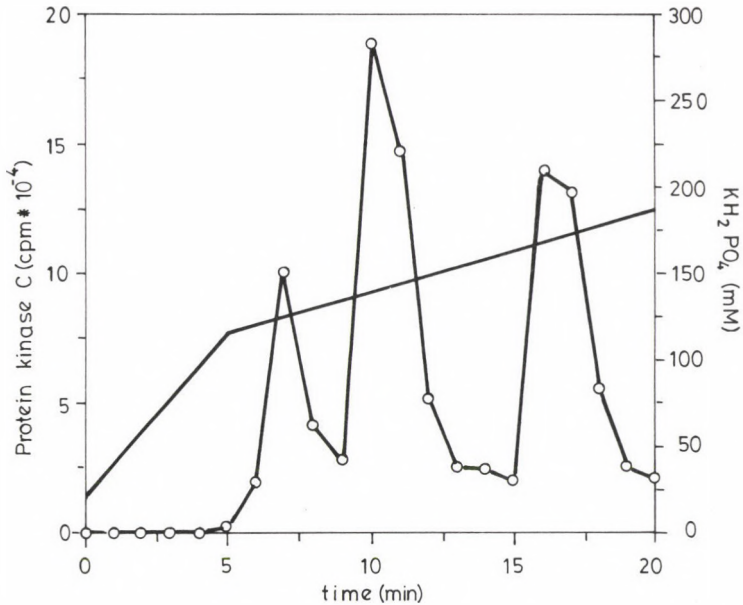


Fig. 1: Separation of rat brain protein kinase C and human T lymphocyte protein kinase C by hydroxylapatite chromatography. Rat brain protein kinase C and human T lymphocyte protein kinase C were semipurified as described and loaded onto a hydroxylapatite HPLC column equilibrated in buffer C. The column was washed for 20 min. at a flow rate of 1 ml/min. and the enzyme was eluted by a linear gradient of potassium phosphate as indicated in the figure. Fractions of 0.5 ml were collected and assayed for protein kinase C activity as described. Fig. 1a: Rat brain protein kinase C.

RESULTS AND DISCUSSION

Protein kinase C activity, obtained from rat brain, was chromatographically separated in three clearly distinct peaks using HPLC-hydroxylapatite chromatography (Fig. 1a). These results are in accordance with previous reports on subtypes of rat brain protein kinase C [7]. Lymphocyte protein kinase C was obtained from the cytosol of unstimulated human T lymphocytes, which have previously been shown to contain nearly no membrane associated protein kinase C [9]. When human T lymphocyte protein kinase C was separated by the same HPLC-technique only two peaks of protein kinase C were revealed (Fig. 1b). These two peaks were observed at exactly the same elution time as peak II and peak III from rat brain and no enzyme activity was

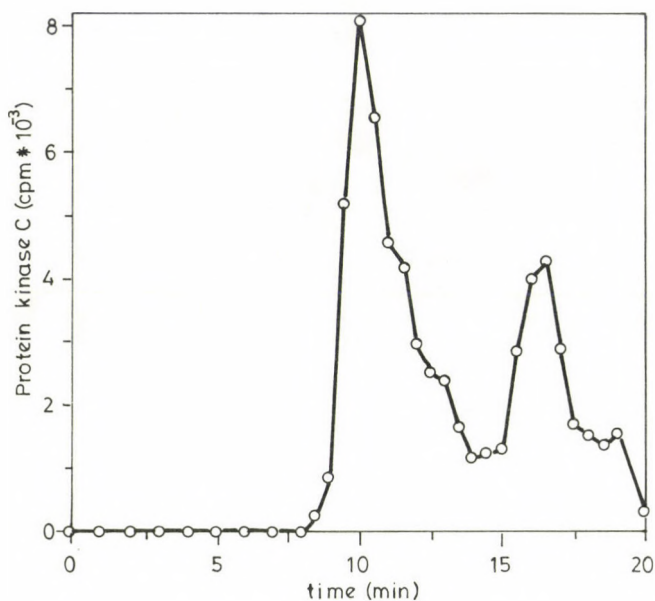


Fig. 1b: Human T lymphocyte cytosol protein kinase C.

obtained in fractions eluting equivalent to peak I from rat brain. In all experiments protein kinase C activity in peak II from human T lymphocytes represented the majority of the kinase activity.

Previously, the existence of two subtypes of protein kinase C in human T lymphocytes has been reported [1]. However, the subtypes were found to be equivalent to type I and type II protein kinase C from rat brain. These results contrast with Shearman et al. who found that T lymphocytes only contain type II and type III protein kinase C [16]. Both data employed hydroxylapatite chromatography and the latter confirmed their results with immunocytochemical analysis which identified both type II and type III protein kinase C [16]. In this context it is of interest that Shearman et al. were unable to raise antibodies against type I lymphocyte protein kinase C [1]. We have no explanation for these contradictory results but can only establish that in repeated experiments we did not find any type I protein kinase C activity, but were only able to demonstrate type II and type III protein kinase C in human T lymphocytes. Our results, therefore, confirm the results published by Shearman et al. [16].

ACKNOWLEDGEMENT

We would like to thank Viggo Esmann for revision of this article, Erik Hagen Nielsen, Else Madsen and Jonna Guldberg for excellent technical assistance, and Lone Manner-Jakobsen for expert secretarial assistance. This work was supported by Fonden af 17-12-1981, the Danish Medical Research Council, The Institute of Clinical Experimental Research, University of Aarhus, Aarhus Universitets Forskningsfond, P. Carl Petersens Fond, and Fhv. director Leo Nielsen og hustru Karen Margrethe Niensens Legat for Laegevidenskabelig Grundforskning.

REFERENCES

1. Beyers, A.D., Hanekom, C., Rheeder, A., Strachan, A.F., Wooten M.W. and Nel, A.E. (1988) *J. Immunol.* 141, 3463-3470.
2. Christiansen, N.O. and Juhl, H. (1986) *Biochem. Biophys. Acta* 885, 170-175.
3. Christiansen, N.O., Larsen, C.S., Juhl, H. and Esmann, V. (1986) *Biochem. Biophys. Acta* 884, 54-59.
4. Depper, J.M., Leonard, W.J., Krönke, M., Noguchi, P.D., Cunningham, R.E., Waldmann, T.A. and Greene, W.C. (1984) *J. Immunol.* 133, 3054-3061.
5. Farrar, W.L. and Ruscetti, F.W. (1986) *J. Immunol.* 136, 1266-1273.
6. Kaibuchi, K., Takai, Y. and Nishizuka, Y.J. (1985) *J. Biol. Chem.* 260, 1366-1369.
7. Kosaka, Y., Ogita, K., Ase, K., Nomura, H., Kikkawa, U. and Nishizuka, Y.J. (1988) *Biochem. Biophys. Res. Commun.* 151, 973-981.
8. Larsen, C.S. (1990) *Scand. J. Immunol.* (in press).
9. Larsen, C.S. and Christiansen, N.O. (1989) *Scand. J. Immunol.* 30, 285-294.
10. Larsen, C.S., Christiansen, N.O. and Esmann, V. (1988) *Scand. J. Immunol.* 28, 167-175.
11. Manger, B., Weiss, A., Imboden, J., Laing, T. and Stobo, J.D. (1987) *J. Immunol.* 139, 2755-2760.
12. Nel, A.E., Bouic, P., Lattanze, G.R., Stevenson, H.C., Miller, P., Dirienzo, W., Stefanini, F. and Galbraith, R.M. (1987) *J. Immunol.* 138, 3519-3524.
13. Nishizuka, Y. (1984) *Nature* 308, 693-698.
14. Ono, Y., Fujii, T., Ogita, K., Kikkawa, U., Igarashi, K. and Nishizuka, Y. (1987) *FEBS Lett.* 226, 125-128.
15. Parker, P.J., Coussens, L., Totty, N., Rhee, L., Young, S., Chen, E., Stabel, S., Waterfield, M.D. and Ullrich, A. (1986) *Science* 233, 853-866.

16. Shearman, M.S., Berry, N., Oda, T., Ase, K., Kikkawa, U. and Nishizuka, Y. (1988) FEBS Lett. 234, 387-391.
17. Truneh, A., Albert, F., Golstein, P. and Schmitt-Verhulst, A.-M. (1985) Nature 313, 318-320.

EM WAVES STANDARDS EFFECTIVENESS

S.B. Diaz

Cadic CC92 (9410) Ushuala, Argentina

Abstract: There are many studies about the effect of electromagnetic radiations on living organisms. Most of these have been carried out with mice, rats, guinea pigs, rabbits, dogs, monkeys, etc; only a limited amount of data is based on effects observed directly on human beings, which were mostly exposed to EM waves because of professional reasons (Epidemiology). In this paper some of these studies have been gathered according to the affected system. At higher frequencies power density is the parameter to be taken into account, at lower frequencies electric and magnetic field are, but in the graph they were expressed in terms of equivalent power density as $E \times H$ when both field strength were given, or as E^2/Z or $H^2 Z$ (where Z is the free space impedance), when only one of them was given. Standards from different countries to human exposure are presented, and finally an analysis of the effects compared with standards from the U.S.A. and U.S.S.R. is presented.

INTRODUCTION

It is well known that EM waves interact with biological tissues. When the field is strong enough the effects are thought to be produced by a temperature rise. Weak fields produce some effects, which are not thermal, generally in a unique frequency range, giving rise to what is called the "window effect".

The effects of the former are irreversible, that is they persist after the EM field ceases. And the latter are reversible, that is the affected system returns to its original state when the field is not present. Both them were extensively studied and are shown as the following items.

NEUROVEGETATIVE SYSTEM (Figure 1)

1. Electric Field Strength: 1800 V/m.
Effect: Changes in the synapses of cells of the brain cortex and in the hypothalamic region structure.
Specimen: Rats.
Reference: 38.
2. Female rats exposed between days 1 and 20 of gestation (Whole gestation 21 days).
Effect: Functional nervous disturbances in offspring.
Specimen: Rats.
Total exposure period: 20 days.
Reference: 1.
3. Electric Field Strength: 300 V/m.
Effect: Increase between 35 and 65% in unconditioned salivation reflex. Only head exposed.
Specimen: Dogs.
Exposure period: 20 min.
Reference: 38.
4. Pulsed Fields. No thermal effect.
Effect: Nervous functional changes.
Specimen: Rodents.
Exposure period: 8 month.
Reference: 38.
5. Experience with human beings in vegetative state.
Magnetic Field Strength: 2.4×10^{-2} A/m.
Effect: Between 1 and 6 Hz calming effect. Between 7 and 20 Hz excitation stimulatory effect even producing taquicardy. At 10 Hz analgesic effect. The effects were detected measuring the skin resistance between left and right hand. The response depends on the person and the state. Strong signals, much more intense than those mentioned previously, cancel the effect.
Specimen: Humans.
Reference: 26.
6. Effect: Smaller number of cells of the brain cortex respond to pain and noise excitation.
Specimen: Rats.
Reference: 1.
7. Effect: Increase in the aberrations of chromosomes of the spinal medulla. The incidence of aberrations in the group exposed to 0.05 mW/cm^2 was higher 2 weeks after the exposition than immediately after it. In the group exposed to 0.5 mW/cm^2 the percentage of aberrations diminished after the second week because damaged cells were eliminated.
Specimen: Pure albino rats.
Reference: 28.

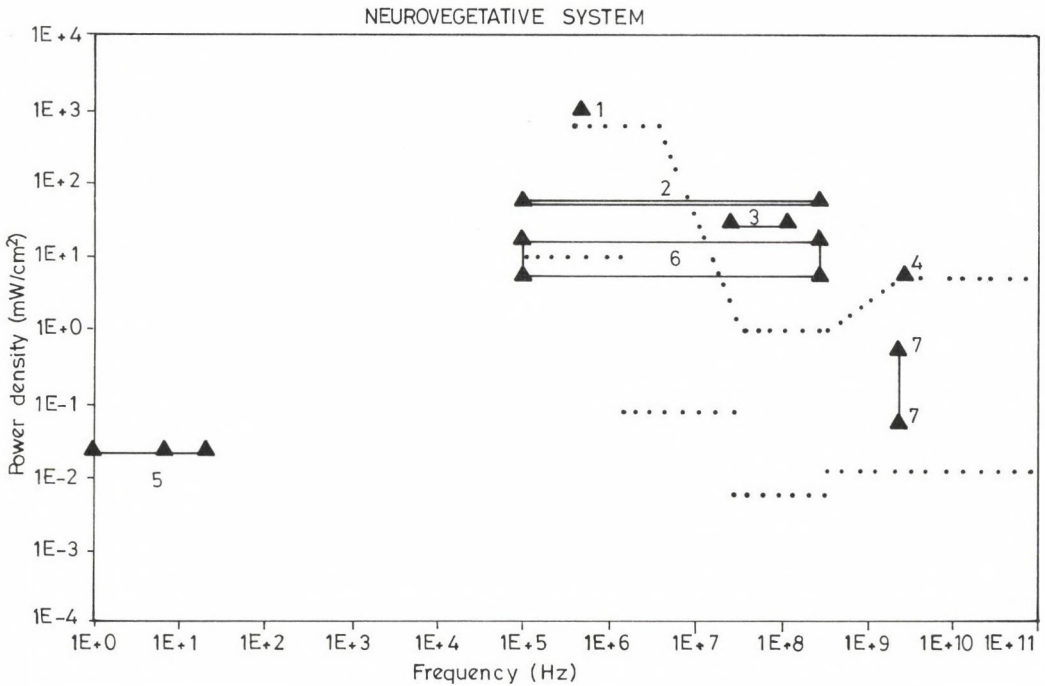


Fig. 1

The hearing of sounds corresponding to the modulation frequency of low power density RADAR was observed in persons exposed, due to professional considerations. It is thought that the effect is produced owing to the bone tissue of the skull acting like a transducer converting electromagnetic waves into mechanical waves [4].

Changes in the electroencephalogram (EEG) and headaches have been observed in humans exposed to RF of low level [1], the intensity of the fields excluded the possibility that the effects could be thermal.

EFFECTS ON EYES

Many experiments have been carried out in RF and microwaves. It is supposed that the range from 1 to 3 GHz may be the most dangerous because eyes have a frequency of resonance in this band.

The most studied effect is the cataract, which are produced by an irreversible process similar to egg white cooking, which heat acts on the protein of the eye diminishing vision.

A special kind of cataract was observed in the posterior capsule of the lenses, produced by RF exposition, distinguishable from other cataract types [29].

Referring to microwave, the experiences observed with animals proved that they could only be produced with levels higher than 100 mW/cm² [29]. Authors have observed cataracts in rabbits with only one exposition in the following cases:

- a) 180 mW/cm² in 60 minutes [18]
- b) 250 mW/cm² from 35 to 40 minutes [29]
- c) 590 mW/cm² in 5 minutes [18]
- d) 600 mW/cm² in 3 minutes [18]

Otherwise it is believed that a daily exposure of 1 hour over 20 days would produce cataracts with a level of 180 mW/cm² and with less than 100 mW/cm² the cataracts could be produced only by an accumulative effect.

With regard to another effect on human eyes, turbidness in the crystalline of personnel exposed to microwave levels of 100 mW/cm² and opacity in the lenses, also in exposed personnel, but with lower levels, were observed. The latter suggest an accumulative effect. Experiments have demonstrated a relationship between the site of damage and the wavelength of the radiation [7].

CARDIOVASCULAR SYSTEM (Figure 2)

1. Electric Field Strength: 80×10^3 V/m.
Effect: No differences in the cardiac rhythm.
Specimen: Birds.
Exposure period: 3 weeks.
Reference: 17.
2. Electric Field Strength: 2.5×10^4 and 5×10^4 V/m.
Effect: Variations in the sanguineous recount. A tendency of white cells to increase and red cells to diminish in number with the exposition level was observed.
Specimen: Mice.
Exposure period: 42 days.
Reference: 17.
3. Electric Field Strength: 96 V/m.
Effect: Increment in eritrocites quantity.
Reference: 12.

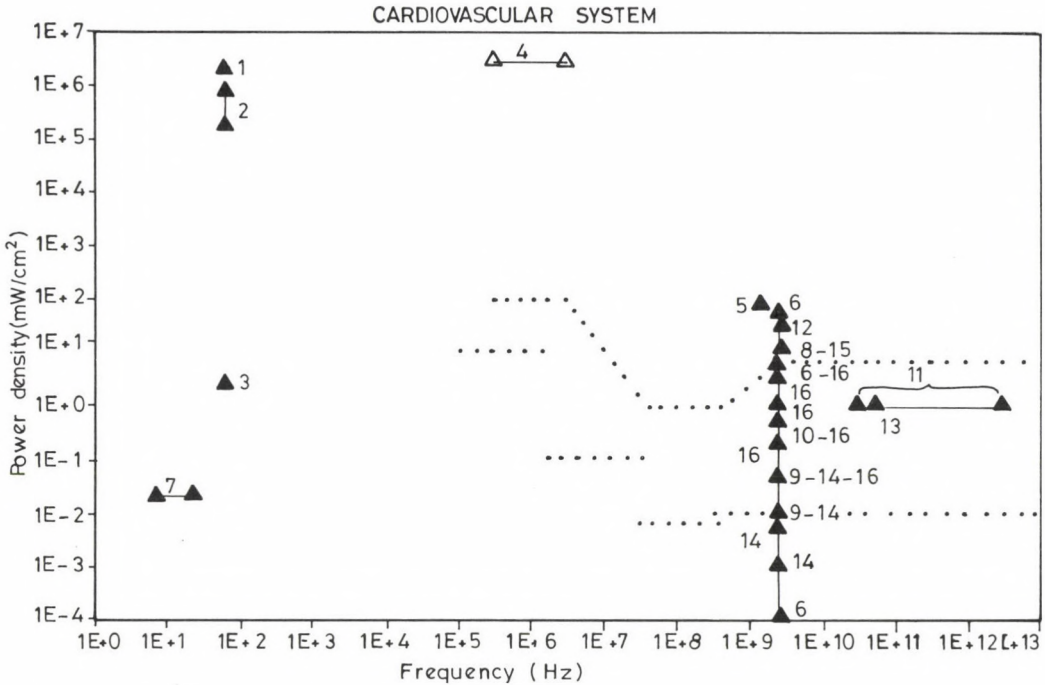


Fig. 2

4. Electric Field Strength: 100 kV/m.
Effect: Diminution in the cardiac rhythm and the blood pressure. Personnel exposed by professional reasons.
Specimen: Humans.
Exposure period: Chronic.
Reference: 38.
5. Effect: Increment in the cardiac rhythm.
Specimen: Isolated frog hearts.
Reference: 6.
6. Effect: Changes in the velocity of transformation and reduction in the frequency of mitosis in lymphocytes.
A morphological and cytogenetic study subsequent to the irradiation revealed a transitory and reversible change in the transformation rate, which depends on the dose.
Reference: 19.
7. Magnetic Field Strength: 2.4×10^2 A/m.
Effect: Taquicardy. (See also neurovegetative system, effect 5.)
Specimen: Humans.
Reference: 26.

8. Pulsed fields. Pulse width 3×10^{-6} seconds. Pulse repetition frequency 350 Hz.
Effect: Diminution of the activity of the enzyme Colinesterase Butitrilic of the blood serum. Until day 29 no effect was observed, on day 42 diminution of the general activity began.
Specimen: Rats.
Exposure period: 1 hour/day during 42 days.
Reference: 28.
9. Effect: Increment of the neutrophils metabolic processes. The effect was detected through the leucocytes cytochemical indexes. The analysis were performed at days 3, 7, 10, 14, 21 and 30 during exposition. The metabolic processes augmented during the first three weeks and then they fell to the control group level.
Specimen: Rats.
Exposure period: 7 hours/day during 30 days.
Reference: 28.
10. Effect: Diminution in the glycogen content owing to the activation of the glycolysis of neutrophils. The effect was detected through leucocytes cytochemical studies extracting blood from the caudal vein at days 3, 7, 10, 14, 21 and 30. The effect was produced towards the end of the fourth week.
Specimen: Rats.
Exposure period: 7 hours /day during 30 days.
References: 28.
11. Study carried out during 3 years with engineers and techniques between 20 and 50 years old exposed to EM radiation by occupational reasons (generators repairing).
Effect: Changes in blood recount. Diminution of: Hemoglobin, erythrocytes, leucocytes, reticulocytes and trombocytes. Increment in lymphocytes. Hypercoagulation tendency.
Specimen: Humans.
References: 28.
12. Pulsed fields. Pulse width 2.6×10^{-6} seconds. Pulse repetition frequency: 395 Hz.
Effect: Diminution in blood recount, minimal values were obtained at the second half of the irradiation period, they reached the normal levels 10 weeks after the irradiation finished. An increment in the alkaline phosphatase activity was observed during the first week of irradiation and transiently after exposition.
Specimen: Rats.
Exposure period: 4 hours/day, 5 days/week, during 7 weeks.
Reference: 28.
13. Effect: Diminution in peripheral blood leucocytes.
Specimen: Mice.
Exposure period: 15 minutes/day, during 20 days.
Reference: 28.

14. Effect: Increment in the neutrophils phagocytosis in blood serum. Analysis was performed before the exposition, at the second and fourth weeks after the start, and second, fourth and eighth weeks after exposure. The greatest effect was observed at 0.01 mW/cm², then this diminished with the field.
Specimen: Guinea pigs.
Reference: 28.
15. Effect: Peripheral vasodilation.
Specimen: Monkeys.
Exposure period: 5 min.
Reference: 2.
16. No changes in the hematocritic recount of hemoglobin and white cells were observed, and in basic studies of blood coagulation, also.
Specimen: Rabbits.
Exposure period: 23 hour/day, 7 days/week, during 6 months.
References: 18.

It was observed that the pulsed fields from 1 to 100 MHz produce a chain effect in leucocytes and erythrocytes, observing a frequency range at which the effect is obtained with minimal power density [38].

An alteration of the electrophoretic model of gammaglobuline with pulsed fields from 10 to 200 MHz was obtained [38].

In rabbits exposed to frequencies from 9.5 to 0.01 kHz an augment proportional to frequency, in blood sugar percentage was obtained, 0.01 kHz to 9.8 MHz a diminution was observed. Otherwise, to the range at which the effect is produced and independent of frequency, the variation was higher when the head was exposed than when the liver was [38].

An experiment was carried out at 960 MHz with a sea turtle isolated heart. The obtained effect was a diminution in heart rate. Then, when power density was increased, diversified effects were observed. The explanation of this disparity of these results resides in that: in the isolated heart part of the parasympathetic and the sympathetic nerves remain; if both are excited, the heart rate is diminished, because the effect on the first nerve is stronger; but when the power density is increased the first is blocked and the dominant effect is the second one [24].

GASTROINTESTINAL SYSTEM (Figure 3)

1. Electric Field Strength: 300 V/m.
Effect: Variation between 87 and 100% in the protein content of saliva. Only head exposed.
Specimen: Dogs.
Exposure period: 20 min.
Reference: 38.
2. Electric Field Strength: 1500 V/m.
Effect: Diminution in the glucose content in isolated liver cells.
Reference: 38.

In personnel exposed to radiation from 30 to 300 GHz an increment in sowing of microbes of self-flora in the buccal cavity was observed [28].

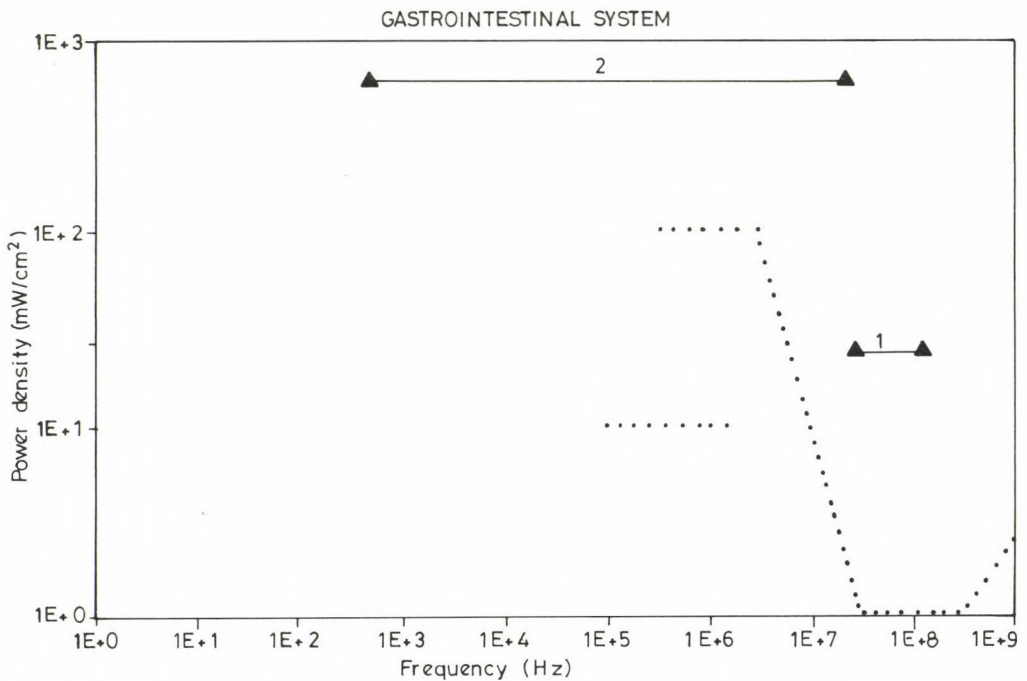


Fig. 3

**FERTILITY, GESTATION, OFFSPRING:
DEVELOPMENT AND THERATOLOGICAL EFFECTS (Figure 4)**

1. Electric Field Strength: 0-700, 700, 7×10^3 and 6.7×10^4 V/m.
Effects: Differences in whole gestation time, but not consistent for each species.
Irradiation after laying.
Specimen: Birds.
Exposure period: Three weeks.
Reference: 12.
2. Electric Field Strength: 8×10^4 V/m.
Effect: Augment in the early growth. Important but not permanent and higher in males than in females.
Specimen: Birds.
Exposure period: Three weeks.
Reference: 12.
3. Effect: Females exposed during gestation. Offspring weaker than the unexposed and with nervous disturbance.
Specimen: Rats.
Reference: 1.

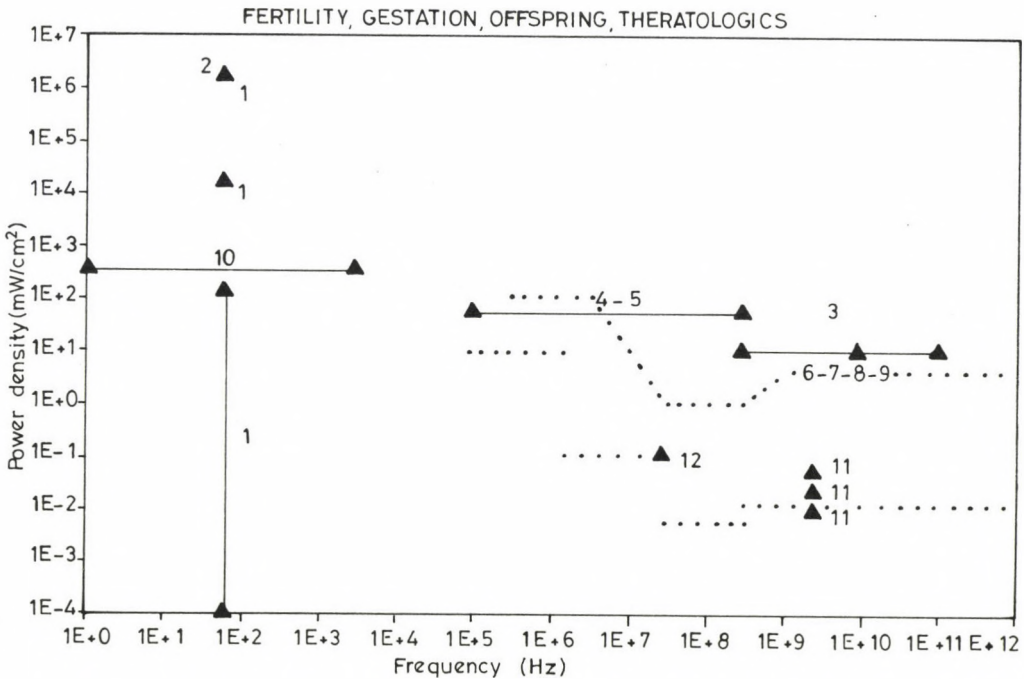


Fig. 4

4. Effect: Females exposed from day 1 to day 20 of pregnancy (Total pregnancy period: 21 days). The offspring presented malformations and disturbances in nervous functions.
Specimen: Rats.
Exposure period: 20 days.
Reference: 1.
5. Effect: Males exposed and then mated with unexposed females. The resulting offspring was weaker than the unexposed and with growth disturbances in it.
Specimen: Rats.
Reference: 1.
6. Pulsed fields. Modulation frequency from 1 to 4 kHz. Peak power: 20 KW.
Effect: Larvae exposed. Abnormalities in development.
Specimen: Coleoptera (*Tenebrio Molitor*).
Reference: 9.
7. Effect: Larvae exposed. Abnormalities of first grade: 23%. Abnormalities of second grade: 20%. Abnormalities in the control group: 10%.
Specimen: Coleoptera (*Tenebrio Molitor*).
Reference: 10.
8. Continuous and pulsed fields.
Effect: Larvae exposed. Abnormalities. It was observed that the damage was a function of the total received energy dose, and not of the power level.
Specimen: Coleoptera (*Tenebrio Molitor*).
Reference: 22.
9. Effect: Larvae exposed. Abnormalities. It was observed that the effect did not vary with the orientation of the specimen.
Specimen: Coleoptera (*Tenebrio Molitor*).
Reference: 23.
10. Electric Field Strength: 20 V/m.
Magnetic Field Strength: 160 A/m.
Effect: Increment in growing rate.
Specimen: Monkeys.
Exposure period: 22 hours each day over 3 years.
Reference: 28.
11. Effect: Female mice. Decrease in the reproductive activity. Increment in offspring death, born from 1.1% at 0.01 mW/cm² to 7% at 0.05 mW/cm². Offspring of smaller size at the moment of birth. Changes in the post-embryonic development. Theratological effects were not observed. The magnitude of the changes was a function of the exposition level.
Specimen: Mice.
Reference: 28.

12. Electric Field Strength: 20 V/m.
Magnetic Field Strength: 5×10^{-2} A/m.
Effect: Pregnant female rats. Total resorption of fetus in 50% of cases was observed when exposure was carried out between days 0-20 and 0-6 of gestation; and in 20% of cases when the exposure was from day 6 to 15. Another effect in the offspring was the incomplete ossification of skull bones.
Specimen: Rats.
Reference: 39.

ENDOCRINE SYSTEM (Figure 5)

1. Pulsed fields. Pulse width 2.6×10^{-6} seconds. Pulse repetition frequency 395 Hz.
Effect: Important increment in the activity of the alkaline phosphatase in leukocytes during the first week of irradiation. Blood samples were taken in the first, third, fifth and seventh week of irradiation. During the second half of the period of irradiation smaller values were obtained, getting normal values at the tenth week after exposure was finished.
Specimen: Male rats (20 specimens).
Exposure period: 4 hours/day, 5 days/week, over 7 weeks.
Reference: 28.
2. Effect: Increment in adrenocorticotropine secretion. Diminution in thyroid glands and growth hormone secretion (the hypophysial hormonal changes are the model of stress reaction in animals).
Specimen: Rats.
Exposure period: 1 hour.
Reference: 25.
3. Effect: Increment in the interorganic metabolism and diminution in excretion of copper, manganese, nickel and molybdenum. Three exposed groups and one control were used. For the final 5 days of exposure the animals were kept in special metabolic cages, which allows the recollection of urine and excrements. The values of the parameters were obtained by quantitative spectroscopy. Finally the animals were sacrificed.
Specimen: Male white rats.
Exposure period: 8 hours/day, over 3 months.
Reference: 28.
4. Effect: Deficiencies in pyridoxine and riboflavin enzymes.
Specimen: Male white rats.
Exposure period: 3 hours/day, over 15 days.
Reference: 28.

Besides changes in the activity of the enzyme, alpha-amylase were obtained with radiation of 11.8 MHz at a temperature of 27.7 and 28.2°C [38].

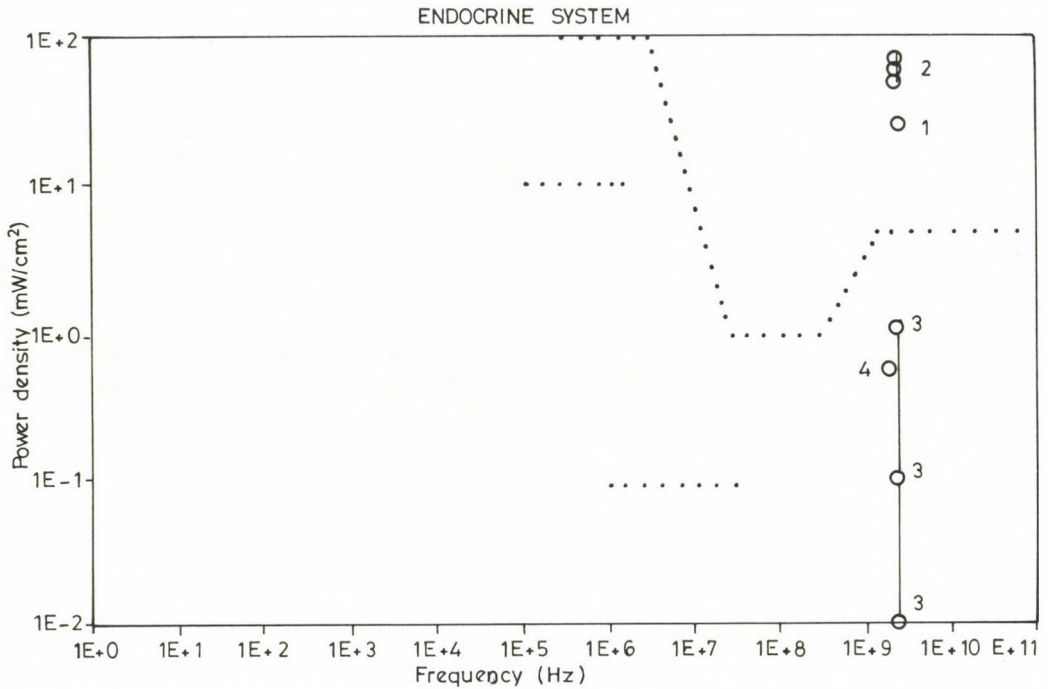


Fig. 5

MICROSCOPIC LEVEL (Figure 6)

1. Electric Field Strength: 96 V/m.
Effect: Increment in glucose percentage.
Reference: 12.
2. Electric Field Strength: 1800 V/m.
Effect: Changes in the synapses of brain cortical cells.
Specimen: Rats.
Reference: 38.
3. Electric Field Strength: 300 V/m.
Effect: Alteration in the protein content of saliva between 87 and 100%. Only head exposed.
Specimen: Dogs.
Exposure period: 20 min.
Reference: 38.
4. Pulsed fields.
Electric Field Strength: 250 to 6000 V/m
Effect: Abberations in garlic root cells.
Specimen: Vegetables.
Reference: 38.

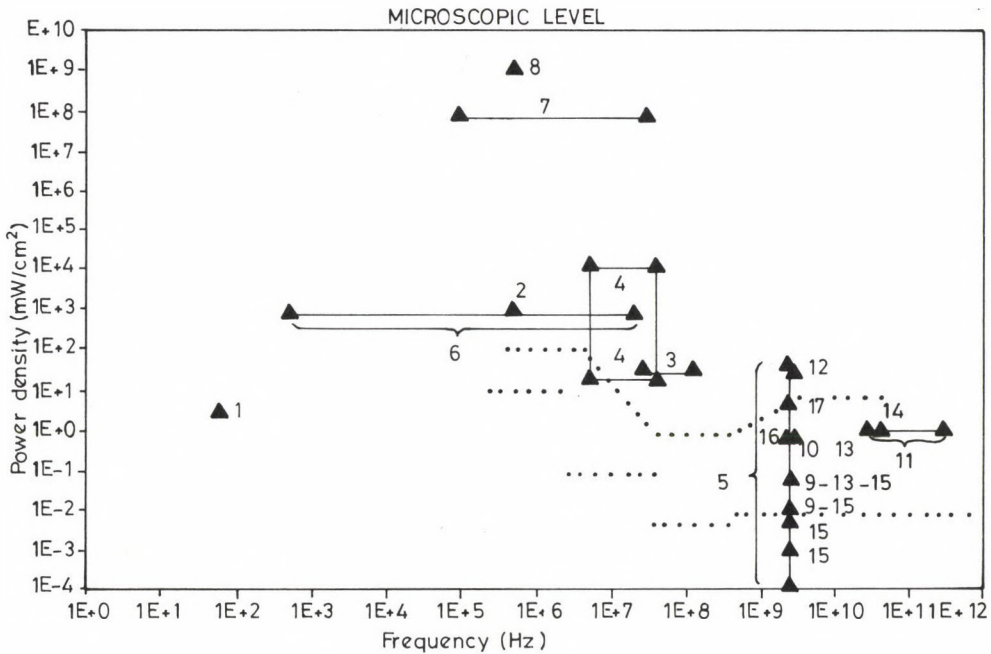


Fig. 6

5. Effect: A morphological and cytogenetic study after irradiation revealed a reversible change, which was a function of dose in cell transformation rate, having a maximum at 30 mW/cm². Also a reduction in the mitosis frequency of lymphocytes was observed.
Reference: 19.
6. Electric Field Strength: 1500 V/m.
Effect: Reduction in glucose content in isolated liver cells.
Reference: 38.
7. Electric Field Strength: 5×10^5 V/m.
Effect: Changes in the peripheral shape of cells and cellular societies, and alignment of the axis of bacteria and plant cells of no filiform algae with the field were observed. Owing to the fact that the threshold for each frequency is the same in all the species, it is thought that the mechanism of reaction is the same in all of them.
Reference: 34.
8. Magnetic Field Strength: 5×10^3 A/m.
Effect: No effect was observed on cells or bacteria.
Reference: 34.

9. Effect: An increment in the metabolic process of neutrophils was observed through studies on cytochemical indices of leukocytes. Blood analyses were carried out on days 3, 7, 10, 14, 21 and 30. The increments in the metabolic processes were observed during the first three weeks, then the levels fell to the control group ones.
Specimen: Albino white rats (10 specimens).
Exposure period: 7 hours/day, over 30 days.
Reference: 28.
10. Effect: An activation in the neutrophils glycolysis which produced a diminution in the glycogen content was observed toward the fourth week.
Specimen: Albino white rats (10 specimens).
Exposure period: 7 hours/day, over 30 days.
Reference: 28.
11. Effect: Diminution in the osmotic and acid resistance in erythrocytes. Study carried out over 3 years with engineers and technicians from 20 to 50 year old, exposed by professional reasons (generator repairing).
Specimen: Humans.
Reference: 28.
12. Pulsed fields, pulse width: 2.6×10^{-6} seconds, pulse repetition frequency: 395 Hz.
Effect: An important activity of the alkaline phosphatase in the neutrophils of leucocytes was observed during the first week. (See also Endocrine System 1.)
Specimen: Male rats (20 specimens).
Exposure period: 4 hours/day, 5 days/week, over 7 weeks.
Reference: 28.
13. Effect: Increment in aberrations in chromosomes of cells of spinal medulla. The highest incidence of the aberrations, at the level of 0.05 mW/cm^2 , was observed two weeks after irradiation finished, while at the group exposed to 0.5 mW/cm^2 the aberration quantity diminished at the end of the second week by elimination of the damaged cells.
Specimen: Pure white rats.
Exposure period: 7 hours/day, over 10 days.
Reference: 28.
14. Effect: Inhibition of adenovirus, which then were used to infect a culture of human kidney cells.
Exposure period: 2 hours.
Reference: 28.
15. Effect: Increment of neutrophils phagocytosis in serum (phagocytic reaction of neutrophils is the nonspecific immunological reaction indicator). The effect was more important with the smallest field (0.001 mW/cm^2). Analyses were performed before (second and fourth weeks), during and after exposure (second, fourth and eighth weeks).
Specimen: Guinea pigs.
Reference: 28.

16. Effect: Deficiencies in pyridoxine and riboflavin.
Specimen: Male white rats.
Exposure period: 3 hours/day, over 15 days.
Reference: 28.

A chain effect was observed on particles in suspension irradiated with modulated fields from 1 to 100 MHz. This effect consists of the alignment of the particles with the field forming chains. There is a frequency range for each kind of particle to which the effect is obtained with a minimal strength [38].

A study was carried out comparing a group of *Pisum sativum* L. in normal environmental conditions with others inside a Farad camera, which was free of radiation in the range 100 kHz to 300 MHz. It was observed that an increment in DNA in stems and roots of 31 and 37%, respectively, and also an increase in RNA was obtained in the camera group. The same experiment was performed with *Cucumis Sativus* L. observing an increment of 41% in DNA in stems and of 9% in roots (32).

Pulsed magnetic fields of 2.4×10^5 A/m strength were applied to leech cells nervous Retzius cells obtaining: a depolarisation of the cell, a transient increment in clamp frequency and a diminution after the pulse in the input resistance of the cell with direct polarisation was observed [37].

Lymphoblastic transformations were observed when microwaves were applied to lymphocytes (see also cardiovascular system) [30].

BEHAVIOR (Figure 7a)

1. Electric Field Strength: 1.77×10^3 V/m.
Effect: Detection of fields. Rats were located decision point of a device with "Y" shape which both branches were constructed equal and had food at the ends. When no EM field was present the animals went about 50% of times to each branch. When one of the branches was exposed to an EM field the animal avoided that one.
Specimen: Rats.
Reference: 38.
2. Pulsed fields.
Effect: Irritability. Owing to the level it is thought that it is not a thermal effect.
Specimen: Rodents.
Exposure period: 8 months.
Reference: 38.

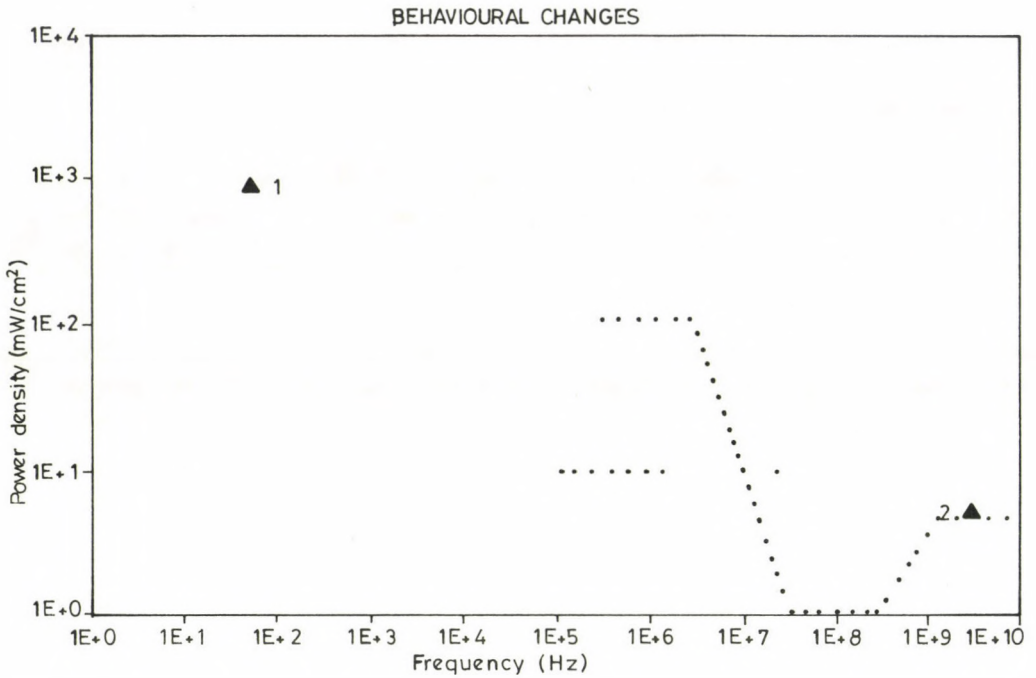


Fig. 7a

STATIC ELECTRIC FIELDS (Figure 7b)

Effect: Fields detection. A device with gradual strength variation was used. Larvae went towards the place where the field was lower.
 Specimen: Coleoptera.
 Reference: 10.

STATIC MAGNETIC FIELDS (Figure 7c)

Effect: Fields detection. The device was similar to the described above. The same result was obtained.
 Specimen: Coleoptera.
 Reference: 10.

There are several symptoms like headaches, sleepiness, memory loss, difficulties in concentration, etc, that are attributed to exposition to EM fields. Also a diminution in the activity of rodents exposed to fields from 300 to 920 MHz preceded by a high activity and emotional instability was observed [1].

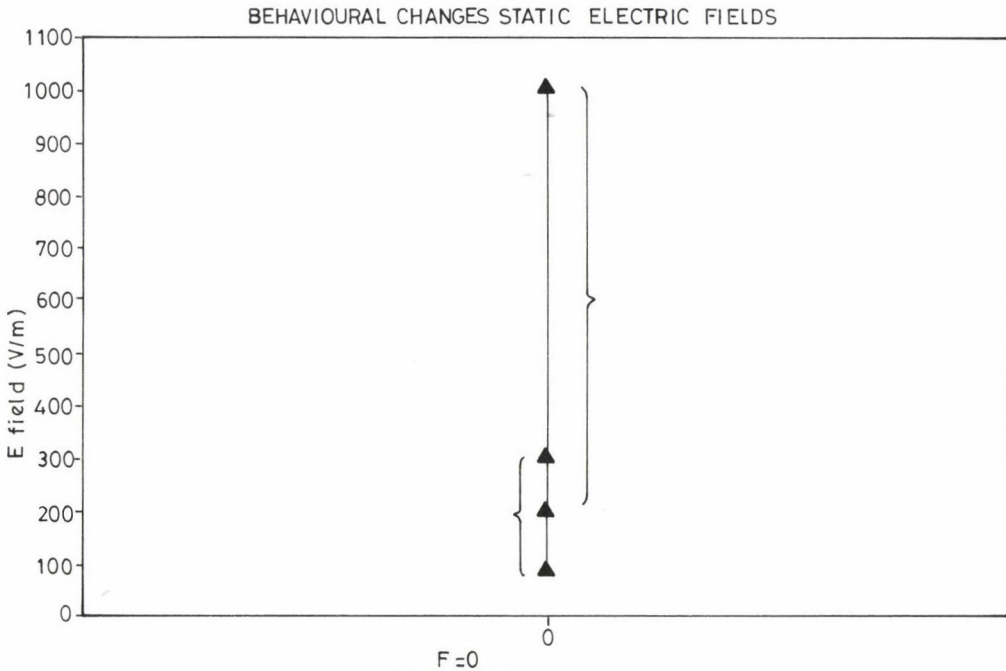


Fig. 7b

OTHER EFFECTS

Frequency: 1-6 Hz and 7-20 Hz.
 Magnetic Field Strength: 2.4×10^{-2} A/m.
 Equivalent Power Density: 0.022 mW/cm².
 Effect: Variation of the skin resistance.
 Reference: 26.

Frequency: 27.12 MHz.
 Electric Field Strength: 20 V/m.
 Magnetic Field Strength: 5×10^{-2} A/m.
 Effect: Pregnant female rats. Uncompleted ossification of the skull bones in the offspring.
 Specimen: Rats.
 Reference: 39.

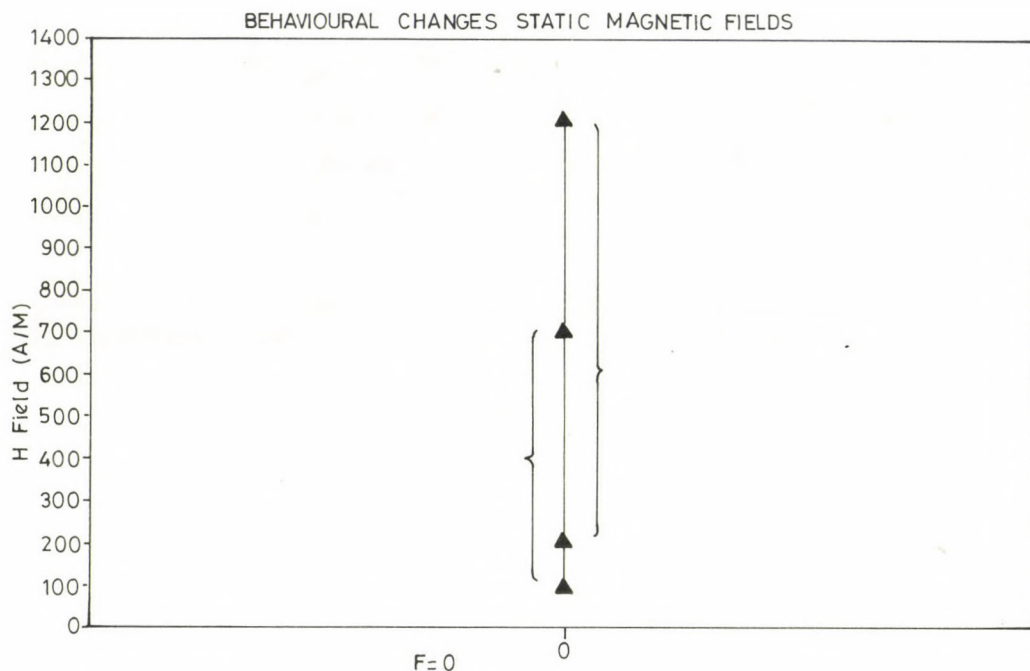


Fig. 7c

STANDARDS

From the previous items it may be inferred that the levels of electromagnetic radiation must be limited in places where human beings are found.

But safety levels are not uniform for all frequencies, owing to different parts of the body and the whole having their own resonance frequency in the VHF band. Some of them are: 31 to 47 MHz for the whole body with Earth effect, 62 to 77 MHz for the whole body in free space, 300 to 400 MHz for the head, 1 to 3 GHz for the eyes and 1.7 to 2.5 GHz for the brain [11] [13] [14] [15] [16] [20] [33]. So in such bands more conservative levels should be considered.

In principle the accidental standards have been defined taking into account the thermal effects of electromagnetic radiation, in such conditions the standards were stabilised in a similar way to those referred to in high temperature working places, where other subjects, besides temperature itself must be taken into account, for example: air temperature, relative humidity, air velocity, duration of the exposure and clothes, which all influence tolerance.

Moreover, when safety levels are being determined the following possibilities must be considered: wavelength of the radiation, exposure time, relationship between the time of exposure and not exposure, possibility of reflection, focusing and dispersion of the radiation, quantity of heat absorbed or generated by the body previously, zone of the body irritated, weight of the person and its distribution, position of the body

related to the radiation, "window effect" in frequency or strength, possibility of "hot spots" owing to focusing or metallic implants, possible increment in the sensibility in persons with health problems, owing to the physical state itself or to medicines that are being taken [5] [30] [31].

Figure 8 shows safety standards for several countries to exposures for periods of more than 8 hours (continuous exposure) [2] [8] [21] [29] [38].

Regarding the U.S.A., the levels correspond to ANSI 82, which are more strict than the previous standards of that country. In Table 1 a more detailed list is given [2] [8] [21] [29] [38].

It is observed that there is not a consensus between different countries about safety levels. For example, Soviet standards are more conservative than North American, and it is originated in criteria to establish the levels. As it was pointed out before, U.S.A. standards are determined considering only irreversible effects, meaning effects that remain after exposure. Instead the U.S.S.R. standards consider also factors that disappear after exposure, like headaches, hearing of RADAR modulation frequencies, detection of fields, etc. The other countries have an intermediate position between the U.S.A. and U.S.S.R.

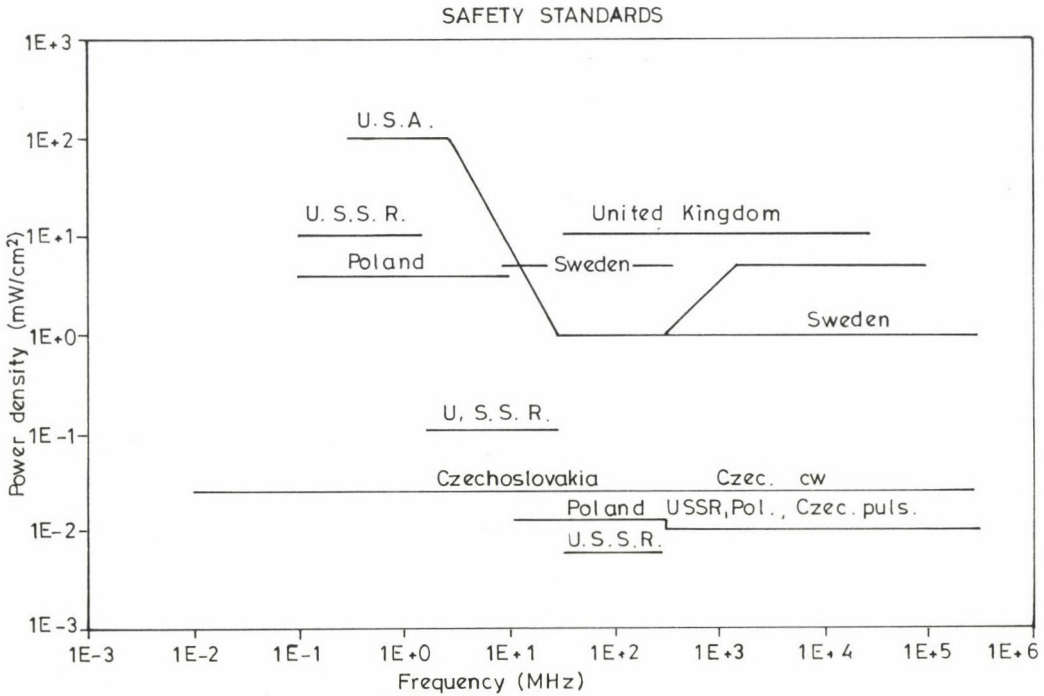


Fig. 8

Table 1

Country	Freq. Range	Exp. Level	Exp. Condition
U.S.A. (ANSI 82)	300 kHz -3 MHz	100mW/cm ²	$E^2 = 4 \times 10^5 [V/m]^2$ $H^2 = 2.5 [A]^2$ Continuous Exposure (that is t>8 hours)
	3 MHz-30 MHz	900/f ² mW/cm ²	$E^2 = 4 \times 10^5 (9/f^2) [V/m]^2$ $H^2 = 2.5 (9/f^2) [A/m]^2$ Cont. Exp.
	30 MHz-300 MHz	1 mW/cm ²	$E^2 = 4 \times 10^3 [V/m]^2$ $H^2 = 0.025 [A/m]^2$ Cont. Exp.
	300 MHz-1.5 GHz	f/300 mW/cm ²	$E^2 = 4 \times 10^3 (f/300)$ [V/m] ² $H^2 = 0.025 (f/300)$ [A/m] ² Cont. Exp.
	1.5 GHz-100 GHz	5 mW/cm ²	$E^2 = 2 \times 10^4 [V/m]^2$ $H^2 = 0.125 [a/m]^2$ Cont. Exp.
U.S.S.R.	0.1 MHz -1.5 MHz	20 V/m-5 A/m	P=10 mW/cm ² (P=Power Density)
	1.5 MHz- 30 MHz	20 V/m	Pe=0.1 mW/cm ² (Pe=Far Field Equivalent Power Density)
	30 MHz- 300 MHz	5 V/m	Pe=6 uW/cm ²
	>300 MHz	1 mW/cm ² 0.1 mW/cm ² 10 uW/cm ²	Up to 20 minutes daily Up to 2 hours daily Up to 6 hours daily Cont. Exp.
United Kingdom	30 MHz -30 GHz	10 mW/cm ²	Up to 8 hours daily Cont. Exp.
Sweden	10 MHz -300 MHz	5 mW/cm ²	t=8 hours daily Average value over any 0.1 hour.

		25 mW/cm ²	Upper limit must never be exceeded. Average over 1 second.
	300 MHz-300 GHz	1 mW/cm ²	t=8 hours daily. Average value over any 0.1 hour.
Czecho-slovakia	10 kHz-300 MHz	10 V/m	Pe=0.026 mW/cm ² t=8 hours daily Cont. Exp.
	>300 MHz	25 uW/cm ²	t=8 hours daily Cont. Exp. CW
		10 uW/cm ²	t=8 hours daily Cont. Exp. Pulsed Waves
Poland	0.1 MHz-10 MHz	>1000 V/m > 250 A/m	Pe=2.4x10 ⁴ mW/cm ² Danger Zone
		1000>E>70V/m 250>H>10 A/m	2.5x10 ⁴ >Pe>70 mW/cm ² Risk Zone
		70>E>20 V/m 10>H>2 A/m	70>Pe>4 mW/cm ² Intermediate Zone
		<20 V/m <2 A/m	Pe<4 mW/cm ² Safe Zone
			At all cases t=560/E; t=80/H (t in hours)
	100 MHz-300 MHz	>300 V/m	Pe>24 mW/cm ² Danger Zone
		300>E>20 V/m	24>Pe>0.11 mW/cm ² Risk Zone
		27>E>7 V/m	0.11>Pe>0.013 mW/cm ² Intermedius Zone
		<7 V/m	Pe<0.013 mW/cm ² Safe Zone
			At all cases t=3200/E ² (t in hours)
	>300 MHz	1 mW/cm ²	Up to 20 minutes daily
		0.1 mW/cm ²	Up to 2 hours daily
		10 uW/cm ²	Up to 6 hours daily

EVALUATION OF STANDARDS

In figures 1 to 7 the levels for U.S.A. and U.S.S.R. standards are drawn as a dotted line.

In the mentioned figures it may be observed that there are many effects that are produced at levels under the North American standards; even, in few cases, under the Soviet, which are the most conservative.

The extrapolation of the results obtained in animals and humans is very difficult because of size and other factors like thermoregulation which seem to be different in men and animals. Owing to the fact that the relation ratio frequency/dimensions, which is related with the resonance frequency, is not the same in both cases, the absorbed power will differ, too. Besides the studies carried out "in vitro", which take only the portion under study, have the difficulty of not allowing to observe the regenerative effects that may be present in the "in vivo" specimen, so some effects produced in such conditions may not be observed under others. The previous means that the effects shown before may not be observed in a human irradiated with the same level and frequency, necessitating a careful extrapolation of the results.

CONCLUSIONS

It may be observed that certain effects have been obtained at levels that some standards consider safe. But it must be taken into account that the fact that some effects may occur in certain animals, frequency and power density, does not mean that under the same conditions this would occur in humans. That is because there is a change in the dimensions and shape of the specimen, giving a variation in the frequency/dimensions relation, which produces amongst others, a change in the frequency or resonance, and in consequence the absorption and distribution of the power.

The above is important in the extrapolation of effects observed in animals to humans to the determination of standards. One way of doing this, is through models. At the present they may be very realistic, owing to the possibility of use of numerical techniques with a relative small computer capability.

REFERENCES

1. Biological Effects of Electromagnetic Fields. Royal Swedish Academy of Sciences, 1976.
2. Electromagnetic Radiation Hazards. IEEE Standard Test Procedures for Antennas. Section 19. Published by IEEE Inc.
3. Adair, E.R. and Adams, B.W. Science, Vol. 207, N 4437, pp. 1381-1383, Mar. 21, 1980.

4. Adrian, R.J.: Frequency selective and nonlinear characteristics of low-frequency EM sensory effects. IEEE 3rd Symposium and Technical Exhibition on EMC, Montreux, June 28-30, 1977.
5. Budd, R.A.: Can microwave/radio frequency radiation (RFR) burns be distinguished from conventional burns? *Journal of Microwave Power*, 1985, pp. 9-11.
6. Clapman, R. and Cain, C.: Absence of heart-rate effects in isolated frog heart with pulse modulated low-level microwave energy. *IEEE, EMC Symposium Record*, July 16-18, 1974.
7. Cleary, S.F.: Microwave cataractogenesis. *Proc. of the IEEE*, Vol. 68, N 1, pp. 49-55, Jan. 1980.
8. Constant, P.C.: Radiation hazards. *Practical Design for Electromagnetic Compatibility*. Chapter 13. Ed Ficchi, R.F., 1771.
9. D'Ambrosio, G., Ferrara, G. and Transfaglia, A.: Pulsed radiation teratogenic effects. *EMC 80, 5th International Wroclaw Symposium on EMC*, pp. 553-560, Sept. 17-19, 1980.
10. D'Ambrosio, G. and La Manna, V.: Perception of static fields by living organism and teratogenic effects of microwaves. *IEEE, 2nd Symposium and Technical Exhibition on EMC, Montreux, June 28-30, 1977*.
11. Durney, C.H.: Electromagnetic dosimetry for models of humans and animals: A review of theoretical and numerical techniques. *Proc. of the IEEE*, Vol. 69, Jan. 1980.
12. Epstein, M.A. and Ondra, G.W.: The interaction of static and alternating electric fields with biological systems. *IEEE Transactions on EMC*, pp. 45-50, Feb. 1976.
13. Gandhi, O.P.: Frequency and orientation effects on whole animal absorption of electromagnetic waves. *IEEE Transactions on Biomedical Engineering*, Nov. 1975.
14. Gandhi, O.P.: Condition of strongest electromagnetic power deposition in man and animals. *IEEE Transaction on Microwave Theory and Techniques*, Vol. MTT-23, Dec. 1975.
15. Gandhi, O.P.: State of the knowledge for electromagnetic absorbed dose in man and animals. *Proc. of the IEEE*, Vol. 68, N 1, Jan. 1980.
16. Gandhi, O.P., Hunt, E.L. and D'Andrea, J.A.: Deposition of electromagnetic energy in animals and man with and without grounding and reflector effects. *Radio Science*, 12N 6 (S), Nov.-Dec. 1977.
17. Graves, H.B.: Some biological effects of high intensity low frequency (60 Hz) electric fields on small birds and mammals. *IEEE, 2nd Symposium and Technical Exhibition on EMC, Montreux, June 28-30, 1977*.

18. Guy, A.W., Kramar, P.O., Harris, C.A. and Chou, C.K.: Long-term 2450 CW microwave irradiation of rabbits: Methodology and evaluation of ocular and physiological effects. *Journal of Microwave Power*, Vol. 15, N 1, pp. 37-44, Mar. 1980.
19. Huang, A.T. and Engle, M.E.: The effects of microwave radiation (2450 MHz) on the morphology and chromosomes of lymphocytes. *Radio Science*, 12 N 6 (S), pp. 173-177, Nov.-Dec. 1977.
20. Joines, W.T and Spiegel, R.J.: Resonance absorption of microwave by the human skull. *IEEE, Transactions on Biomedical Engineering*, Jan. 1974.
21. Koperski, A. and Smialkowski, T.: Evaluation of radiation hazards caused by HF equipments. EMC 80, 5th International Wroclaw Symposium on Electromagnetic Compatibility. Sept. 17-19, 1980.
22. Lindauer, G.A., Liu, L.M., Skewes, G.W. and Rosebaum, F.J.: Further experiments seeking evidence of nonthermal biological effects of microwave radiation. *IEEE Transactions on MTT*, pp. 790-793f, Aug. 1974.
23. Liv, L.M., Rosebaum, F.J. and Pickard, W.F.: The relation of theratogenesis in tenebrio molitor to the incidence of low-level microwave. *IEEE Transactions on MTT*, Vol. MTT 23, Nov. 1975.
24. Lords, J.L., Durney, C.H., Borg, A.M. and Tinney, C.E.: Rate effects in isolated hearts induced by microwave irradiation. *IEEE Transactions on MTT*, Dec. 1973.
25. Lu, S.T., Lotz, W.G. and Michaelson, S.M.: Advances in microwaves-induced neuroendocrine effects. The concept of stress. *Proc. of the IEEE*, Vol. 68, N 1, pp. 73-77, Jan. 1980.
26. Ludwig, H.W.: Compatibility of weak magnetic ELF fields. *IEEE, 2nd Symposium and Technical Exhibition on EMC, Montreux, June 28-30, 1977.*
27. McCally, R.L.: Nonionizing radiation damage in the eye. *John Hopkins APL Technical Digest*, Vol. 7, N 1, 1986.
28. McRee, D.I.: Soviet and Eastern European research biological effects of microwave radiation. *Proc. of the IEEE*, Vol. 68, N 1, pp. 84-91, Jan. 1980.
29. Mennie, D.: Microwave Ovens. What's cooking?. *IEEE Spectrum*, March 1975.
30. Michaelson, S.M.: Microwave biological effects. An overview. *Proc. of the IEEE*, Vol. 68, N 1, pp. 40-49, Jan 1980.
31. Michaelson, S.M.: The Tri-Service Program - A tribute to George M. Knauf, USAF (MC). *IEEE Transactions on Microwave Theory and Techniques*, Vol. MTT-19, pp. 131-146, Feb. 1971.
32. Nowakowski, W.: The growth and the content of DNA and RNA of seedling of *Pisum sativum* L. and *Cucumis Sativus* L. in the environment without exterior electromagnetic fields. EMC 80, 5th International Wroclaw Symposium on EMC, pp. 586-590, Sept. 17-19, 1980.

33. Quboa, K., Al Hafid, H.T. and Gupta, S.C.: Estimation of induced fields and power absorption of human heads using an ellipsoidal model when exposed to electromagnetic energy. IEEE, 3rd Symposium and Technical Exhibition on Electromagnetic Compatibility, Rotterdam, May 1-3, 1979.
34. Raufman, B.: Influence of electromagnetic fields in the low-medium and high frequency range on biological components. IEEE, 3rd Symposium and Technical Exhibition on EMC, Rotterdam, May 1-3, 1979.
35. Schwartz, J.L.: Influence of a constant magnetic field on nervous tissues. II Voltage clamp studies. IEEE Transactions on BME, April, 1979.
36. Schwartz, J.L.: Chronic exposure of the tobacco hornworm to pulsed microwaves - effects on development. Journal of Microwave Power, 1985.
37. Stamenovic, B., Dekleva, N., Beleskin, B. and Majic, B.: Magnetic field influence on biological material. IEEE, 3rd Symposium and Technical Exhibition on EMC, Rotterdam, May 1-3, 1979.
38. Tell, R.A.: Broadcast radiation. How safe is safe? IEEE Spectrum, August, 1972.
39. Tofani, S.: Effects of continuous low-level exposure to radiofrequency radiation on intrauterine development in rats. Health Physics, Vol. 51, N 4, Oct. pp. 489-499, 1986.
40. White, J.F.: Were you zapped? Microwave Journal, Vol. 24, N 1, pp. 16-24, Jan. 1981.

KINETICS OF HISTONE PROTEIN GLYCATION

Á. Lakatos and K. Jobst

Department of Clinical Chemistry, University Medical School of Pécs,
H-7643 Pécs, Ifjúság u. 13, Hungary

Summary: The kinetics of glycation of histone proteins was studied. The glucose uptake of H1 linker histone reached saturation attained after an exponential course. H2-H4 core histone and total histone exhibited two-phase courses differing in time. With the uptake of glucose, the electromobility of the fractions changed. The kinetic results are explained in terms of interaction between proteins.

Key words: histone, glycation, glycohistone kinetics, gel electrophoresis

The literature covering the agrobiochemistry, clinical aspects and diagnostics of the various glycated proteins has increased considerably recently [Bernstein, 1987]. As no such data were to be found on histone proteins, we began a study of the nonenzymatic glycation of histones by means of chemical and morphological methods [Lakatos and Jobst, 1989; Jobst et al., 1991]. Surprisingly, it emerged that the times of uptake of glucose by the various histones differed. The detailed investigations to be described here, showed that the kinetics of glucose uptake varied with the histone fractions.

MATERIAL AND METHODS

Total histone and its fractions were isolated from calf thymus [Johns, 1971]. For comparison purposes, Boehringer (FRG) and Sigma (USA) histone fractions were chosen. Human and bovine albumine, glucose a.g. (Reanal, Budapest) and protamine (La Roche, Ch) were used. The serum protein was obtained from dialyzed samples of nondiabetic subjects.

The various histones were dissolved in 66% aqueous ethanol at a concentration of 10 mg/ml, then incubated with 300 mM glucose and 10 000 U/l Aprotinin (Boehringer, FRG) at 37 °C for 1-30 days. The aliquots, taken at different points of time, were

dialyzed against water for 48 hrs to remove glucose and, after lyophilization, the glucose uptake of the proteins and their glycation were measured by using the NBT-fructosamine method [Johnson et al., 1982]. Glycation of the albumins and protamine was performed as described previously, but in phosphate buffer of pH 8.9. The glucose uptake of the samples was expressed as changes in absorbance of the NBT reaction and the quotient of the biuret value for protein ($\Delta A/\text{protein}$). All data presented here are average results of three parallel experiments. Electrophoretic separation was carried out in 15% unidimensional, thin-layer polyacrylamide gel containing 3 M acidic urea and 0.15% Triton X 100 [Laemmli, 1970]. The gels were stained with Coomassie blue.

RESULTS

The degree of glycation of the original H1 and total histone, not containing free glucose, and also their lysine content in M% were determined (Table 1). With the exceptions of H1 histone and protamine, no appreciable differences in lysine content and primary glycation were found for proteins examined.

In a pilot experiment, the glucose uptake of the protein samples were measured after 8-10, 15-17 and 30 days (Table 2). The guanidino group of the arginine-rich protamine was not glycated. There was no difference in glucose uptake between human and bovine albumin [Kennedy et al., 1982; Davies et al., 1989] and serum proteins on days 10 and 30. Total histone had taken as much glucose after 10 days as albumin did after 30 days. By then, the initial glucose uptake of H1 histone had increased seven fold.

Table 1

Glycation of various "native" proteins measured with the NBT reaction and expressed as $\Delta A/g$ protein.

Protein	$\Delta A/g$ Protein	Lysine M%
Histone (total) calf thymus	1.5-2.5	15
H1-histone calf thymus	0.1-0.5	30
Bovine albumin	1.5-3.0	10
Human albumin	0.8-1.5	10
Human serum	1.0-1.1	
Protamine	0	0

Table 2

In vitro glucose (300 mmol/l) of various proteins measured with the NBT reaction in 66% aqueous ethanol at 37°C.

Protein	Procedure	$\Delta A/g$ protein
Histone (total) calf thymus	66% EtOH	
	10 days	40-50
	15 days	50-70
	30 days	80-100
H1-histone calf thymus	66% EtOH	
	15 days	150-200
Human albumin	PBS pH 8.9	
	8 days	25-30
	30 days	40-50
Bovine albumin	PBS pH 8.9	
	2-10 days	15-20
	30 days	40-50
Protamine	PBS pH 8.9	
	10 days	3-4

The kinetics of glucose uptake was determined from the data obtained on samples taken every other day (Fig. 1). As compared with the slowly glycating albumin, which served as a control, the curve for H1 linker histone attained saturation after a hyperbola-shaped curve. The glucose uptakes of H2-4 core histone and total histone displayed two-phase kinetics with inflection points differing in time. On day 20 the glucose uptake was nearly identical, at half the value for H1 on day 20.

The electrophoretograms (Fig. 2) clearly reflect the numerical data in Table 2. As a result of the uptake of glucose, in parallel with the increase in mass of the protein fractions and the decrease in their positive charge, there was a decrease not only in their mobility, but also in their acidic Coomassie blue uptake, which resulted from Amadori product formation by the basic amino groups [Kuhn and Weygand, 1937].

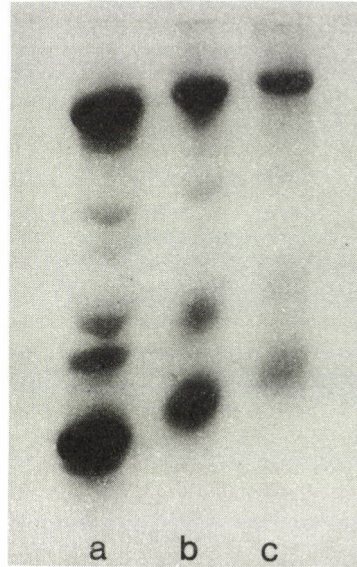


Fig. 1: PAGE-electrophoretic picture of total histone, after Coomassie blue staining: unglycated control (a), Glycated for 10 days (b) and Glycated for 30 days (c).

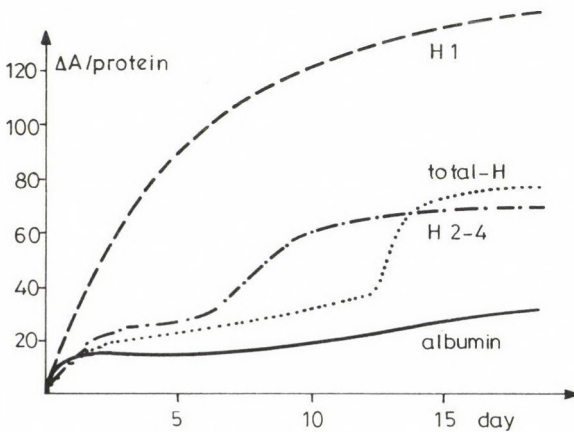


Fig. 2: Kinetics of glucose uptake by H 1 linker histone, H 2-4 core histone, total histone and albumin. The average s.d. of points is ± 4.0 .

DISCUSSION

The uptake of glucose, which was observed in the pilot study to increase in proportion to time, was determined precisely in kinetic and electrophoretic examinations.

An analysis of the uptake of glucose by histones revealed that the kinetics of the most basic, lysine-rich linker H1 histone agreed with expectations: it increased steeply with time. On the other hand, the arginine-rich H2-H4 core fraction, whose lysine content was smaller, attained the glucose level corresponding to three times that of albumin with an inflection after 7 days. For total histone, the inflection developed after day 13. This saturation value is in agreement with that calculated from elementary analysis earlier [Lakatos and Jobst, 1989]: 45 M% glucose uptake after 72 hrs of incubation. The differing kinetics for total histone may be explained by a structural change resulting from an interaction between the core and linker histones, and by a relative decrease in the charge of the basic groups. This is indicated by our observations that the primary glucose content and in vitro glucose uptake of isolated cell nuclei were considerably lower than those for isolated histone (unpublished results). As in the case of acetylation [Thorne et al., 1990], the results presented here will be easier to interpret after the clarification of the time sequence of glucose uptake by the lysine molecules in the conservative protein structure.

ACKNOWLEDGEMENT

This work was supported by Hungarian Science Foundation Grant OTKA 86/1991.

REFERENCES

1. Bernstein, R. E. (1987) *Adv. in Clin. Chem.* 26, 1-78.
2. Davis, L. J., Hakim, G. and Rossi, C. A. (1989) *Biochem. Biophys. Res. Comm.* 160, 362-366.
3. Lakatos, Á. and Jobst, K. (1989) *Acta Biochem. Biophys.* 24, 355-359.
4. Jobst, K., Lakatos, Á. and Horváth, A. (1990) *Acta Histochem.* 88, 183-185.
5. Jobst, K., Lakatos, Á. and Horváth, A. (1991) *Biotechn. and Histochem.* 1, 26.
6. Johns, E. F. The preparation and characterization of histones. In: Phillips, D.M.P. ed. *Histones and nucleohistones*. London & New York: Plenum Press, (1971) 1-83.

7. Johnson, R. N., Metcalf, P. A. and Baker, J. R. (1982) *Clin. Acta* 127, 87-95.
8. Kennedy, L., Mehl, T. D., Elder, E., Varghese, M. and Merimee, T.H.J. (1982) In *Conference on Nonenzymatic Glucosylation and Browning Reaction: Their Relevance to Diabetes Mellitus*, ed. Peterson CHM, *Diabetes* 31, Suppl. 3, p 52-56.
9. Kuhn, R. and Weygand, F. (1937) *Berichte* 70, 768-772.
10. Laemmli, V. K. (1970) *Nature* 227, 680-685.
11. Thorne, A. W., Kmiciek, D., Mitchelson, K., Sautiere, P. and Grance-Robinson, C. (1990) *Eur. J. Biochem.* 193, 701-713.

SINGLE-CHANNEL ANALYSIS OF Pb²⁺ MODIFIED STEADY-STATE Na-CONDUCTANCE IN SNAIL NEURONS

O.N. Osipenko¹ and T. Kiss²

¹Permanent address: Department of General Physiology of Nervous System, A.A. Bogomoletz Institute of Physiology, Academy of Sciences of the Ukrainian S.S.R., Bogomoletz str. 4, Kiev-24, 252601, C.I.S. and ²Balaton Limnological Research Institute of the Hungarian Academy of Sciences, H-8237 Tihany, Hungary

Summary: Patch-clamp technique was used in order to study properties of the steady-state Na-channel in snail neurons. Experiments revealed that Pb-ions, applied extracellularly, close these channels, which are preferably in open state at the resting membrane potential. Elementary currents have a linear current-voltage (I-V) relationship with single channel conductance of 14 pS between -100 and -40 mV both in control saline and in the presence of 50 μ M Pb in the pipette. Pb-ions decreased the mean open and increased the mean closed time. It was found that both open and closed times showed little voltage-dependence, however the probabilities of the open and closed times proved to be voltage-dependent. Open and closed time histograms were fitted by one exponential, therefore first order kinetics were assumed for the blocking effect of Pb²⁺ at the single channel level.

Key words: patch-clamp, Pb²⁺, steady-state Na-conductance, snail neuron

INTRODUCTION

Electrophysiological data from molluscan neurons suggest that the membrane generates transmembrane potentials basically in accordance with electrodiffusion theory [1]. Superimposed, however, on this are processes like electrogenic pumps, membrane rectification and the high Na-conductance in the resting state. The ultimate electrophysiological properties of the neuron is a summation of the processes mentioned above.

It is well known that molluscan neurons have a significant Na-conductance at the resting membrane potential. The complete replacement of extracellular Na⁺ with Tris ions, sucrose or other substances, as well as TTX application, caused a hyperpolarisation in all molluscan neurons studied. The magnitude of this

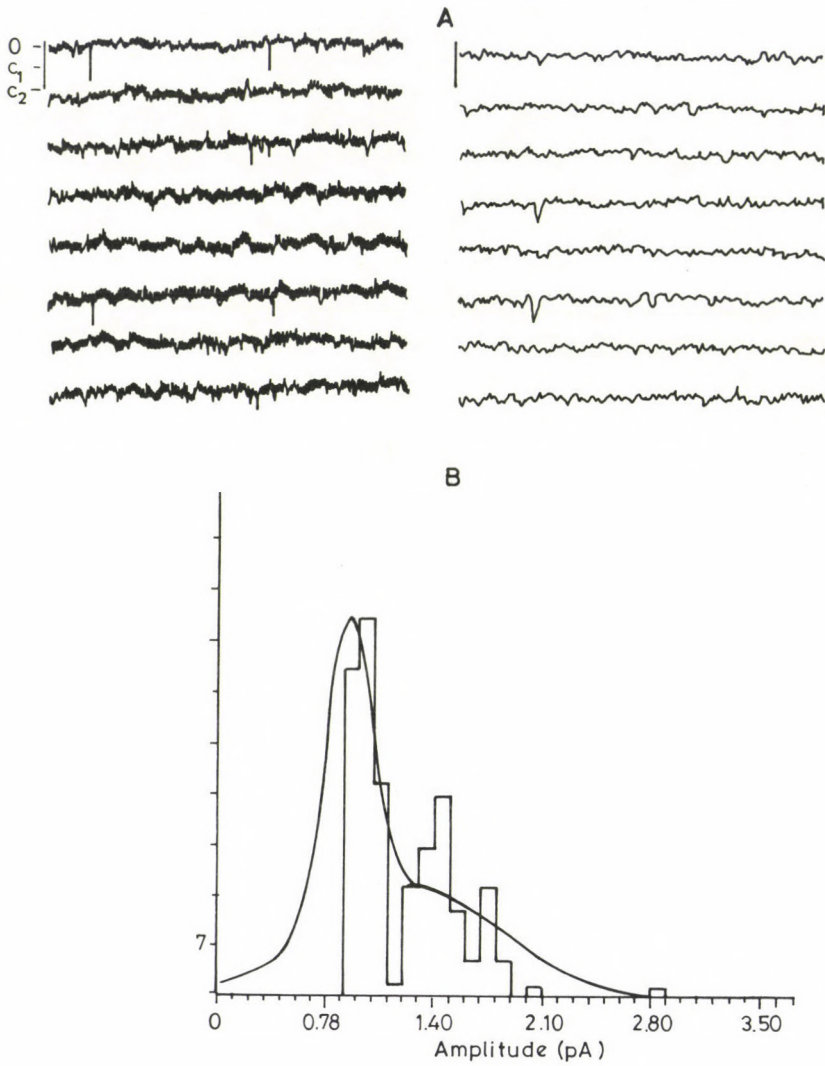


Fig. 1a: Single channel currents recorded in cell-attached mode with control saline in the patch pipette. O - open level, C - closed level. PP= +40 mV. Downward deflections are closings of inward currents shown at two different time scales 200 and 50 ms.

b: Amplitude histogram demonstrating Gaussian distributions of open channel amplitudes. Y axis 7 events/div. Closings shorter than 0.6 ms were not included in the histogram.

hyperpolarisation was generally around 15 mV [2-7]. Molluscan neurons are widely used in different neurophysiological studies, yet little is known about the nature of the leakage channels. Recently it was found that Pb -ions produce an outward current, which was likely due to the closing of the steady-state Na-channels [8].

The aim of the present study was to analyse and describe the kinetic properties of these channels using the single-channel recording technique.

MATERIALS AND METHODS

Single channel activity was recorded in the cell-attached patch configuration, according to the technique of Hamill et al. [9] using List EPC-7 (List-Medical) amplifier. Patch electrodes were pulled from Pirex glass in one or two steps from tubes with or without internal capillaries, and tips were subsequently firepolished and covered with sylgard. Electrodes were filled with extracellular saline the following composition (in mM): NaCl 80, KCl 4, $MgCl_2$ 5, $CaCl_2$ 10, HEPES 5, glucose 10. The pH of the saline was adjusted by 0.1 M HCl to 7.8. 50 or 100 μ M $Pb(NO_3)_2$ was added to the extracellular saline in the patch pipette or to the bathing saline.

Data were recorded on a tape recorder (AKAI 1710) for storage and subsequent analysis. Digitisation was made at a sampling rate of 2 KHz with Labmaster TL-1 (Axon Instruments) A/D-D/A converter and analysed using pClamp software (Axon Instruments). Transitions between open and closed levels were identified using 50% of single open channel amplitude as the threshold criterion. All experiments were made on isolated neurons at room temperature (20°C). The isolation procedure of neurons from brains of *Helix pomatia* L. was described elsewhere [10, 11].

RESULTS

Steady-state Na-channels are open most of the time around the resting membrane potential (zero pipette potential-PP). Fig. 1 shows single channel recordings in the cell-attached mode without Pb^{2+} in the pipette at a +40 mV pipette potential. Brief spontaneous closures can be seen that account for 0.2-0.3% fractional time. The amplitude histogram of the spontaneous closures could be fitted with two Gaussian-distributions with maxima at 0.75 and 1.45 pA (Fig. 1b). The average mean value was calculated to be $A_1=0.83\pm0.15$ pA (S. D.) and $A_2=1.26\pm0.55$ pA (S. D.). The closed time distribution was fitted by one exponential while the open time distribution could not be fitted due to the small number of spontaneous events (Fig. 2). The mean closed and open times were calculated to be 0.48 ± 0.13 ms (S. D.) and 202 ± 187 ms (S. D.), respectively. The mean open and closed times were determined from interval histograms of the channel open and closed times. Since the data recording and analysis system fails to detect brief shut intervals, the observed mean closed time is somewhat overestimated. The distributions of the intervals were fitted to a single

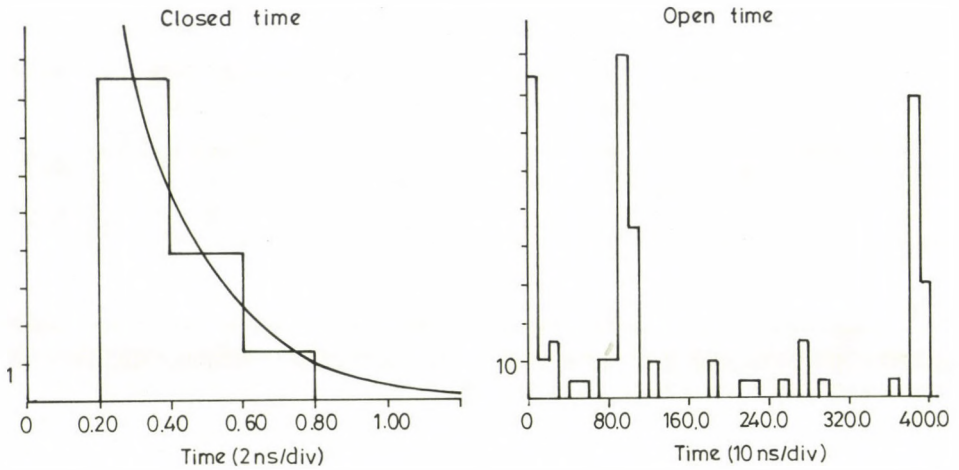


Fig. 2: Closed and open time histograms obtained from the experiment shown on Fig. 1a. A non-linear least-squares curve-fitting routine was used to fit data: $N = \sum W_n / \exp(-T/\tau) dt$ where T is the centre value of a given bin of width dt , τ is the time constant, W_n is the weight of the n -th term and N is the number of counts in the given bin contributing to the term.

exponential, and the mean values were obtained from these fits. Time constants and S. D.-s were determined using a nonlinear least-square algorithm. When patch-pipette in addition contained 50 or 100 $\mu M Pb^{2+}$ closings were more frequently seen. Fig. 3a shows single channel events at different holding potentials with two different Pb^{2+} concentrations in the patch pipette. In both cases the reversal was obtained at zero PP. the amplitude histogram was similar to that obtained in the control saline (Fig. 3b). The I-V curve was linear with a slope conductance of 12 pS with 50 $\mu M Pb$ and 7 pS with 100 $\mu M Pb^{2+}$ in the pipette (Fig. 4a). Fig. 5a shows the open and closed time histograms in the presence of 50 $\mu M Pb^{2+}$ at PP= +20 mV. In both cases histograms were well fitted by one exponential. In some experiments, however, the open time was fitted by two exponentials with a time constant of 1.1 and 19.9 ms, while the closed time histogram was monoexponentially distributed with a 0.98 ms time constant (Fig. 5b).

To demonstrate the voltage dependence of the transition from closed-to-open and open-to-closed states, we calculated the rate of the transitions and plotted the log of the rate versus the pipette potential. In Fig. 6 both the forward (closed-to-open) and

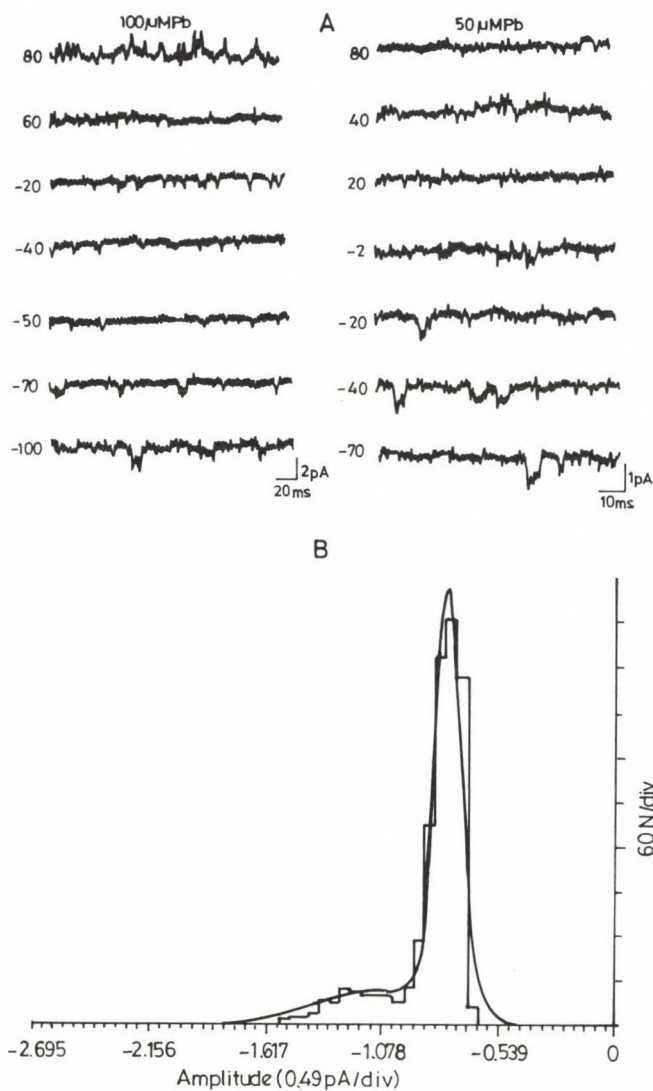


Fig. 3a: Closing of single steady-state Na-channels in the presence of two concentrations of Pb^{2+} in the patch pipette. Cell attached patch. Numbers on the left show the pipette potential. b: Amplitude histogram of single channel current at PP= +40 mV and 50 μ MPb $^{2+}$ in the pipette.

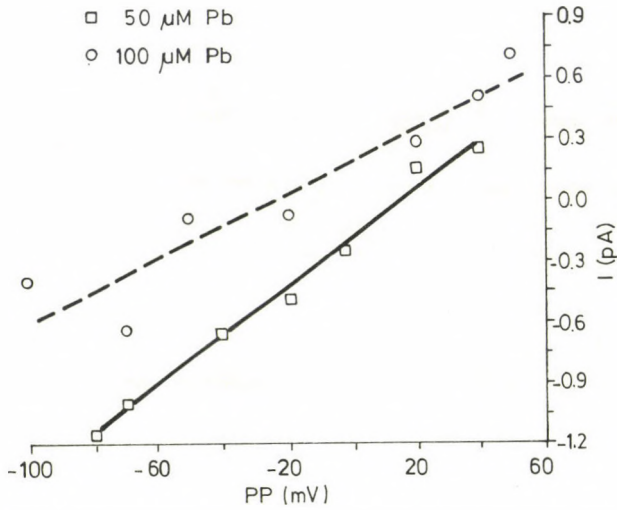


Fig. 4: I-V relationship of single channel currents in the presence of two concentrations of 150 and 100 μM Pb^{2+} , with single channel conductance of 12 and 7 pS, respectively.

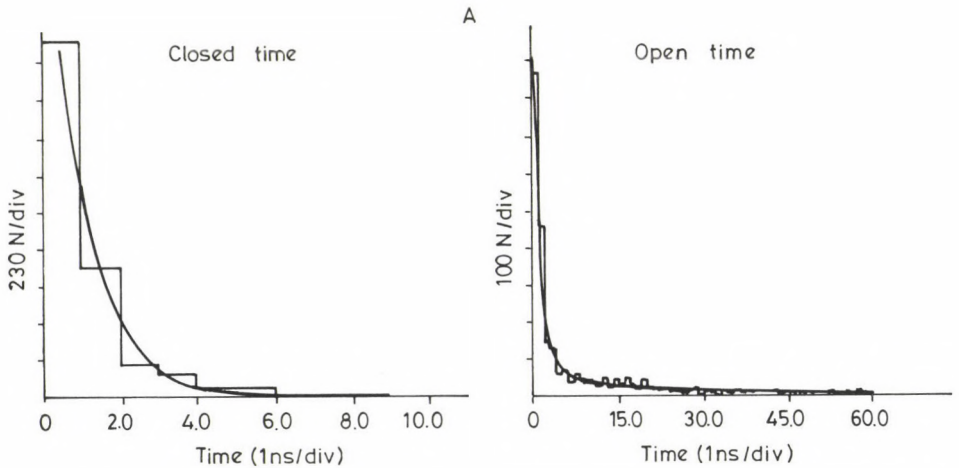


Fig. 5a: Closed and open time histograms at $PP = +20$ mV. On Y axis 230 events/div. and 100 events/div., respectively. A monoexponential distribution was obtained in both cases.

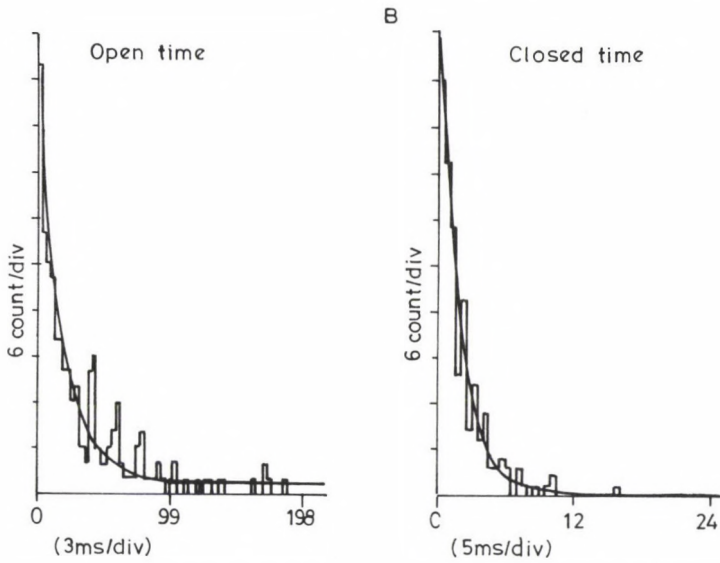


Fig. 5b: Closed and open time histograms which could be fitted by one and two exponentials.

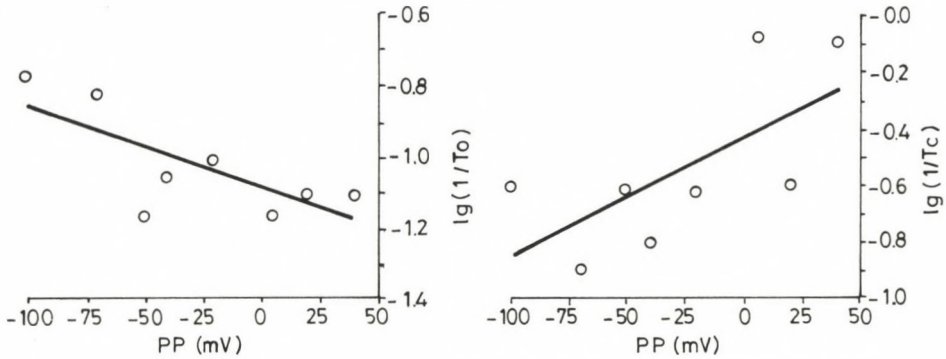


Fig. 6: Closing and opening rate constants plotted on a semilog graph. For details see text.

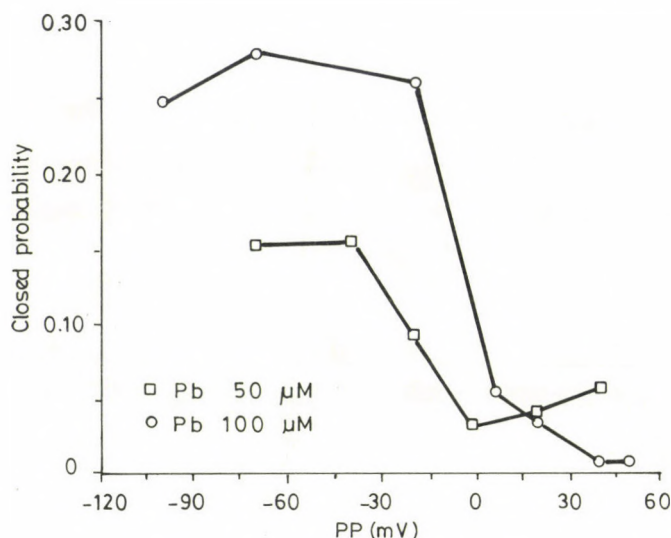


Fig. 7: The probability of the channel being in closed state at two different Pb²⁺ concentrations.

the reverse rate (open-to-closed) have a clear voltage dependence between -100 and 50 mV pipette potential. However, to produce a 10-fold change in the rate constant would require several hundreds of mV change in potential, both for the opening and closing rates. Therefore, membrane voltage itself does not seem likely to be important for normal physiological control of the steady-state Na-channel.

The probability, however, to find a channel in the open or closed state was voltage dependent. Fig. 7 shows that with increasing depolarisation the probability to find a channel in the closed state increased. The probability (P) of channels being closed was determined as the ratio between the time spent in the closed state by all channels and the total recording time: $P_{Cl} = (\sum n_{Cl} \cdot t) / t_{total}$.

Besides outwardly directed channels, inward currents were also observed in several experiments (Fig. 8A). This current reversed around zero mV and gave a linear I-V curve between -20 and +80 mV PP with a single channel conductance of 13 pS (Fig. 8B). The open time probability decreased with increasing depolarisation (Fig. 8C). Both open and closed duration histograms were fitted by one exponential with 1.88 ms mean open and 10.6 ms mean closed times.

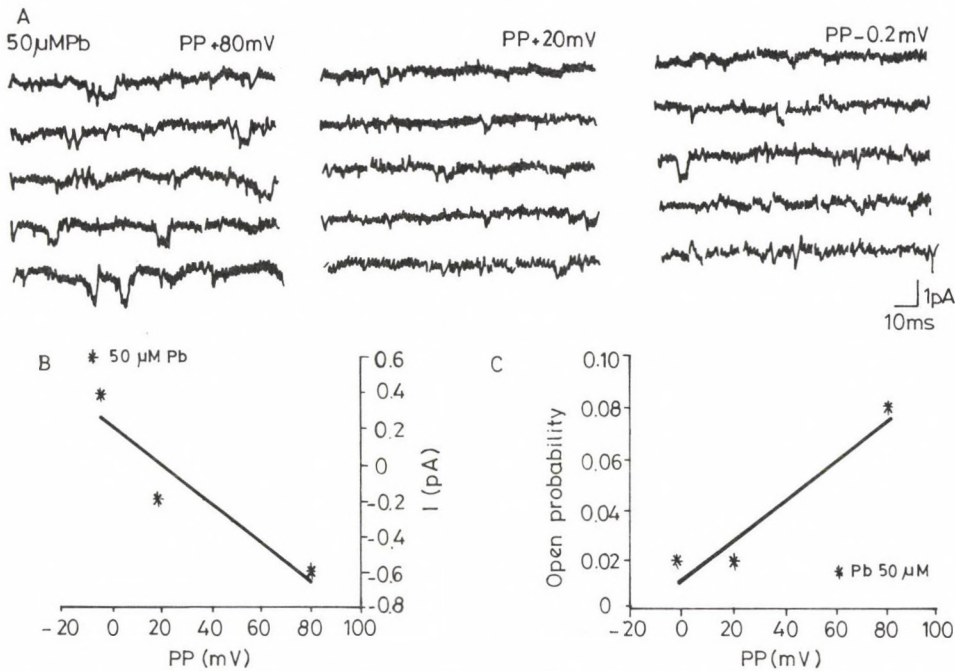
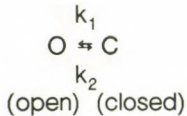


Fig. 8: A: Inward channels induced by Pb^{2+} application at three different PP's. I-V relationship (B) and the probability of finding the channel in an open state (C) with $50 \mu MPb^{2+}$ in the patch pipette.

DISCUSSION

Steady-state Na-channels have been characterised in the presence of extracellularly applied Pb^{2+} in cell-attached patch-clamp experiments. The single channel experiments revealed that Pb^{2+} applied extracellularly, but not intracellularly [8], closed the steady-state Na-channels. These channels have a linear I-V relationship between voltages of -100 and -40 mV, with a single channel conductance of 14 pS for $50 \mu M Pb$ in the pipette. Both open and closed times showed little if any voltage dependence. The mean open time decreased ten fold and the mean closed time increased two fold in the presence of Pb ions. However, the probabilities of the open and closed states proved to be strongly voltage-dependent. At negative pipette potentials (i.e. at depolarised level) the probability of the channel being open decreased while the probability of being in a closed state increased. Since open and closed time distributions were well fitted mostly by one exponential, first order kinetics

were assumed to be responsible for the blocking effect of Pb^{2+} at the single channel level:



Here k_1 and k_2 are the opening and closing rate constants, respectively. Transition rates were measured directly from single channel records assuming that the channel has only two kinetic states, one open and one closed. For such a simple model, single channel recording can be used to estimate the transition rate for opening from the average closed time ($K_1=1/\tau_c$), and the transition rate for closing from the average open time ($K_2=1/\tau_o$) of the channel. Models for gating of ion channels usually assume that the rate constants for transitions among a discrete number of kinetic states are independent of previous channel activity [12-16], i.e. the channel gating might be characterised as the time homogeneous Markov model. Therefore, it can be concluded that the steady-state Na-channels at a first approximation could be described as channels having two kinetic states: one open state, in which channels spent most of the time at the resting potential, and one closed (or Pb-bound) state. Since in control circumstances two amplitudes were found and in the presence of Pb^{2+} only one (see amplitude histograms) and, furthermore, since open life time distributions were sometimes biexponentially distributed, it could be suggested that channel gating kinetics is far more complex than previously thought.

Despite the considerable similarity in the single channel characteristics (e.g. single exponential approximation of the closed and open time distribution, reversal potential and single channel conductance) between steady-state Na- and Pb^{2+} -activated inward channels, it is proposed that these channels could be different. It was found that Cu and Pb activate a new type of inward current, both in *Aplysia* and neuroblastoma cells [17, 18]. It could be suggested, therefore, that in *Helix* neurons the Pb^{2+} -activated inward current is likely to be similar to this current.

ACKNOWLEDGEMENT

This work was supported by a grant from OTKA (Hungary), (N 1-600-2-86-1-546).

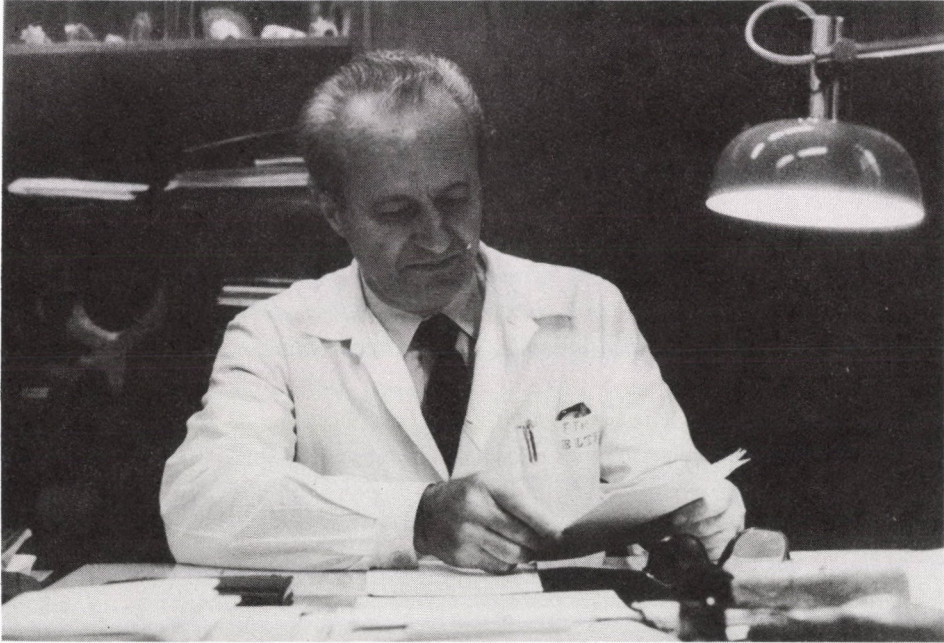
REFERENCES

1. Hodgkin, A.L. (1958) *Proc. Roy. Soc. B.* 148, 1-23.
2. Gerasimov, V.D., Kostyuk, P.G. and Maiskii, V.A. (1965) *Biophysics* 10, 88-96.
3. Chiarandini, D.J. and Stefani, E. (1967) *J. Gen. Physiol.* 50, 1183-1200.
4. Geduldig, D. and Junge, D. (1968) *J. Physiol.* 199, 347-365
5. Meves, H.(1968) *Pflügers Arch.* 304, 215-241.
6. Carpenter, D.O. and Gunn, R. (1970) *J. Cell. Physiol.* 75, 121-128.
7. Gorman, A.L.F. and Marmor, M.F. (1970) *J. Physiol.* 210, 897-917.
8. Osipenko, O.N., Győri, J. and Kiss, T. (submitted for publication)
9. Hamill, O.P., Marty, A., Neher, E., Sakmann, B. and Sigworth, F.J. (1981) *Pflügers Arch.* 391, 85-100.
10. Kostyuk, P.G. (1982) *Ann. Rev. Neurosci.* 5, 107-120.
11. Győri, J., Kiss, T., Shcherbatko, A.D., Belan, P.V., Tepikin, A.V., Osipenko, O.N. and Salánki, J. (1991) *J. Physiol.* (accepted for publication).
12. Colquhoun, D. and Hawkes, A.G. (1977) *Proc. Roy. Soc. B.* 199, 231-262.
13. Neher, E. and Stevens, C.F. (1977) *Ann. Rev. Biophys. Bioeng.* 6, 345-381.
14. Hille, B. (1984) *Sinauer Associates Inc. MA*, 426 pp.
15. Horn, R. (1984) *Current Topics in Membranes and Transport* 21, 53-97.
16. Bezanilla, F. (1980) *J. Membrane Biol.* 88, 97-111.
17. Weinreich, D. and Wonderlin, W.F. (1987) *J. Physiol.* 394, 429-443.
18. Oortgiesen, M., M. van Kleef, R.G.D. and Vijverberg, H.P.M. (1990) *J. Membrane Biol.* 113, 261-268.

PROCEEDINGS
from presentations
of the Annual Meeting of the Neuroscience Section
of Hungarian Physiological Society,
Visegrád, January 23-25, 1992.

About the President of the Meeting

György Ádám



György Ádám, full professor, Member of the Hungarian Academy of Sciences is 70 years old now. He was born August 25, 1922, in Nagyvárad, Romania, where he attended both his elementary and secondary schools. He graduated from the Budapest University Medical School as a physician (M.D.) in 1949. He started to work as a clinician, then he became a staff member at the Institute of Physiology of the Medical School. Here he studied kidney physiology and also taught physiology for undergraduate students. In 1952 he became a fellow of the Pavlovian Institute in Leningrad (now St. Petersburg), where he had first got in touch with research in neurophysiology and psychophysiology. He defended his thesis in 1955. After returning home he had an opportunity to organize a neurophysiology research group and laboratory, which he had headed until 1966. He obtained his Doctor of Science title in 1965.

In 1966 he moved to the Eötvös Lóránd University to be a full professor and to establish the new Department of Comparative Physiology. Since then until now he had been the Head of this Department. Meanwhile, he served as Director of the

Institute of Physiology of the Hungarian Academy of Sciences between 1970 and 1972, and from 1972 to 1978 he was the Rector of the University. His work in the education and research was recognized with the State Prize in 1988. He is "Doctor Honoris Causa" of the State University of Leningrad (St. Petersburg). He is the member of numerous scientific institutions, like the: European Academy of Sciences, Arts and Humanities; Hungarian Physiological Society (board member); Hungarian Psychological Society; Hungarian IBRO Committee (president); Association des Physiologistes (France); Pavlovian Society of America (president for one year); CIANS; ENA; Governing Council of IBRO; Academy of Behavioral Medicine Research (USA).

György Ádám is a recognized university teacher of Physiology and related disciplines. He has taught many generations of young students of biology, medicine and psychology. He emphasizes the importance of appropriate textbooks and other written texts, consequently he published a series of books and lecture notes. He has always stressed that without proper experimentation it is impossible to learn real Physiology. With this in mind he organized the lectures and practical work in the Department of Comparative Physiology with his colleagues. Lectures and experimentation at the University, however, are not the only means of his teaching activity. He has practiced popular scientific education since his youth. He has had many lectures, talks, published papers and monographs in the framework of the Hungarian Society of Scientific Education (TIT), and had many lectures in the TV and Radio programmes. He had also been the President of the Society for many years. In this field he has always stressed the priority of the common sense ("ratio") to the irrationality. Although he knows that the human thinking and behavior are frequently motivated by other factors than the clear mind, he still believes the world is mostly governed by the genuine common sense. In his young years Voltaire and Erasmus were, among others, his favourite philosophers.

György Ádám is a dedicated researcher in Psychophysiology. He has made a lot of efforts to establish the financial and scientific basis of a regional psychophysiology research programme. He had to do everything by himself, without a tradition of any already existing school or significant predecessors. As a result, he established and has been leading the Psychophysiology Research Group of the Hungarian Academy of Sciences, in the frame of the Department of Comparative Physiology of the Eötvös University. At the beginning, his small group studied visceral sensation, and also dealt with the neuronal and molecular mechanism of learning and memory. This latter topic was summarized in an international symposium organized by them in Tihany in 1969. While some topics been carried over since then, new ideas and problems have also been raised. This was marked by the commencement of the sleep research among the first labs in Hungary, and the Department has also

become one of the most significant centres of the hypnosis research. This tendency has not been ceased up to now, when mostly the second generation of teachers and researchers work in the laboratories. Recently, new methods of micro electrophysiology, micro chemistry, cell culture and other in vitro techniques were introduced for investigating minute molecular mechanisms of the nervous system.

György Ádám has been frequently invited to deliver lectures and talks in other institutes and on international conferences all around the world. He himself is also always ready to organize symposia and other scientific events. He was one of the leading organizers of the International Congress of the Physiological Sciences (1980) and the 2nd World Congress of the Neurosciences (IBRO, 1987) both held in Budapest with great success. He also organized a Joint Symposium of the Pavlovian Society of America and the Hungarian Physiological Society in 1980, and was asked to organize and host an International Symposium on the Gastrointestinal Psychophysiology in 1989. Many other events are in his list besides those mentioned above.

He can be characterized by modesty. Although he, as everybody else in science, has always worked for new results and ideas, looked for recognition and success, he has never felt the necessity to push himself forward anywhere. Science has always been first in his mind! His attitude toward his colleagues and coworkers was always friendly and helpful, his doors were open for anybody's problems. While doing his best in whatever he was trusted with, he has always tried to keep his humanity, personality and integrity. He feels there is no situation in human life when we should give up our integrity. This is the principle that has governed him throughout his 70 years of life, studies, research and teaching.

Budapest, August 1992

Tibor Kukorelli

EFFECT OF ELECTROPHORETICALLY APPLIED NEUROCHEMICALS ON ACTIVITY OF EXTRAPYRAMIDAL AND LIMBIC NEURONS IN THE RAT

A. Czurkó, B. Faludi, I. Vida, Cs. Niedetzky, A. Hajnal, Z. Karádi and L. Lénárd

Institute of Physiology, Neurophysiology Research Group
of the Hungarian Academy of Sciences, University of Pécs,
School of Medicine, H-7643 Pécs, Szigeti u. 12, Hungary

Key words: single neuron recording, multibarrel microelectrophoretic technique, catecholamines, glucose sensitive cells, extrapyramidal and limbic regions

The caudate nucleus (CN), globus pallidus (GP) and amygdaloid body (AMY), and especially their local and passing catecholamine (CA) elements, have been demonstrated to play important roles in the central feeding control [1,3,4,5]. Despite the large amount of relevant data in the literature [2,7], little is known yet about the functional attributes of local cells in these structures. Since the neurochemical characteristics belong to the most important factors that determine the functional capacity of a neuron, in the present experiments, the effects of electrophoretically administered neurotransmitters and glucose were examined on the activity of single neurons in the 1) CN, 2) GP and 3) AMY.

Eleven adult CFY rats of both sexes were used. Experiments were performed under urethane anesthesia (20%, 1.5 ml/300g). Carbon fiber multibarreled glass microelectrodes were employed for single neuron recordings and electrophoretic applications. Each electrophoretic micropipette was filled with one of the following solutions: 0.5 M Na-L-glutamate (Glut); 0.5 M GABA; 0.5 M noradrenaline-HCL (NA); 0.5 M dopamine-HCL (DA); 0.5 M D-glucose (Gluc) and 0.5 M acetylcholine-Cl (ACh). Two additional barrels (one for current balancing and another one for general current test) were filled with physiological saline (0.15 M NaCl). Constant currents of appropriate polarity were used to release the chemicals from their respective barrels (NeuroPhore

BH-2, Med. Syst. Corp., U.S.A.). The extracellular single neuron action potentials were led into a high input impedance preamplifier with capacity compensation, than to a high gain amplifier with low and high cut filters and to a window discriminator to obtain standard, formed pulses. Both action potentials and pulses were continuously monitored on oscilloscope (HAMEG HM-2037, Germany). Pulses were fed into an IBM PC-compatible microcomputer for real-time analysis. Analog signals, commentaries and application markers were stored on magnetic tapes for off-line analyses. Stereotaxic coordinates of the recording sites were localized histologically.

The activity of altogether 114 neurons was recorded in these experiments. Basic discharge rates largely varied in the CN, GP and AMY. The neurochemical sensitivities, however, showed distinct characteristics of cells of these three brain regions (Table 1).

Table 1

	GP	CN	AMY	Number of cell tested
GABA	- -	- -	- -	80
Dopamine	- - +	+ -	- -	77
Noradrenaline	- - +	+ -	- -	76
Glucose	- - +	0	- -	72
Acetylcholine	- - +	+ -	+ -	27

Total number of cells tested: 114

(+: facilitation; -: inhibition; 0: no effect; the - - signs refer to stronger effects)

The CN neurons displayed both inhibitory and excitatory activity changes to NA, DA and ACh and the ratio of the two response types was nearly the same. The GABA elicited firing rate changes were identical to those sharp inhibitory patterns seen in the other two structures. In contrast to the relatively high Gluc-responsiveness of GP and AMY cells, no neuronal response was found in the CN to Gluc applied microelectroretically.

In the GP, the primary response to the CAs and ACh was inhibition, though a small set of neurons exhibited facilitation to these respective chemicals. The GABA-applications resulted in exclusive activity decrease. In contrast to the lack of sensitivity in the CN, more than one fourth of all GP cells responded to Gluc. The predominant effect of electroosmotically applied Gluc was inhibition (22% of neurons tested), whereas a few pallidal cells (appx. 4%) showed excitation to this same chemical. Thus, both the so-called glucose-sensitive (inhibitory response) and glucose-receptor (excitatory response) neurons were identified in the GP.

The neurotransmitter sensitivity of GP cells represented a transition between the characteristics of CN and AMY neurons. The CAs and GABA elicited only inhibitory firing rate changes of AMY cells, whereas ACh administrations, when effective, were followed either by facilitation or inhibition. In a few cases, the DA caused especially long-lasting (for several minutes) suppression of neuronal activity. The responsive AMY cells, in concordance with previous findings in the rhesus monkey [6], were exclusively suppressed by electrophoretically applied Gluc (appx. 25% of all neurons tested).

The results demonstrated that a characteristically high proportion of extrapyramidal and limbic neurons receive multiple neurotransmitter inputs. These neurochemical attributes of the cells appear to be important constituents of their functional heterogeneity. In addition, the often antagonistic neurotransmitter actions (e.g. DA & ACh in the CN) can serve as the underlying neural mechanism for complex regulatory processes. Our finding provided further evidence for the existence of Gluc-responsive units in the GP and the AMY of anesthetized rats. These neurons can be of particular significance in the integrative mechanism of the feeding regulation.

ACKNOWLEDGEMENTS

This project was supported by the Hungarian National Research Found (OTKA 1404/1990; L.L.) and the Ministry of People's Welfare of Hungary (ETT T-565 / 1990) and by the Foundation for the Hungarian Science, Hungarian Credit Bank (H.A.).

REFERENCES

1. Fonberg, E. (1974) Amygdala functions within the alimentary system. *Acta Neurobiol. Exp. (Vars.)* 34, 435-466.
2. Karádi, Z., Oomura, Y., Nishino, H., Scott, T. R., Lénárd, L. and Aou, S.: Lateral hypothalamic and amygdaloid neuronal responses to chemical stimuli in rhesus monkey. In: Morita, H., ed. *Proc. of the 22nd Japanese Symposium on Taste and Smell*. Gifu: Jasts, Asahi University Press; 1988: 121-124.

3. Lénárd, L. (1977) Food and water intake in rats after bilateral caudate and putamen lesions. *Acta Physiol. Acad. Sci. Hung.* 50, 27-34.
4. Lénárd, L. (1977) Sex-dependent body weight loss after bilateral 6-hydroxydopamine injection into the globus pallidus. *Brain Res.* 128, 559-568.
5. Morgane, P. J. (1961) Alterations in feeding and drinking behaviour of rats with lesions in globi pallidi. *Am. J. Physiol.* 204: 420.
6. Nakano, Y., Oomura, Y., Lénárd, L., Nishino, H., Aou, S., Yamamoto, T. and Aoyagi, K. (1986) Feeding-related activity of glucose- and morphine-sensitive neurons in the monkey amygdala. *Brain Res.* 399, 167-172.
7. Nishino, H., Ono, T., Muramoto, K., Fukuda, M. and Sasaki, K. (1984): Caudate, pallidal and nigral unit activity during sensory integration and motor execution in bar press feeding behaviour of monkey. Modulation of sensorimotor activity during alterations in behavioral states, pp. 151-164.

DYNAMIC PHENOMENA IN THE OLFACTORY BULB

T. Gröbler and P. Érdi ^x

Biophysics Group, KFKI Research Institute for Particle and Nuclear Physics of the
Hungarian Academy of Sciences, H-1525 Budapest P.O. Box 49, Hungary

^x This work have been done on leave at the Microelectronics Laboratory,
Tampere University of Technology, Finland

Summary: A mathematical model of the olfactory bulb is presented to study the dynamics of the bulbar information processing. A two level model is adopted to describe both neural activity and synaptic modifiability. The model takes explicitly into account the existence of lateral interactions in the mitral layer, and the synaptic modifiability of these connections. A series of bifurcation phenomena among fix points, limit cycle and strange attractors have been demonstrated. Chaos occurred only in the case of excitatory lateral connections. Coexistence between oscillation and chaos, and synaptic modification induced transition have also been found.

The model attempts to demonstrate the associative memory character of the olfactory bulb. Odour qualities are coded in distributed spatial amplitude patterns. Differential equations for the mitral and granule cell activities have been supplemented by a continuous-time local learning rule. A nonlinear forgetting term and a selective decreasing term is added to the Hebbian learning rule. A learned odour can be recalled by a subset of the pattern. There is a strict restriction on the parameters: only those values can be admitted which generate physiologically justified activity signals.

BIFURCATION SEQUENCES, COEXISTENCE OF PERIODICITY AND CHAOS, SYNAPTIC MODIFICATION INDUCED TRANSITIONS

Many details of different aspects of olfaction such as the nature of olfactory stimuli, mechanism of reception and of central processing, olfactory coding, learning and memory have extensively been studied (for a recent monograph see [1]), still the mechanism of information processing in the olfactory system is not well-known. Neurodynamic approach offers a conceptual framework to unify concepts and experimental data coming from different field of neurobiology such as anatomy, neurochemistry, physiology and behavioral studies.

Models of the first relay station of the olfactory system, i.e. the olfactory bulb (OB) have been studied earlier [2-7]. Mechanism of pattern generation and of pattern recognition in the OB have to be explained in terms of dynamic system theory, as it was suggested by Freeman and his school [2, 3, 7]. Decision states during odour discrimination have been assumed as cycles (as opposed to point attractors). The excitatory-inhibitory interactions between mitral and granule cell populations (with fixed synaptic weights) have been suggested as anatomical and physiological substrates providing oscillatory activity [Li-Hopfield model: 5, 6].

A new mathematical model of the olfactory bulb (OB) has been set up and its dynamic properties are studied, mostly numerically, to have a more detailed view on the dynamic aspects of the olfactory bulb. The model is based on the Li-Hopfield model, but it takes explicitly into account (i) the lateral interactions in the mitral layer, (ii) the modifiability of certain synapses.

Because of the lack of firm data on the physiological nature of the lateral interactions in the mitral layer, the effects of both lateral inhibition and excitation on the dynamic behaviour have been studied. In the first part of our simulations, the strengths of lateral connections are taken as constant over time, and can be varied through a control parameter (c). The sign of c determines whether the lateral connections are interpreted as excitatory or inhibitory synapses.

The underlying differential equations for the mitral and granule cell activities are respectively as follows:

$$\dot{m}_i(t) = -am_i(t) - b \sum_{j=1}^N G_{ij} f(g_j(t)) + c \sum_{j=1}^N L_{ij} f(m_j(t)) + I$$

$$\dot{g}_i(t) = -dg(t) + e \sum_{j=1}^N M_{ij} f(m_j(t)) + J$$

where f is a nonlinear (sigmoid) function, a, b, d, e are positive constants, I and J are the receptor and cortical inputs, respectively.

Simulation experiments show the occurrence of a series of bifurcation phenomena: Hopf bifurcation, transition from fix point to large amplitude oscillation, infinite-period bifurcation, period doubling bifurcation to chaos. The qualitative character of the attractors in the function of the control parameter has been determined. It is remarkable to observe that chaos is only generated if lateral excitation is assumed. (The simulations have been evaluated at the individual mitral cell level, but "synthetic EEG curves" based on granule cell activities have also been considered).

In another series of simulation experiments, the effect of continuous time

synaptic modification on the qualitative dynamics has been studied. Here the excitatory mitral-mitral interactions are modified by the Hebb rule (see e.g. [8]), while the activity equations are the same as previously. Adopting a moderately slow learning process, transitions between different regimes have been demonstrated. In particular, a continuous time transition from oscillation to chaos is shown.

In part I, constant sensory input is considered enabling to study the details of activity dynamics. To have a more realistic model, time-varying input ("sniff cycle") is also taken into account. Furthermore, a more realistic learning rule has been used containing a nonlinear forgetting term, and a selective decreasing term. This model is capable of behaving as a simple associative memory (see next section).

MODEL FOR A SIMPLE ASSOCIATIVE MEMORY

Albeit a lot of work have been done on models of associative memory of artificial neural networks, there are only very few anatomically and physiologically justified memory models [4]. Real neural networks can have recurrent anatomical structure, both excitatory and inhibitory populations can be found, and their interactions might imply the occurrence of periodic and chaotic neural activity.

Olfactory bulb (OB) is one of the newest "working horse" of theoretical neurobiology to study the mechanism of information processing in "real" neural network models. In part II, an extension of the model introduced in Part I is given to demonstrate the capability of OB to learn and recognize odour patterns.

In Section 1, the input was assumed to be constant over time and the synaptic weights were only modified by the original Hebb rule. Here the temporal character of the sensory input ("sniff cycle") is also taken into account. From technical point of view, the input can be interpreted as a nonautonomous term in the right hand side of the otherwise autonomous system of differential equations. Nonautonomous systems do not generally have attractors, therefore the notion of "computation with attractor" cannot be adopted. The substitution of a set of fix point attractors by periodic attractors does not provide a proper analogy to generalize the notion of associative memory. The collapse of initial conditions and inputs in some degenerate cases were essentially utilized by Baird [7]. He also introduced a "one-shot" learning rule to modify synaptic strengths.

In our model (i) odour qualities are coded in spatial amplitude patterns; (ii) the representation of the qualities has a distributive character; (iii) lower stimulus intensity implies the stimulation of less "receptor" cells; (iv) learning is considered as a

continuous temporal process; (v) the Hebb rule is supplemented by a nonlinear forgetting term and a selective decreasing term. Neurobiologically motivated constraints not only preform the possible structure of associative models but also give strict restrictions for the form of the mitral and granule cell activity responses. Only those parameters of the learning process can be accepted which provide physiologically well-defined responses (bursts) (Figure 1).

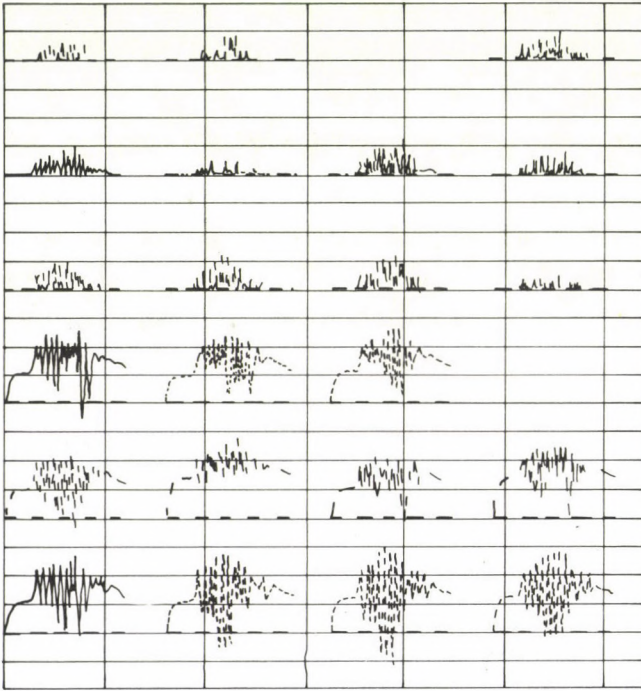


Fig. 1: Burst activities of the model mitral (top) and granule (bottom) cells.

More specifically, the synaptic weights of the lateral connections among mitral cells were modified by the learning rule:

$$L_{ij}(t) = -k_1 L_{ij}^2(t) + k_2 f(m_i(t)) f(m_j(t)) - k_3 L_{ij}(t) (f(m_i(t)) - f(m_j(t)))^2$$

The quality and intensity of the odour are coded by the amplitude-pattern of the input over the bulb. In our model, the values 1 and 0 are assigned to high and low amplitudes, respectively. Thus, a complete odour pattern corresponds to the set of mitral cells, potentially receiving input during the sniff. In reality, however, only subsets of this set are stimulated.

In the learning stage, a random sequence of such incomplete patterns is presented as input. The specifically constructed learning rule with proper parameter values insures the separation of the synaptic weights, without violating their boundedness and sign-preserving property. In the recall stage, incomplete inputs are recognized by the retrieval of the complete odour pattern, while mitral and EEG temporal patterns exhibit physiologically justified burst activities.

ACKNOWLEDGEMENTS

Many discussion with Prof. Kimmo Kaski and Dr. György Barna are highly appreciated.

REFERENCES

1. Halász, N. (1990) The Vertebrate Olfactory System: Chemical Neuroanatomy, Function and Development. Akadémiai Kiadó, Budapest.
2. Freeman, W.J. and Skarda, Ch.A. (1985) Spatial EEG Patterns, Non-Linear Dynamics and Perception: The Neo-Sherringtonian View, *Brain Res. Rev.* 10, 147-175.
3. Baird, B. (1986) Nonlinear Dynamics of Pattern Formation and Pattern Recognition in the Rabbit Olfactory Bulb, *Physica* 22D, 150-175.
4. Haberly, L.B. and Bower, J.M. (1989) Olfactory Cortex: Model Circuit for Study of Associative Memory. *Trends in Neurosciences* 12, 258-264.
5. Li, Z. and Hopfield, J.J. (1989) Modeling the Olfactory Bulb and its Neural Oscillatory Processings, *Biol. Cybernetics* 12, 349-392.
6. Li, Z. (1990) A model of Olfactory Adaptation and Sensitivity Enhancement in the Olfactory Bulb, *Biol. Cybernetics* 62, 349-361.
7. Baird, B. (1990) Bifurcation and Category Learning in Network Models of Oscillating Cortex, *Physica* 42D, 365-384.
8. Skarda, Ch. and Freeman, W.J. (1987) How Brains Make Chaos in Order to Make Sense of the World, *Behav. Brain. Sci.* 10, 161-195.

HUNGER- AND SATIETY-RELATED CHANGES OF AMYGDALOID CATECHOLAMINES: A MICRODIALYTIC STUDY IN FREELY MOVING RATS

A. Hajnal, I. Ábrahám, I. Vida, Z. Karádi, and L. Lénárd

University of Pécs, School of Medicine, Institute of Physiology,
H-7643 Pécs, Szigeti u. 12, Hungary

Key words: food deprivation, glucose, insulin, catecholamines, amygdala, microdialysis, HPLC, freely moving rats

The amygdaloid complex (AMY), similarly to the 'classic' feeding centres in the hypothalamus, has a dual catecholamine (CA) innervation: its dopamine (DA) input originates from neurons located in the tegmental DA cell groups (A8 and A10) and the noradrenaline (NA) fibers ascend from the locus coeruleus and the medullary clusters of NA cells [1, 5]. Our previous experiments with bilateral 6-hydroxydopamine injections into the central or basolateral AMY showed that a relative DA deficit caused weight loss and hypophagia, whereas hyperphagia occurred after a relative decrease of NA level [3, 4].

The actual alterations of extra- and intracellular CAs were previously detected by less sensitive fluorimetric method [2]. In the present study, therefore, the chronic microdialysis-HPLC technique was employed in freely moving rats to investigate whether food deprivation or satiation elicit specific changes of the extracellular level of amygdaloid CAs and their metabolites. In a further series of experiments we aimed to define the similarities between the amygdaloid CA release in relation to natural feeding states or chemical manipulations with insulin or glucose applied intraperitoneally.

Seven adult CFY (LATI, Gödöllő, Hungary) male rats weighing 320-340 g were used. Microdialysis probes were implanted unilaterally into the central nucleus of AMY (coordinates according to Pellegrino and Cushman: A:5.2; L:4.3 V:7.8 from the dura).

Probes (active length of the polycarbonate membrane, 1 mm; 5 kDa MW cut-off) were attached to the skull with dental cement and acrylic. A constant flow ($2 \mu\text{l}/\text{min}$) of the perfusion media (Ringer's solution) through the dialysis setup was ensured. Inlet and outlet of the probes were run through a liquid swivel to allow free movement of the animals. Sampling (20 min sequential collections) started 24 hr after the probes had been implanted. Sample analysis, by means of an HPLC equipment with electrochemical detection was performed immediately after each collection period.

Chromatograms were stored and analysed using a specific software package designed in our laboratory for IBM PC/AT compatible microcomputers. The mean concentrations of substances were (in a self-controlled manner) calculated for the samples taken before, during and after treatments. At the end of the experiments histological analysis was performed with cresyl violet staining of frozen sections for verification of the probe's placement as well as for visualization of glial reaction.

Food and water deprivation resulted in a significant decline in the extracellular levels of amygdaloid NA, L-DOPA, DOPAC, and HVA in freely moving rats. The NA and metabolite values decreased to 20-30 % of the baseline level within the first 12 hrs after food withdrawal. The concentration of DOPAC continued to decline towards the detection limit of our system. By contrast, a sharp increase (about 500 %) was found in the DA levels from the beginning of the 24th hr. After attaining this peak value, DA levels declined to a stable low value (20-25 % of baseline). No significant change of 5-HIAA levels was observed during deprivation. The above changes were all reversible, extreme values recovered to the initial levels within 6 hrs after refeeding.

Similar response patterns were induced by i.p. injection of insulin (Insulin-s-Richter, Hungary, 20 IU/kg). The short-lasting (4 hr) duration of the biochemical responses in the AMY was in correlation with the time-course of decline of simultaneously measured blood glucose levels.

The effect of peripherally administered glucose (10 ml, 20%, i.p.) on the amygdaloid CAs and their metabolites in deprived animals was similar to the consequences of the natural satiation: the initially detected low concentrations rapidly increased back to the original baseline values. The dynamics of these changes in the AMY was closely related to the alteration of blood sugar levels seen after glucose injection. Duration of changes of the CA metabolite levels, however, was longer (about 300 min) than the duration of the hyperglycemic period itself.

The results demonstrate that the natural hunger and satiety states were accompanied by opposite changes of the extracellular levels of amygdaloid CAs and

their metabolites. These findings confirmed the results of our previous neurochemical lesion studies [2, 3] that demonstrated differential changes in food intake and body weight depending on actual shifts of amygdaloid DA/NA ratios.

Since similar transient neurotransmitter alterations were observed, in concert with changes of the blood glucose concentration, after peripheral glucose or insulin administrations, the existence of a basic metabolic regulation is further supported at the neuronal level. To elucidate the underlying neurochemical mechanism of these feeding-related extracellular metabolite responses in the AMY, further behavioral and neurochemical experiments are needed. The chronic microdialysis combined with other techniques appears to be a useful tool for these further studies.

ACKNOWLEDGEMENTS

This work was supported by the Hungarian National Research Fund (OTKA/1404; L. Lénárd) and the Ministry of People's Welfare of Hungary (ETT T-565/1990; L. Lénárd). A. Hajnal was supported by the Foundation for the Hungarian Science, Hungarian Credit Bank.

REFERENCES

1. Fallon, J. H., Koziell, D. A. and Moore, R. Y. J. (1978) Catecholamine innervation of the basal forebrain. II. Amygdala, suprarhinal cortex and entorhinal cortex. *J. Comp. Neurol.* 180, 509-532.
2. Hahn, Z. (1980) Centrifugal microfiltration: A simple way to enhance the sensitivity of the classical aluminium oxide adsorption of fluorimetric catecholamine determination. *J. Biochem. Biophys. Meth.* 2, 163-169.
3. Lénárd, L. and Hahn, Z. (1982) Amygdalar noradrenergic and dopaminergic mechanism in the regulation of hunger and thirst-motivated behaviour. *Brain Res.* 233: 115-132.
4. Lénárd, L., Hahn, Z. and Karádi, Z. (1982) Body weight changes after neurochemical manipulations of lateral amygdala: noradrenergic and dopaminergic mechanism. *Brain Res.* 249, 95-101.
5. Lindvall, O. and Björklund, A. (1974) The organization of the ascending catecholamine neuron system in the rat brain. *Acta Physiol. Scand.* [Supp 1.] 412: 1-48.

LOCAL AND DISTANT EFFECTS OF AMYGDALOID KAINATE LESIONS IN THE RAT: A SILVER IMPREGNATION STUDY

A. Hajnal, A. Czurkó, Z. Karádi and L. Lénárd

University of Pécs, School of Medicine, Institute of Physiology,
H-7643 Pécs, Szigeti u. 12, Hungary

Key words: kainic acid, microiontophoresis, amygdala, hippocampus, 'collapsed' state of neuron, silver impregnation

Kainic acid (KA) is a widely used powerful excitotoxin to induce neuron specific lesions in different brain structures. Due to its high excitatory and diffusion capabilities, however, it usually causes extensive brain destruction: distant lesions from the site of injection were found and electrical seizure activities were also recorded [1]. Despite the abundance of relevant data, little is known yet about the pathomorphological nature and time-course of distant effects of the KA lesions.

In the present experiments, therefore, both 'conventional' light microscopic staining and silver impregnation methods were used to determine the extent and dynamics of local and distant damages produced by microiontophoretic administration of KA into the amygdala (AMY). For demonstration of affected, so-called 'collapsed' ('dark', 'contracted', etc.) neurons - that appear as acute or delayed consequences of various pathological conditions including cerebral ischemia, brain injury, pronounced changes in metabolic status (e.g. hypoglycemia), excessive stimulation, status epilepticus, deafferentation and poisoning with various agents (e.g. 6-hydroxydopamine, colchicine, hyperbaric oxygen and KA [3], etc.) - a modification of a Golgi-like argyrophil III physical developing procedure according to Gallyas et al. was employed [2].

Forty two adult CFY male rats weighing 290-320 g were used. Eighteen animals served as sham-operated controls. Twelve of them were operated with micropipettes filled with isotonic saline to demonstrate the electric and/or mechanic effects of the

iontophoresis. Small holes in the skull (3 mm in dia.) were drilled in 6 rats. Three additional rats served as intact controls. Unilateral lesions of the central part of the AMY were carried out under ketamine anaesthesia. KA was administrated iontophoretically by means of glass micropipettes. Parameters were as follows: concentration of KA, 80 mMol; tip diameter, 30 μm ; current, 10 μA for 5 min. At the appropriate survival time (0., 6., 12., 24., 48. hr and 10., 15. day), animals were deeply anesthetized and perfused according to Gallyas et al. [2]. The brains were removed 24 hr later and immersed in the same fixative for at least 1 week. The brains were frozen and cut into 60 μm sections. Every 12th section was stained by the silver impregnation method for 'collapsed' neurons [2]. Adjacent sections were stained with toluidine blue.

In intact control brains, no cell bodies, axons or dendrites of any neuron type were stained by silver impregnation. In other control brains, only neurons near the cortical surface where the skull was exposed and around the tracks of micropipettes were stained. There was no significant difference in number of collapsed neurons between controls with or without current application. By contrast, argyrophilic cells appeared in the AMY immediately after the KA lesions. The extent of silver stained area in the AMY was maximal at the 6th postoperative hr. During the next 6 hr, the region of degeneration had spread rostrally and laterally to involve the claustrum and the pyriform cortex. Later, 24 and 48 hr after the surgery, decreasing number of argyrophilic neurons and increasing amount of silver granular deposits or argyrophilic debris were found in the target area. In these early postoperative stages, amygdaloid cells appeared to be intact in the toluidine blue-stained material. Neural degeneration and reactive gliosis started by the 24th hr after the intervention. In two cases, collapsed neurons were observed in the ipsilateral septal area 12 hr after the lesion. Four distant regions were found to be especially vulnerable to effect of amygdaloid KA lesions: (1) CA1, CA3 and CA4 areas of the hippocampus (HPC); (2) fascia dentata (FD); (3) entorhinal cortex (Ent), and (4) subiculum (S). 'Collapsed' neurons in these regions appeared in two waves: first, 6 hr after the surgery numerous pyramidal cells were visible at the ipsilateral CA3 and CA4 regions and in the FD; second, huge amount of 'collapsed' neurons were found bilaterally in the Ent, S, FD and CA1 HPC regions by the 12th postlesion hr. The amount of affected neurons in these above distant regions reached its maximum by the 24th hr. 'Collapsed' neurons, however, were not found 10 and 15 days after the lesions. By contrast, cell loss or degenerative signs were not seen at all by toluidine blue staining in any distant structures of identical brains at any survival times.

Our results showed that (1) KA microlesions affected neurons not only locally in the AMY but also in broad areas of the rat brain. (2) The regions most vulnerable to KA were the hippocampal formation, S and Ent, but the extent and time course of the degeneration varied. (3) The spatial and temporal distribution of neuronal degeneration processes could be revealed by the silver impregnation technique for 'collapsed' neurons. (4) The conventional light microscopic staining method appeared not to be sensitive enough to demonstrate neuronal damages in the early postoperative period and especially in distant brain regions.

Although details of cellular and subcellular mechanism responsible for development of the 'collapsed' state are not known yet, the specific silver impregnation method proved to be a sensitive, useful tool for fine histological analyses of consequences of various physiological interventions in the rat brain.

ACKNOWLEDGEMENTS

This work was supported by the Hungarian National Research Found (OTKA/1404; L. Lénárd) and the Ministry of People's Welfare of Hungary (ETT/ T-565/1990; L. Lénárd). A. Hajnal was supported by the Foundation for the Hungarian Science, Hungarian Credit Bank.

REFERENCES

1. Ben-Ary, Y., Tremblay, E., Otterson, O.P., and Meldrum, B.S. (1980) The role of epileptic activity in hippocampal and "remote" cerebral lesions induced by kainic acid. *Brain Res.* 191, 79-97.
2. Gallyas, F., Güldner, F.H., Zoltay, G. and Wolff, J.R. (1990) Golgi-like demonstration of "dark" neurons with an argyrophil III method for experimental neuropathology. *Acta Neuropathol. (Berl.)* 79, 620-628.
3. Sperk, G., Lassmann, H., Baran, H., Kish, S.J., Seitelberger, F. and Hornykiewicz, O. (1983) Kainic acid induced seizures: neurochemical and histopathological changes. *Neuroscience* 10, 1301-1315.

DRUGS ACTING AT CALCIUM CHANNELS CAN INFLUENCE THE HYPNOTIC-ANESTHETIC EFFECT OF DEXMEDETOMIDINE

Gy. Horváth¹, M. Kovács², M. Szikszay² and Gy. Benedek²

¹Department of Physiology, and ²Division of Health Visitors,
Albert Szent-Györgyi Medical University, H-6720 Szeged, Dóm tér 10, Hungary

Summary: The effects of chronic administration of the calcium channel antagonist verapamil on the anesthetic effects of a novel specific α_2 -receptor agonist (dexmedetomidine) were studied in rats. It is presumed that this agonist acts on both pre- and postsynaptic α_2 -adrenoceptors. To determine whether the central postsynaptic receptors are involved in the anesthetic interactions between these drugs, rats were treated with DSP-4 to deplete endogenous norepinephrine. Loss of the righting reflex was used to determine the presence of anesthesia and the duration of hypnosis. Chronic treatment with verapamil (1 or 5 mg/kg) significantly increased the duration of the hypnotic-anesthetic effect of dexmedetomidine. Neither acute treatment with verapamil nor the calcium channel agonist BAY K 8644 (0.5 or 1 mg/kg) influenced the dexmedetomidine-induced hypnosis after DSP-4 treatment. The results seem to support the idea that the hypnotic action of dexmedetomidine can be affected via modulation of the transmembraneous calcium movement in the central nervous system. Further, the data on catecholamine-depleted rats with DSP-4 suggest that the interactions between verapamil and dexmedetomidine may be mediated through presynaptic or homoreceptors on noradrenergic neurons.

INTRODUCTION

Calcium channel antagonists are employed widely in the treatment of angina pectoris, hypertension and other cardiovascular disorders. With such widespread use, the possibility exists of drug interactions between calcium channel antagonists and many concurrently administered drugs. Given the important role that calcium plays within muscle cells, at the neuromuscular junction, and in the central nervous system, reports of drug interactions with calcium channel antagonists and agents applied during

anesthesia are not surprising. There is strong experimental evidence that calcium channel blockers influence various neuronal processes, including analgesia and anesthesia [5, 19]. Calcium channel antagonists have been reported to increase the anesthetic potency of a variety of structurally dissimilar drugs (pentobarbitone, ethanol, argon, nitrous oxide and midazolam) in rodents, although calcium channel antagonists do not themselves produce a state of anesthesia [7, 8, 9]. The mechanisms by which calcium agonists and antagonists influence the effects of anesthetic drugs are unclear. Dolin and Little suggest that anesthetic agents may alter the state of the calcium channels. Alterations in the state of the calcium channels by anesthetic agents allow the calcium blockers to act [7].

There has recently been substantial interest in the anesthetic properties of α_2 -adrenergic agonists. Numerous studies have demonstrated that α_2 -adrenergic agonists promote anesthesia, while the centrally acting α_2 -adrenergic antagonists (e.g. atipazemole and idazoxan) dose-dependently attenuate it [10, 14, 16]. Dexmedetomidine, a novel selective α_2 -agonist, has been shown to reduce anesthetic requirements by 90% in dogs and rats [25, 26, 27, 28]. In human studies, it has been found that dexmedetomidine reduces the anesthetic requirements without adverse effects, and inhibits harmful sympathetic reflexes during intubation [1, 4]. We have demonstrated previously that the anesthetic effects of the α_2 -adrenergic agonists are increased by acute administration of a calcium channel antagonist, verapamil, and decreased by a calcium channel agonist, BAY K 8644 [17, 18].

Since a number of patients undergo anesthesia after chronic calcium channel antagonist treatment, it seemed worthwhile to investigate the alterations in the anesthetic potency of an α_2 -adrenergic agonist after chronic verapamil treatment. The exact mechanism of the hypnotic-anesthetic action of dexmedetomidine is unknown, but it is presumed to act on both pre- and postsynaptic α_2 -adrenoceptors in the central nervous system [14, 26, 27]. To determine whether the central postsynaptic receptors are involved in the anesthetic interactions between the above drugs, rats were treated with DSP-4 to deplete endogenous norepinephrine.

MATERIALS AND METHODS

Male Wistar rats weighing 150-300 g were used. They were kept on a 12-h light:12-h dark cycle, with food and water ad libitum. All experiments were carried out at the same time of the day (8.00-13.00) to exclude diurnal variations in pharmacological effects. Each rat was tested only once.

Loss of the righting reflex was used to determine the presence of anesthesia;

its length in minutes is referred to as the duration of the hypnotic-anesthetic effect. This technique is widely used for assessment of anesthesia in rodents, and there has been good agreement between various papers on general anesthetics [22]. Hypnosis was established when an animal could be placed on its back without righting itself. The duration of hypnosis is reported in minutes, as mean \pm SEM. Data were analysed for statistical significance by using one-way analysis of variance. Probability less than 0.05 was considered significant. Post hoc comparisons were made by Student's *t* test.

Drug solutions were made up immediately prior to their injection and were administered by the intraperitoneal (ip) route. The only exception was verapamil, which was injected subcutaneously. Injection volumes were adjusted to 2 ml/kg in all instances. Dexmedetomidine HCl was a gift from Farnos-Group Ltd. (Turku, Finland), verapamil HCl was purchased from Orion (Helsinki, Finland) and BAY K 8644 was a gift from Bayer AG (Leverkusen, FRG). DSP-4 (N-2-chloroethyl-N-ethyl-2-bromobenzylamine hydrochloride) was a generous gift from Astra Research Centre AB (Södertälje, Sweden).

In the first experiment, the rats were treated randomly according to one of the following protocols: controls received vehicle; experimental animals were injected with verapamil (1 and 5 mg/kg twice a day). These injections were given for 2 weeks. On the 15th day, dexmedetomidine (200 μ g/kg) was given.

In the second experiment, DSP-4, 50 mg/kg ip, was used to deplete endogenous norepinephrine in the central nervous system. Ten days later, the effects of verapamil (0.25, 1 or 2.5 mg/kg) or BAY K 8644 (0.5 or 1 mg/kg) on dexmedetomidine anesthesia (150 or 200 μ g/kg) were studied.

The experimental protocols were approved by the Animal Investigation Committee of Albert Szent-Györgyi Medical University.

RESULTS

Chronic verapamil treatment

Pretreatment with 1 or 5 mg/kg verapamil significantly increased the duration of the hypnotic-anesthetic effect of dexmedetomidine ($F(2,15)=4.89$, $p<0.05$ Fig. 1) from 128.3 ± 19.63 min to 155.4 ± 18.70 min or 196.1 ± 10.61 min, respectively.

Effects of the DSP-4 pretreatment

The co-administration of verapamil (0.25, 1 or 2.5 mg/kg) with 150 or 200 μ g/kg dexmedetomidine did not increase the anesthetic effect of dexmedetomidine in these animals (Fig. 2). Similarly, BAY K 8644 (0.5 or 1 mg/kg) did not influence dexmedetomidine-induced (150 μ g/kg) hypnosis.

DISCUSSION

There has recently been substantial interest in the anesthetic properties of α_2 -adrenergic agonists. The α_2 -agonists in themselves exert hypnotic-anesthetic action in animals [10, 14, 16, 21]. The centrally acting α_2 -adrenergic antagonists

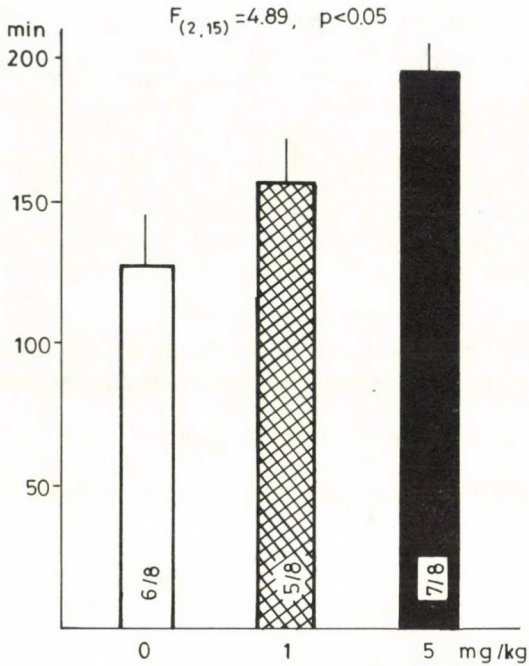


Fig. 1: The effects of chronic verapamil treatment on dexmedetomidine-induced (200 $\mu\text{g}/\text{kg}$) anesthesia. Ordinate: duration of hypnosis in min. Each column represents the mean \pm SEM. The figures in the columns indicate the numbers of rats falling asleep as a ratio of the total.

dose-dependently attenuate the hypnotic-anesthetic action of dexmedetomidine in rats [10]. Our results seem to support the idea that the hypnotic action of dexmedetomidine can be affected by modulation of the transmembraneous calcium movement in the central nervous system. It has recently been demonstrated that α_2 -receptor activation by clonidine decreases the synaptosomal free Ca^{2+} level [2]. All used calcium channel blockers exert their pharmacologic activity against the L channels, one of the three separate voltage sensitive calcium channels (T, L and N) which have been described [24]. The N channels appear to play the predominant role in the calcium-mediated release of transmitters [15, 23, 24]. It has been demonstrated that the α -adrenergic inhibition of sympathetic neurotransmitter release is mediated by modulation of the N calcium channel gating [20]. Clonidine decreases calcium accumulation in the synaptosomes by inhibiting N, but not L voltage-sensitive calcium channels, and the additive effect of an L channel antagonist with that of clonidine has been observed [3, 29]. The present study shows that the hypnotic-anesthetic action of dexmedetomidine is increased not only by acute, but also by chronic pretreatment with the calcium channel antagonist verapamil. It is conceivable that the state of the calcium channels

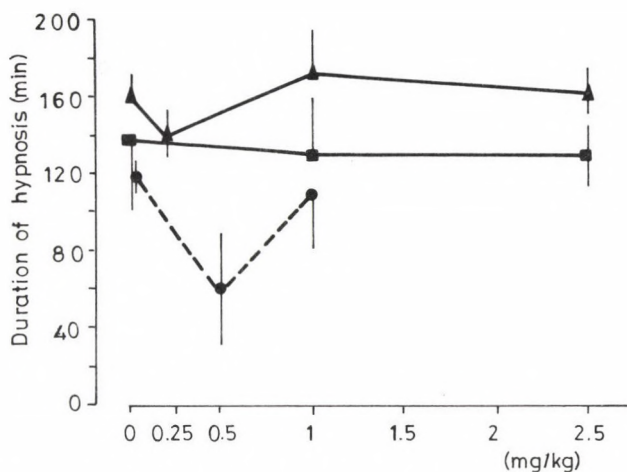


Fig. 2: The effects of different doses of verapamil or Bay K 8644 on dexmedetomidine-induced anesthesia in DSP-4 treated rats.

(Δ - Δ : 200 μ g/kg dexmedetomidine + verapamil, \blacksquare - \blacksquare : 150 μ g/kg dexmedetomidine + verapamil, \circ - \circ : 150 μ g/kg dexmedetomidine + Bay K 8644).

does not undergo adaptive changes after repeated treatment of rats with verapamil.

The noradrenaline-containing nerve cell bodies are prominent in the locus coeruleus and project diffusely throughout the cortex; this nucleus is an important area for the main ascending and descending noradrenergic pathway [6, 12]. DSP-4 treatment produces very marked noradrenaline reductions in the locus coeruleus innervated regions (frontal and occipital cortex, hippocampus, cerebellum and spinal cord) [13]. It appears that the locus coeruleus may play a role in paradoxical sleep and the mechanisms underlying vigilance and behavioral arousal [11].

Data on catecholamine-depleted rats by treatment with DSP-4 from Segal's laboratory, suggest that the mediating mechanism of dexmedetomidine anesthesia must involve sites other than or in addition to the presynaptic α_2 -adrenergic receptors on noradrenergic neurons [26]. Our finding that DSP-4 treatment inhibits the effects of drugs acting at the calcium channels on dexmedetomidine-induced anesthesia suggests that these interactions may be mediated through presynaptic or homoreceptors on noradrenergic neurons.

Overall, these results provide evidence of a potentiated anesthetic effect of

dexmedetomidine after chronic verapamil administration. This may offer a possibility for clinical evaluation of the effects of dexmedetomidine in patients after chronic calcium channel antagonist treatment.

REFERENCES

1. Aantaa, R., Kanto, J., Scheinin, M., Kallio, A. and Scheinin, H. (1990) *Anesthesiology* 73, 230-235.
2. Adamson, P., McWilliam, J.R., Brammer, M.J. and Campbell, I.C. (1987) *Eur. J. Pharmacol.* 142, 261-266.
3. Adamson, P., Xiang, J., Mantzourides, T., Brammar, M.J. and Campbell, I.C. (1989) *Eur. J. Pharmacol.* 174, 63-70.
4. Aho, M., Lehtinen, A-M., Erkola, O. and Kortilla, K. (1990) *Anesth. Analg.* 70, S1-S450.
5. Benedek, G. and Szikszay, M. (1984) *Pharmacol. Res. Commun.* 16, 1009-1018.
6. Dahlström, A. and Fuxe, K. (1964) *Acta Physiol. Scand.* 232, 1-55.
7. Dolin, S.J. and Little, H.J. (1986) *Br. J. Pharmacol.* 88, 909-914.
8. Dolin, S.J. and Little, H.J. (1989) *Anesthesiology* 70, 91-97.
9. Dolin, S.J., Patch, T.L., Rabbani, M., Taberner, P.V. and Little, H.J. (1991) *Neuropharmacology* 30, 217-224.
10. Doze, V.A., Chen, B-X. and Maze, M. (1989) *Anesthesiology* 71, 75-79.
11. Ferrarese, C., Mennini, T., Pecora, N., Pierpaoli, C., Frigo, M., Marzorati, C., Gobbi, M., Bizzi, A., Codegoni, A., Garattini, S. and Frattola, L. (1991) *Neuropharmacology* 30, 1445-1452.
12. Fuxe, K., Hamberger, B. and Hökfelt, T. (1968) *Brain Res.* 8, 125-131.
13. Hallman, H. and Jonsson, G. (1984) *Eur. J. Pharmacol.* 103, 269-278.
14. Harsing, L.G., Kapocsi, J. and Vizi, E.S. (1989) *Pharmacol. Biochem. Behav.* 32, 927-932.
15. Hirning, L.D., Fox, A.P., McCleskey, E.W., Olivera, B.M., Thayer, S.A., Miller, R.J. and Tsien, R.W. (1988) *Science* 239, 57-61.
16. Holman, R.B., Shillito, E.E. and Vogt, M. (1971) *Br. J. Pharmacol.* 43, 685-695.
17. Horvath, Gy., Szikszay, M. and Benedek, Gy. (1992) *Acta. Anaesthesiol. Scand.* 36, 170-174.
18. Horvath, Gy., Szikszay, M. and Benedek, Gy. (1992) *Anesth. Analg.* in press.

19. Kirch, W., Kleinbloesem, C.H. and Belz, G.G. (1990) *Pharmacol. Ther.* 45, 109-136.
20. Lipscombe, D., Kongsamut, S. and Tsien, R.W. (1989) *Nature (London)* 340, 639-642.
21. MacDonald, E., Scheinin, H. and Scheinin, M. (1988) *Eur. J. Pharmacol.* 158, 119-127.
22. Miller, K.W., Paton, W.D.M., Smith, E.B. and Smith, R.A. (1972) *Anesthesiology* 36, 339-351.
23. Miller, R.J. (1987) *Science* 235, 46-52.
24. Nowycky, M.C., Fox, A.P. and Tsien, R.W. (1985) *Nature (London)* 316, 440-443.
25. Scheinin, H., Virtanen, R., MacDonald, E., Lammintausta, R. and Scheinin, M. (1989) *Prog. Neuro-Psychopharmacol. & Biol. Psychiat.* 13, 635-651.
26. Segal, I.S., Vickery, R.G., Walton, J.K., Doze, V.A. and Maze, M. (1988) *Anesthesiology* 69, 818-823.
27. Vickery, R.G., Sheridan, B.C., Segal, I.S. and Maze, M. (1988) *Anesth. Analg.* 67, 611-615.
28. Virtanen, R., Savola, J.-M., Saano, V. and Nyman, L. (1988) *Eur. J. Pharmacol.* 150, 9-14.
29. Xiang, J., Morton, J., Brammer, M.J. and Campbell, I.C. (1990) *J. Neurochem.* 55, 303-310.

THE MATHEMATICAL ANALYSIS OF SPONTANEOUS AND INDUCED POTENTIALS IN NEURAL CULTURES

V. Jánosy¹, K. Krinizs¹, B. Lukács¹, A. Rác¹,
A. Gyévai² and E. Madarász³

¹Central Research Institute for Physics, H-1525 Budapest 114, P.O. Box 49, Hungary;

²Institute of Experimental Medicine, H-1083 Budapest, Szigony u. 43, Hungary and

³Lóránd Eötvös University, H-1088 Budapest, Múzeum krt. 6-8, Hungary

Summary: We compare the power spectra of activities of neural cultures from the cortex and spinal cord of embryonic rat. The measurements were made in a microelectrode culture chamber by non-invasive methods. The data suggest that the fundamental frequencies of cortical and spinal cultures significantly differ, while the general patterns of the spectra are rather similar.

INTRODUCTION

The present paper is a comparison between electric activities of spinal and cortical neural cultures of rat embryos. The compared quantities are some parameters of the Fourier spectra of the activities.

As it is well known, the brain and spinal cord have common phylogenetic origin, and in the *Amphioxus* these two fundamental parts of the central neural system do not yet show serious qualitative differences. Therefore common features may be expected in *Vertebrata*, so the comparison is possible.

MATERIALS AND METHODS

The cell cultures originate from rat embryos, the embryonic age is indicated by EX in days; the cells are first dissociated and then cultured for a time indicated as DIC X in a culture chamber whose bottom contains a number of microelectrodes. The details of the method were published by Jánosy et al., 1990. The nearest neighbour distances of microelectrodes were 60 μm . Generally 5 microelectrodes were used for simultaneous measurement of electric activity of the system. The culture chamber is shown by Fig. 1, while Fig. 2 gives the block diagram of the electronics. All further details can be found in Ref. 2 [Jánosy et al., 1991].

Here we investigate the power spectra of the activities and the delayed cross correlations between electrode pairs. The comparison will be made between the power spectra.

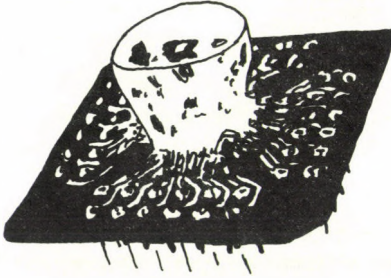


Fig. 1: The culture chamber.

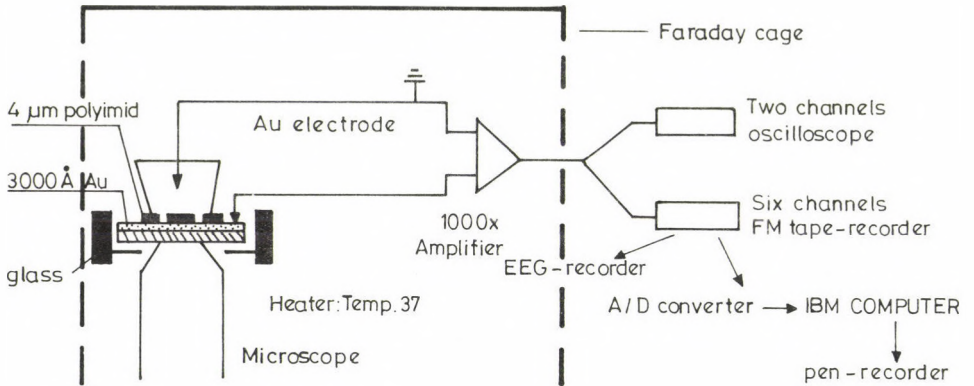


Fig. 2: The block diagram of the measurement.

RESULTS

Fig. 3 is the power spectrum of an E13 DIC 9 spinal culture. The main feature of the spectrum is the sequence of expressed peaks at the integer multiples of a frequency in the neighbourhood of 50 Hz. Of course, this frequency is disturbingly close to the standard AC frequency, however the fifth electrode, which was empty, definitely did not show any peak there. We will return to this question after the cortical samples;

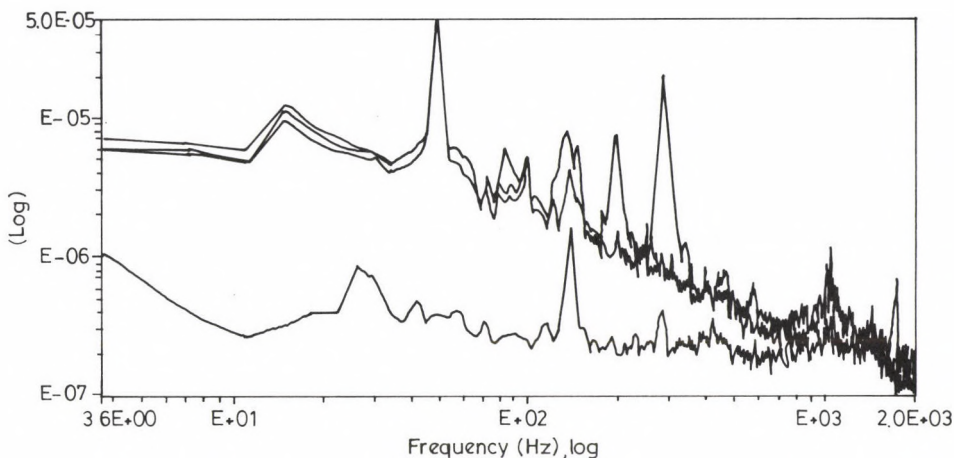


Fig. 3: The power spectrum of an E13 DIC 9 rat spinal sample. One electrode was empty and can be used as measurement for noises.

now for a while let us assume that the peaks are genuine. There is one more characteristic frequency at 13 Hz.

Samples of various other ages discussed in Refs. 3 and 4 showed the same main frequency; different embryonic and culture ages cause differences in the relative weights of higher harmonics. The general rule is that higher maxima become more and more expressed with increasing time in culture.

Fig. 4 is, on the other hand, the power spectrum from an E15 DIC 9 forebrain culture. We note that the same E and DIC ages may belong to different stage of development in spinal and cortical assemblies. First observe the overall similarity to the previous Figure. However now the fundamental frequency is 38 Hz, while the modulating one is 17 Hz. Fig. 5 is a similar culture but of E15 DIC 12 age. The fundamental frequency is again 38 Hz, but the pattern is different, because now the higher harmonics are strongly suppressed and some other (low) maxima appear as well.

Finally, Fig. 6 shows the delayed cross correlation coefficients for 6 pairs of electrodes for the sample whose power spectra were given as Fig. 3. The highest cross correlation is cca. 0.55 at 0 delay time.

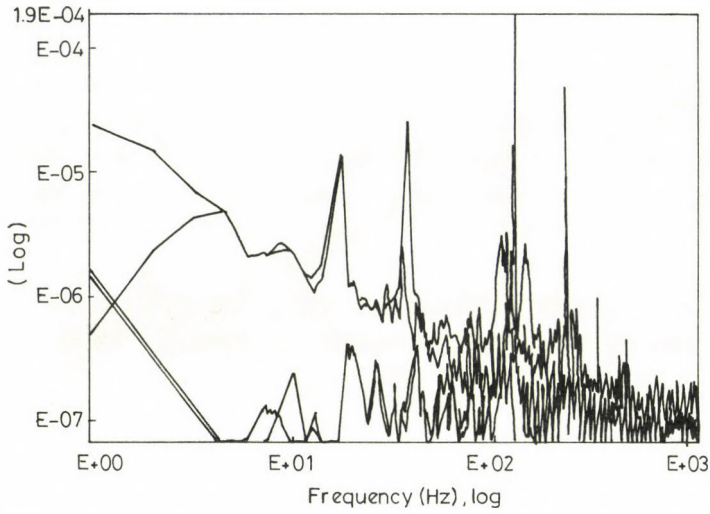


Fig. 4: Power spectrum for an E15 DIC 9 rat cortical sample. The main peak is at 38 Hz.

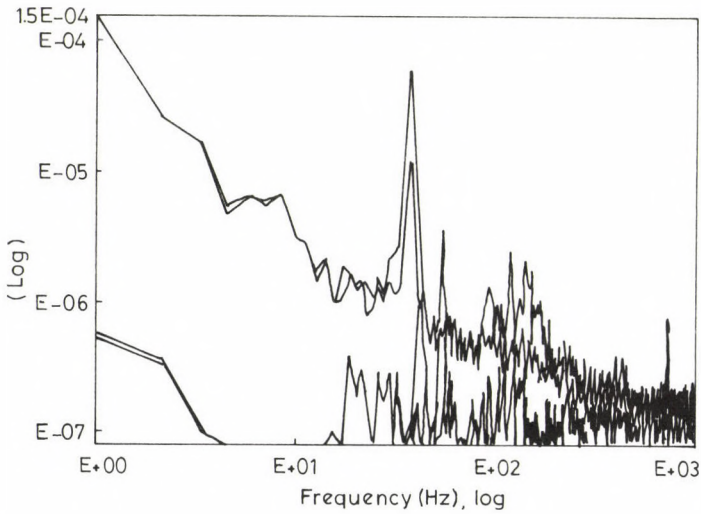


Fig. 5: As Fig. 4, but for E15 DIC 12. The location of the main peak remains the same but the higher harmonics are obscure.

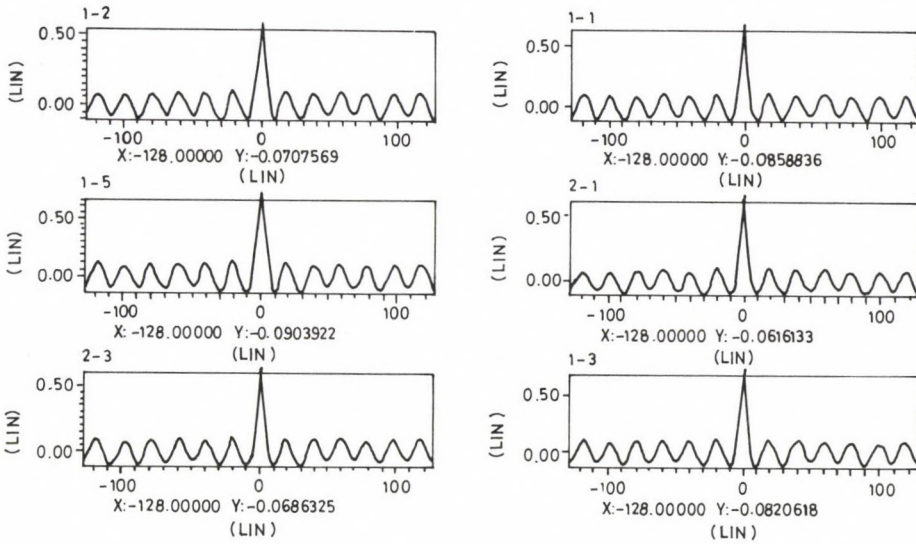


Fig. 6: Delayed cross correlation coefficients for the spinal sample. Note that the maximum is at cca 0 ms, and is ≤ 0.55 .

CONCLUSIONS

Since both spinal and cortical power spectra show the same structure, namely peaks at the multiples of a fundamental frequency + a lower frequency modulation, the 50 Hz peak for spinal samples must correspond to the 38 Hz peak for cortical ones, which latter frequency cannot be in any connection with the standard AC currents. This is the reason why we accept the previous one as well to be genuine.

For both spinal and cortical assemblies the power spectra suggest an almost periodic sequence of individual pulses, with a repetition time 20 or 26 ms (the fundamental frequency) but with a 4-6 ms characteristic time of the changes in the signal (according to the dominant higher harmonics). The timing of repetition suggests the existence of an underlying mechanism.

Cross correlation coefficients show that the electrodes measure at least partly local activities, otherwise the maximum would be near to 1. The 0 delay time in maximum indicates that in these networks there is no preferred signal transmission path.

A definite difference is obtained for fundamental frequencies. The reason is still unknown and further investigations are needed to clear the mechanism behind.

There is also a slight indication for different evolution with aging: increasing DIC age causes more expressed higher harmonics in spinal samples, while in the two available cortical ones the change is the opposite. However, note that the younger cortical sample has the same DIC age as the spinal one. Furthermore it is better not to generalize from two data, so further measurements are needed to draw a solid conclusion in this point.

ACKNOWLEDGEMENT

This lecture shows up new results of a collaboration going on for years. Details and a complete list of collaborators can be found in Refs. 1-4. The present authors acknowledge the previous work of all collaborators mentioned there.

The present work was partly supported by the OTKA grant N°1845.

REFERENCES

1. Jánossy, V. et al., *Acta Biol. Hung.* 41: 289 (1990)
2. Jánossy, V. et al., KFKI-1991-12
3. Jánossy, V. et al., *Proc. 14th Annual Meeting of the European Neurosci. Ass.*, Cambridge 8-12 Sept., 1991.
4. Jánossy, V. et al., *Proc. 39th Ann. ETCS Meeting*, Krakow 16-19 Sept. 1991.

VIMENTIN IMMUNOPOSITIVITY IN THE BRAIN OF THE ADULT FROG

M. Kálmán

1st Department of Anatomy, Semmelweis University of Medicine,
H-1450 Budapest, Tűzoltó u. 58, Hungary

Adult frog brains were processed for immunohistochemical staining against glial fibrillary acidic protein (GFAP) and vimentin. No GFAP immunopositivity was observed. The glial elements which proved to be vimentin-immunopositive, were long, usually radial fibers: no astrocytes could be seen. The vimentin found in mammals in the immature glia can be considered as a usual cytoskeletal protein of mature glia in amphibians.

Glial fibrillary acidic protein (GFAP, an important cytoskeletal protein and immunohistochemical marker of astroglia) shows an immunohistochemical cross-reactivity in the different groups of vertebrates: mammals, birds, reptiles, bony and cartilaginous fishes [1, 2, 3]. The frog brain proved to be immunonegative to GFAP in these experiments, although other authors demonstrated the presence of GFAP in urodeles [4, 5]. The presence and distribution of vimentin, the cytoskeletal protein of the immature glia of mammals [6, 7] has not been investigated in frogs although there are some data on urodeles [5]. The similarity of the outward appearance of immature radial mammalian glia and that of mature amphibian glia, which is also built up by long fibers mainly of ependymal origin [4, 5, 8], urges the investigation of whether vimentin can be the cytoskeletal protein of mature glia in frogs.

Brains of frogs (*Rana esculenta*) were removed after deep cooling and decapitation, and were fixed in 4% paraformaldehyde buffered with 0.1 M phosphate buffer (pH 7.4). After a 48-h fixation and an overnight washing in phosphate buffer the brains were embedded in agar and sectioned by a Vibroslice vibrating microtome (70 μ m thickness). Parallel series of sections were processed for either GFAP or vimentin immunohistochemistry. The monoclonal antibodies against GFAP and vimentin were obtained from Boehringer (Mannheim) or prof. Viklicky (Prague), respectively, and were applied in 1:100 dilution in a phosphate buffer containing 0.5% Triton X-100 at 4°C for 48 hours. The immunoreaction was developed by a Streptavidin-biotin system (Amersham, 1:100, for 1.5 hours at room temperature) and the reaction product was visualized by diaminobenzidin reaction.



Fig. 1: Vimentin-immunopositive radial glial fibers in the frog telencephalon. Bar represents 60 μm .

Concerning GFAP, we failed to demonstrate any immunopositivity in the frog brain although the rat brain slices incubated in the same medium showed a fine reaction. Vimentin-immunopositive long fibers were found throughout the brain but no star-shaped astrocytes could be seen. The vimentin-containing fibers were usually straight, arranged radially to the outer brain surface (Fig. 1). Such a radial pattern characterized the telencephalon, the inferior lobe of hypothalamus, the outer rim of thalamus, the optic tectum and the brain stem. Corresponding to the posterior commissure the radial fibers gathered into a broom-shaped raphe-like structure. In the deeper parts of diencephalon some irregular patterns of sinuous immunopositive fibers could be observed (Fig. 2). Unusually thick straight fibers were also observed in these areas (Fig. 3). Their precise connections remained to be investigated.



Fig. 2: Irregular vimentin-positive fibers in the diencephalon. Bar represents 200 μm .

Considering these results together with the other data published [1-5] we can suppose the vimentin to be a usual cytoskeletal protein of the mature glia in amphibians along with (urodeles) or replacing (frogs) GFAP. The reason can be the similar outward appearance of mature amphibian and immature radial mammalian glia or the persistence of some glial functions (e.g. a possibility of regeneration) in the adult amphibian brain, which functions disappear in the mammalian brain during glial maturation [5, 7].



Fig. 3: Thick immunopositive fibers (arrow) in the diencephalon. Note the difference from the other fibers (arrowheads). Bar represents 200 μm .

REFERENCES

1. Dahl, D. and Bignami, A. (1973) *Brain Res.* 61, 279-293.
2. Dahl, D., Crosby, C. J., Sethi, A. and Bignami, A. (1985) *J. Comp. Neurol.* 239, 75-88.
3. Onteniente, B., Kimura, H. and Maeda, T. (1983) *J. Comp. Neurol.* 215, 427-436.
4. Naujoks-Manteuffel, C. and Roth, G. (1989) *Brain Res.* 487, 397-401.
5. Zamora, A. J. and Mutin, M. (1988) *Neuroscience* 27, 279-288.

6. Dahl, D., Rueger, D. C. and Bignami, A. (1981) *Eur. J. Cell Biol.* 24, 191-196.
7. Pixley, S. R. and de Vellis, J. (1984) *Develop. Brain Res.* 15, 201-209.
8. Korte, G. E. and Rosenbluth, J. (1981) *Anat. Rec.* 199, 267-279.

CALRETININ ONTOGENESIS IN THE DEVELOPING DRG OF CHICKEN

E. Király¹ and M.R. Celio²

¹Department of Anatomy, Albert Szent-Györgyi University, H-6701 Szeged, Kossuth Lajos sgt. 40, Hungary and ²Institute of Histology and General Embryology, University of Fribourg, Rte A. Gockel, CH-1700, Fribourg, Switzerland

Calcium ions play an important role in some critical developmental events of the nervous system such as neurulation and neurite elongation [1, 2]. Evidence is accumulating about the role of different calcium-binding proteins in the maintenance of the normal calcium level, therefore their presence may be of developmental importance. It was recently reported that chicken sensory neurons are predominantly marked by two calcium binding proteins, calbindin D-28k and an other very similar one, calretinin (CR). Calbindin has been shown to be present in sensory neurons of chicken embryo from embryonic day (E), 10 on [4]. The aim of our experiments was to investigate the developmental profile of CR immunoreactivity in chicken sensory ganglia.

METHODS

Eggs were incubated for 5-21 days. Embryos were taken at the end of each incubation day, and immersed in Bouin's fixative and embedded in paraffine. From older embryos after perfusion the lumbosacral spinal ganglia were dissected and stored in the same fixative. Paraffine or free floating sections were processed for immunostaining using a polyclonal antibody raised against calretinin.

RESULTS

By day 9 of embryonic development a few faintly stained large cells appeared in the ventrolateral portion of the ganglia. From E10 on, the number of immuno-positive cells was increased and these cells were scattered throughout the ganglia. Immunoreactivity was detected not only in the cell bodies but also in their processes.

Quantitative measurements revealed a progressive increase in the number of CR-positive ganglion cells with a peak between E10-E13 days. Furthermore, most CR-containing nerve cells appeared to belong to the large and medium sized populations of sensory ganglion neurons.

CONCLUSIONS

In the light of the present results we suppose that the E10-E13 period in chickens could be an important landmark in the development of DRG as it is proved by the followings:

1. The time period corresponds to the termination of cell death and differentiation in both neuronal groups [5].
2. For this time the afferents occupied their innervation field on the periphery [6].
3. The primary afferents show a dense projection in the dorsal horn and monosynaptic reflexes can be elicited [7].
4. The appearance of an other calcium binding-protein, calbindin D-28k takes place also in this developmental stage [4].

Our results suggest that the expression of the calcium binding proteins may be associated with the morpho-functional maturation of a certain population of primary sensory neurons.

REFERENCES

1. Anglister, L., Farber, I.C., Shahar, A. and Grinvald, A. (1982) *Dev. Biol.* 94, 351-365.
2. Cohan, Ch.S., Connor, I.A. and Kater, S.B. (1987) *J. Neurosci.* 7, 3588-3599.
3. Rogers, J.H. (1989) *Neuroscience* 31, 697-709.
4. Philippe, E. and Droz, B. (1988) *Neuroscience* 26, 215-224.
5. Pannese, E. (1974) *Adv. Anat. Embryol. Cell Biol.* 47, 1-97.
6. Honig, M.G. (1982) *J. Physiol.* 330, 175-202.
7. Davis, B.M., Frank, E., Johnson, F.A., Scott, Sh.A. (1989) *J. Comp. Neurol.* 279, 556-566.

REGENERATION OF DORSAL COLUMN PATHWAYS IN PERIPHERAL BYPASS AUTOGRAFTS IMPLANTED IN THE SPINAL CORD OF ADULT RATS

E. Knyihár-Csillik¹, Á. Török², S. Mohtasham¹ and B. Csillik¹

¹Department of Anatomy and ²Department of Anesthesiology,
Albert Szent-Györgyi Medical University, H-6701 Szeged, P.O. Box 512, Hungary

Summary: Sciatic nerves were implanted into the cervical spinal cord as bypass autografts. Nerve fibers growing into the bypass were shown to be authentic dorsal column axons. Ingrowth of axons is dependent of intact basal laminae in the autograft.

Elongation of axons of the central nervous system in peripheral nerve grafts implanted into the spinal cords of adult rats was first reported by Aguayo et al. (1981) and by Benfey and Aguayo (1982). Regenerative propensity in sensory neurons was shown to be enhanced by peripheral axonal injury [Richardson and Verge, 1987]. However, peripheral nerve grafts implanted into the central nervous system are prone to be innervated by alien peripheral sources [Richardson et al., 1980; Bray et al., 1987] and, not less importantly, it has been proposed that viable Schwann cells of full structural and functional value are indispensable for axonal elongation in grafts [Smith and Stevenson, 1988]. Therefore, we addressed the questions whether (a) axons elongating in dorsal column bypass autografts are of dorsal root ganglion origin; (b) whether it is the Schwann cell micro-environment itself or rather the proteoglycane (laminin) content of basement membranes which is decisive in the process of regenerative propensity and (c) whether the bypass autografts represent a suitable model for the estimation of efficiency of various chemical compounds promoting (or retarding) axonal elongation.

Experiments were performed on 28 albino rats, R-Amsterdam (CFY) strain. The sciatic nerve was excised and implanted in the cervical dorsal column, thus establishing an open-end bypass. Survival time of the animals varied between 3 months and 2½ years.

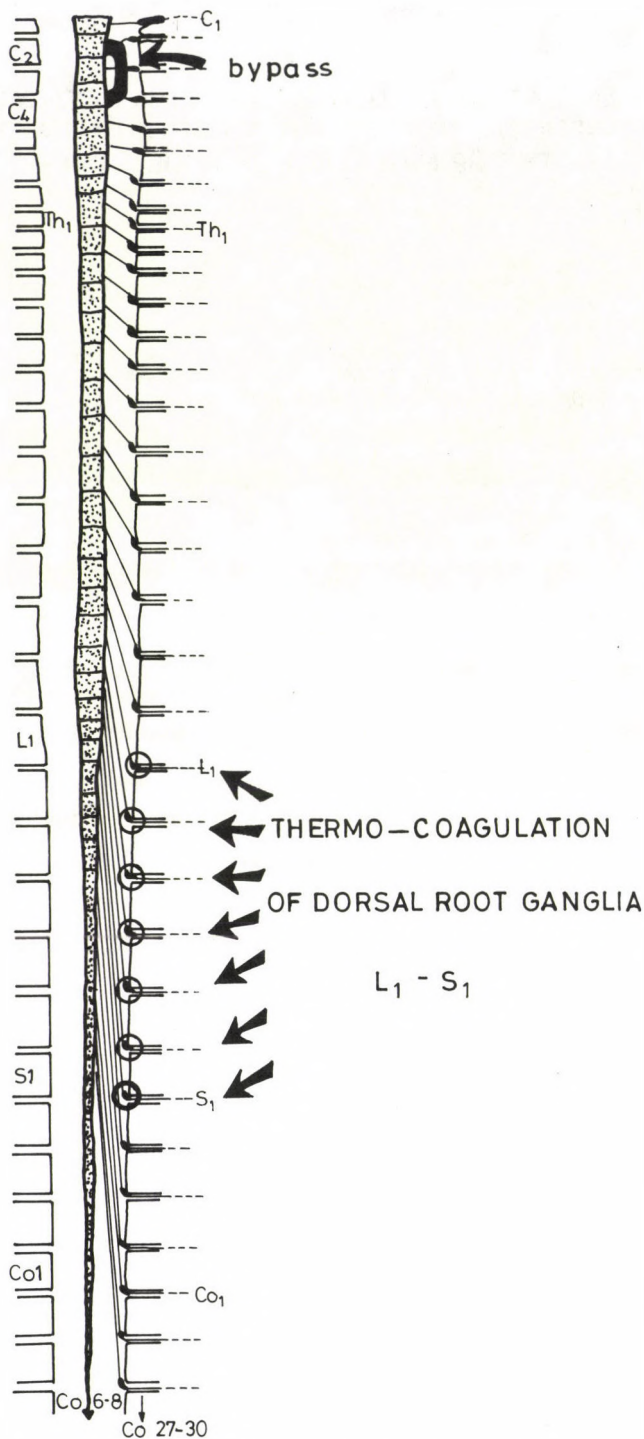


Fig. 1: Schematic drawing of the experimental set-up. The bypass is implanted in the cervical spinal cord. Three months later, dorsal rhizotomy or coagulation of ganglia L₁-S₁ was performed.

Question (a) has been answered by performing dorsal rhizotomies (L2-S1) three months after implanting a sciatic bypass autograft into the cervical dorsal column. Five days after rhizotomy, a considerable number of myelinated axons in the homograft showed Wallerian degeneration proving their dorsal root origin. Similar results were obtained after extrathecal electrocauterization of ipsilateral dorsal root ganglia L1-S1 (Fig. 1). Thus not only the suspicion of alien peripheral sources, but also the presence of postsynaptic dorsal column pathways and cortico-spinal axons, both proceeding under normal conditions, in the rat dorsal column, can be excluded with certainty. More properly, this corollary experiment proves that at least the far great majority of axons in the implant are of dorsal root ganglion origin (Figs. 2, 3).

In addition to experimentally induced Wallerian degeneration of myelinated axons proceeding in the bypass autograft, also cytochemical analysis of the normal autografts supports the notion that these axons are, in reality, extensions of dorsal column pathways. Most of these axons exhibit intense carbonic anhydrase activity, characterizing dorsal column pathways in general [Riley et al., 1984]. Such axons proceeding in the graft, are equipped with axonal growth cones, also exerting carbonic anhydrase activity. A few nerve fibers in the autografts showed acetylcholinesterase activity, also occasionally exhibited by some dorsal column axons. On the other hand, none of the enzymes, neuropeptides or monoamines, characterizing other pathways in the spinal cord, but consistently absent from the dorsal columns, could be detected in the bypass autografts (Table 1).

Table 1

Histochemical characteristics of nerve fibres grown in the graft

Carbonic anhydrase	+
Acetylcholinesterase	(+)
Substance P	-
CGRP	-
VIP	-
NPY	-
Somatostatin	-
Norepinephrine	-
5-HT	-

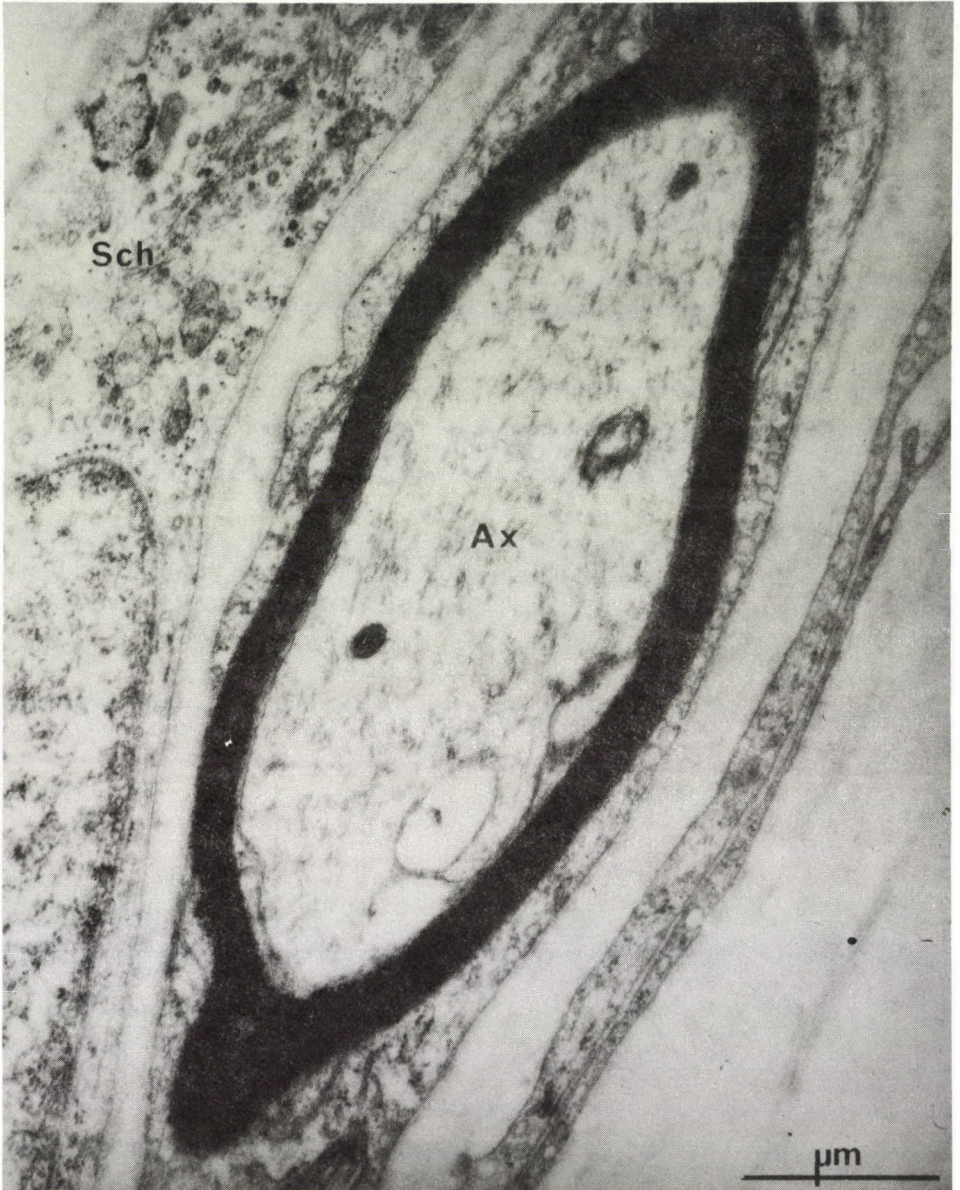


Fig. 2: Electron micrograph of the graft, 4 months after implantation. Note well-preserved, myelinated axons in cross section. Ax, axon; Sch, Schwann cell.

Table 2

Effects of physical treatments on the regenerative propensity

Types of implant	Result (content of graft 1-5 months after implantation)
Normal sciatic nerve (n=13)	Myelinated axons
Frozen (-200°C) sciatic nerve (n=4)	Non-myelinated axons
Heated (+100°C) sciatic nerve	No axons

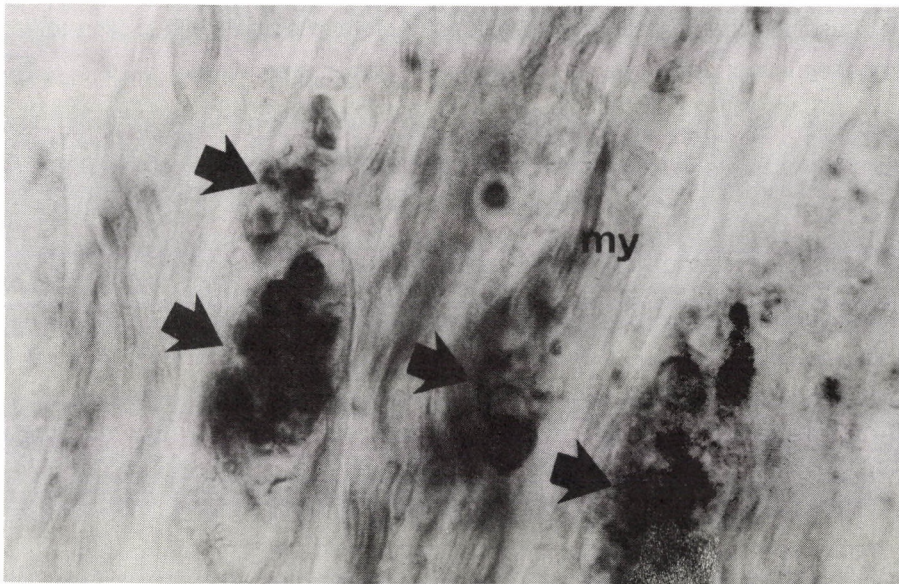


Fig. 3: Wallerian degeneration of myelinated dorsal column axons in the graft, 11 days after dorsal rhizotomy (arrows). Note normal myelinated nerve fibers (my).

Question (b) has been approached by implanting, in addition to native sciatic nerves in control experiments, sciatics which had been frozen in liquid nitrogen and other ones, boiled in isotonic saline. There was no ingrowth of axons to be seen in the heat-treated implants where both the Schwann cells and the laminin type proteoglycans had been destroyed. In contrast, axonal prolongation was observed in the frozen implants; however, these axons lacked myelin sheaths characterizing normal sciatic autografts. Since freezing would damage Schwann cells but would not destroy

laminin deemed essential for axonal growth by numerous authors [Barondes, 1984; Hantaz-Ambroise et al., 1987; David, 1988] it stands for reason to assume that success of regeneration in dorsal root implants depends on the persistence of basal laminae or basement membranes, while a prerequisite for the production of myelin sheaths is the presence of viable Schwann cells (Table 2). These observations, essential for any further clinical trials, are at variance to those of Berry (1982) and Smith and Stevenson (1988), but are consistent with recent studies of Giftchristos and David (1988).

The third question (c) we are studying recently with the aid of the implanted bypass autografts is the promoting or retarding activity of various substances upon the regenerative propensity of dorsal column axons. Though these studies are at the very beginnings at best (Table 3), they clearly prove that the bypass autograft paradigm is a useful model to estimate the efficiency of various treatments aiming to improve regeneration of central nervous pathways in human neurosurgery.

Table 3

Effects of systemic^x or local^{xx} chemical treatments on the regenerative propensity (length of the area occupied by myelinated axons in the graft, 1 month after implantation)

Control (n=3)	12±4 mm
^x Co-ATP, 1 mg/d (n=3)	18±9 mm
^x NGF, 10 µg/d (n=3)	13±5 mm
^{xx} anti-NGF, 20 µg/d (n=1)	6 mm

REFERENCES

1. Abbott, N.J. (1988) *Nature* 332, 490-491.
2. Aguayo, A.J. (1987) In: "Encyclopedia of Neuroscience", ed. G. Adelman, Birkhäuser, Boston, pp. 1040-1043.
3. Aguayo, A.J., David, S. and Bray, G.M. (1984) *J. Exp. Biol.* 95, 231-240.
4. Barnes, C.D. and Worrall, N. (1968) *J. Neurophysiol.* 31, 689-695.
5. Barondes, S.H. (1984) *Science* 223, 1259-1264.

6. Benfey, M. and Aguayo, A.J. (1982) *Nature* 296, 150-152.
7. Berry, M. (1982) *Bibl. Anat.* 23, 1-11.
8. Bray, G.M., Vidal-Sanz, M. and Aguayo, A.J. (1987) In: "Neural Regeneration", eds. F.J. Seil, E. Herbert and B.M. Carlson, *Progr. in Brain Res.* 71, 373-379.
9. Cajal, S.R.Y. (1928) *Degeneration and Regeneration of the Nervous System*. Oxford University Press, London.
10. Csillik, B. and Knyihár-Csillik, E. (1986) *The Protean Gate. Plasticity of the primary nociceptive analyzer*. Akadémiai Kiadó, Budapest.
11. David, S. (1988) *J. Neurocytol.* 17, 131-144.
12. Gristochristos, N. and David, S. (1988) *J. Neurocytol.* 17, 385-397.
13. Hantaz-Ambroise, D., Vigny, M. and Koenig, I. (1987) *J. Neurosci.* 7, 2293-2304.
14. Ide, C., Tohyama, K., Yokota, R., Nitatori, T. and Onodera, S. (1983) *Brain Res.* 288, 61-75.
15. Linzzi, F.J. and Lasek, R.J. (1985) *J. Comp. Neurol.* 232, 456-465.
16. Richardson, P.M. and Verge, V.M.K. (1986) *J. Neurocytol.* 15, 595-617.
17. Richardson, P.M. and Verge, V.M.K. (1987) *Brain Res.* 441, 406-408.
18. Riley, D.A., Ellis, S. and Bain, J.L.W. (1984) *Neuroscience* 13, 189-206.
19. Smith, G.V. and Stevenson, J.A. (1988) *Exp. Brain Res.* 69, 299-306.

THEOREMS SPEAKING FOR THE ASYMMETRY OF ALL ANIMAL BRAINS

E. Lábos

Semmelweis University, Medical School. 1st Dept. of Anatomy, Neurobiology Unit.
H-1450 Budapest, Tűzoltó u. 58, Hungary

Summary: In random graph theory [1, 2, 3, 4] it has been proved that with the increasing size of a graph, the proportion of the non-symmetric graphs increases and this class becomes the dominant one [5, 6, 7, 8] while the number of symmetric cases turns to be 'negligible'. Thus the asymmetry (AS) is the generic property. Since nervous systems are representable by graphs or better with special digraphs, the networks, it follows that the brains are asymmetric in a strong sense according to which all cells are distinguishable from each other alone by their internal connections [6]. Such a consequence holds perfectly only if a random evolution or generation of neural networks is supposed. Thus apparent symmetries have to come from heavily controlled (i.e. non random) ontogenetic processes. At the present time the possible total cellular heterogeneity of the various nervous systems has still unclear functional implications. In small nervous systems the odd [11] number of neurons alone is neither a sufficient nor a necessary condition of the asymmetry in the outlined sense.

INTRODUCTION

It occurs rarely in neurosciences -like elsewhere- that an existing and seemingly important - feature of a given nervous system is supported sufficiently by special theoretical (mathematical) argument. This circumstance justifies the presentation of the present case study as follows.

MATERIALS AND METHODS

Facts originating of the theory of random graph [1, 2, 3, 4] are used which are capable of explaining various existing asymmetries [5, 8, 9] occurring in real nervous systems.

RESULTS

The main result is the application of a class theorems taken from (random) graph theory in order to clarify and even interpret special kinds of asymmetries supposed to occur in every nervous system.

1.1. *Graph and digraph* [10]: It is a pair of two sets: (1) a P set of items called points, vertices and (2) an E set of edges, lines or interconnections corresponding to (directed) pairs of vertices. In short notation: $G = (P, E)$.

1.2. *Symmetry* [8, 9, 11, 12]: A transformation or mapping applied to a set of items. This map keeps at least one property invariant in the resulting, transformed image. Examples are displayed in Fig. 1.

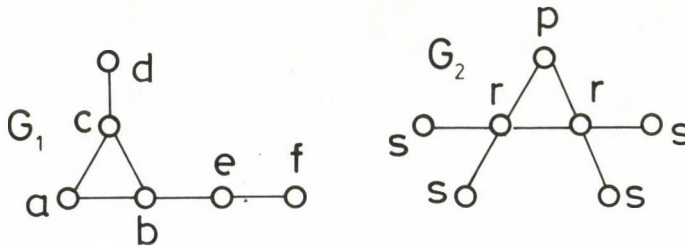


Fig. 1: Two examples of graphs. The G_1 is a non-symmetric (asymmetric). Its automorphism group is trivial (with one permutation only). The graph G_2 is a partially symmetric graph, whose the automorphism group consists of 48 different permutations.

1.3. *Automorphism group (AG) of a graph* [9]: Definition of vertex-isomorphism of graphical items is based on the existence of one-to-one correspondence (a permutation over the vertex set) which preserves adjacencies. Thus G and H are isomorphic if and only if for all (v_i, v_j) or (w_i, w_j) pairs of vertices in G or in H are interconnected by an edge only simultaneously: either both pairs or neither of them are adjacent in this sense.

1.4. *Asymmetric and symmetric graphs* [5, 6]: A graph (tree, directed graph, partially labelled graph, etc.) is called asymmetric if all of their points may be distinguished from each other based alone on the relationship of points determined by interconnections (edges). With other nomenclature a graph (digraph) is called asymmetric if its automorphism group is trivial. Since in the asymmetric case all the points are distinguished from each other without using supplementary markers (colour, number), thus only the identical or trivial permutation is suitable to point out which vertices can be exchanged with other ones and which are not interchangeable. The automorphism group of asymmetric graphs is thus -per definitionem- trivial.

The symmetry of adjacency matrix of the digraphs or graphs does not reflect this group-theoretically founded symmetry [12]. It is something else.

2. The relevant *theorem* of random graph theory. Supposing that the generation of graphs is random with equal probability for all cases. The theorem which is important here in its less formal exposition is as follows: if the number of points (p) in a graph is increased and the different non-labelled graphs are enumerated [14, 15, 16], then the majority of cases proves to be asymmetric. Furthermore as p goes to the infinite then the asymptotic value of distinct graph is essentially identical to the number of asymmetric graphs. Thus [7, 4] the ratio of all labelled graph (L_p) and unlabelled graphs (U_p) is in the following asymptotic relationship holds:

$$U_p \sim L_p/p!$$

No comparably elaborated theorem I know with respect of digraphs. However, attributing directions to edges never destroys graph asymmetry but it may eliminate symmetry. A more detailed elaboration of this generalization is required. Remark that such an approximation becomes valid at relatively large number of points.

3. *The argumentation.* - Neural networks in nervous systems are representable by graphs or better with double labelled digraphs [12]. Thus if a suitable randomness condition was satisfied then the dominance of asymmetric graphs (in the theoretical case) at large size of graph can be used as an argument for the asymmetry of central nervous systems and brains in general. The possible objections might be incorporated in the ontogenesis of brains, if it was strictly deterministic and some control process could block the manifestation of this expected asymmetry. In reality, however, at least in lower animals the individuality of nerve cells is a well founded experience. Problems emerge as soon as 'higher animals' are considered with their huge number of individual neurons. Nevertheless, the bilateral deviation of human and numerous animal brains appears to be well supported facts or can be predicted (!) in advance.

DISCUSSION

1. *Symmetries are more surprising than asymmetries.* - As a consequence of the dominating majority of asymmetric graphs already at small size of graphs (compared to the thousands or 10^{10} neurons in CNS) it is the actual degree of bilateral symmetries occurring in real nervous systems are less expected than the opposite. This argument is reasonable only if supposed that various symmetry conservation control processes occur and operate during the 'neurogenesis'.

2. *The limits of symmetry and asymmetry concepts.* - It is fair to call the attention again that 'symmetry in general' is always accompanied with some invariant property remaining unchanged after the transformations. This is a widely accepted concept [17]. However, to an arbitrary transformations some 'invariant quantities or qualities' almost surely can be found. That is why it is important to specify the meaning of symmetry or asymmetry in any context. This has been done here: it is related to automorphism groups of graphs.

3. *Functional implications.* - It would be too extravagant to claim that if all neurons were distinguishable from each other thus they necessarily have distinct functional significance as well. At the actual state of art this problem seems to be hardly decidable and always will depend strongly on the context, too.

4. *Deductive procedures* are sometimes efficient tools to understand causes of realities. - One of the messages of this short communication underlines the conviction. Namely, theoretical tools even in the special form of an application of already proven or very plausible mathematical statements (restricted originally to a branch of mathematics) may also provide fruitful conclusion even in neurosciences. Furthermore, these conclusions seems to be hardly avoidable.

ACKNOWLEDGEMENTS

The work was born under the umbrella of an OTKA-grant support. The author is grateful to Mrs M. Csati for her help in manuscript processing.

REFERENCES

1. Erdos, P. and Renyi, A. (1960) On random graphs I. Publ. Math. Debrecen, 6, 290-297.
2. Palmer, E. (1985) Graphical Evolution. J. Wiley & Sons, New York.

3. Karonski, M. (1982) A review of random graphs. *J. Graph Theory*, 6, 349-389.
4. Bollobas, B. (1985) *Random Graphs*. Academic Press, New York. Section IX/4. pp. 219-224.
5. Erdos, P. and Renyi, A. (1963) Asymmetric Graphs. *Acta Math. Acad. Sci. Hung.* 14, 295-315.
6. Labos, E. (1991) Enumeration of network structures of various symmetry types. In: *Symmetry and Topology in Evolution* (Lukacs, B. et al. eds.) pp. 107-110. KFKI-1991-32/C report series.
7. Wright, E. M. (1971) Graphs on unlabelled nodes with a given number of edges. *Acta Math.* 126, 1-9.
8. Ford, G. W. and Uhlenbeck, G. E. (1957) Combinatorial problems in the theory of graphs. *Prot. Natn. Acad. Sci. USA*, 43, 163-167.
9. Cameron, P. J. (1983) Automorphism groups of graphs. In: *Selected Topics in Graph Theory 2*. (Beinecke, L. W. and Wilson, R. J., eds.), Academic Press, New York, pp. 89-127.
10. Harary, F. (1969) *Graph Theory*. Addison-Wesley, Reading, Mass.
11. Foster, R. M. (1932) Geometrical circuits of electrical networks. *Trans. Amer. Inst. Elec. Engrs.* 51, 309-317.
12. Wright, E. M. (1974) Asymmetric and symmetric graphs. *Glasgow Math. J.* 15, 69-73.
13. Labos, E. (1990) On the rise and decline (R&D) of the brains. In: *Evolution: from Cosmogenesis to Biogenesis* (Lukacs, B. et al. eds.) pp. 109-116. KFKI-1990-50/C report series.
14. Harary, F. and Palmer, A. (1973) *Graphical Enumeration*. Academic Press, New York.
15. Palmer, E. (1979) The enumeration of graphs. In: *Selected Topics in Graph Theory* (Beinecke, L. W. and Wilson, R. J., eds.) pp. 385-416. Academic Press, New York.
16. Read, R. C. (1979) Some Applications of Computers in Graph Theory. (Beinecke, L. W. and Wilson, R. J., eds.) pp. 417-444. Academic Press, New York.
17. Lukacs, B. (1991) On geometric symmetries and topologies of forms. In: *Symmetry and Topology in Evolution* (Lukacs, B. et al. eds.) pp. 47-51. KFKI-1991-32/C report series.

EFFECTS OF MENTAL LOAD ON THE SPECTRAL COMPONENTS OF HEART PERIOD VARIABILITY IN TWINS

E. Láng¹, N. Szilágyi², J. Métneki³ and J. Weisz¹

¹Psychophysiology Research Group, Hungarian Academy of Sciences, H-1088 Budapest, Múzeum krt. 4/A, Hungary; ²Department of Comparative Physiology, Eötvös Loránd University, Budapest and ³Department of Human Genetics, National Institute of Hygiene, Budapest

Summary: The contribution of genetic and environmental control to stress-related cardiovascular reactions was investigated in 10 monozygotic and 10 dizygotic twin pairs during mental arithmetics. Non-invasive indices reflecting vagal and sympathetic activity were used, namely: indices of myocardial contractility based on impedance cardiogram, and spectral components of heart period variance. Autoregressive algorithms were developed for heart period power spectral density estimation providing automatic decomposition of heart period spectra into individual spectral components. During the mental task spectral energy of the mid-frequency (central frequency ≈ 0.1 Hz) and high frequency (around respiratory frequency) components of heart period variance significantly decreased indicating vagal withdrawal. A task-related increase of the mid-frequency component relative to the high-frequency component was obtained. This change in the ratio of the two components as well as the considerable shortening of the contractility indices are pointing to sympathetic activation. When comparing intraclass correlations computed separately for monozygotic and dizygotic twins highly significant correlations were found for the mid-frequency component in monozygotic but not in dizygotic twin pairs in resting condition indicating a substantial genetic contribution to the control mechanisms involved in the baroreflex. Contribution of genetic factors to the control of stress-related interplay of autonomic outflows has been shown.

INTRODUCTION

A number of studies [8, 9, 19, 22, 28] has shown that increasing mental load causes a decrease in heart rate variance (HRV). Sayers [29] found that consistent changes occur in the heart period (HP) spectrum especially in the band 0.05-0.15 Hz. According to Mulder [23] the mid-frequency (MF) band of HRV (0.07-0.14) appeared to

be more sensitive to mental workload than total variance or respiratory fluctuations. HR fluctuations in the mid-frequency range reflecting baroreceptor response to third order blood pressure fluctuations [7] were studied by different authors in somewhat different frequency ranges. This can be explained by their approach based on Fast Fourier Transfer (FFT) algorithm relying on the selection of predetermined frequency bands. The approach based on autoregressive (AR) algorithms for HP variance (HPV) analysis used by Baselli and cov. [5], Pagani and cov. [25], Lombardi and cov. [18], Szilágyi and Láng [13, 14, 33, 34] provides automatic decomposition of HP spectra into individual components. It is of great importance, since it does not require any a priori subdivision of frequencies into bands and arbitrary recognition of power peaks [5].

Our goal was to investigate the effect of mental arithmetics on spectral components of the HPV revealed by decomposition of HP power spectra using AR method. Since HP oscillations in different frequency bands are shown to be differentially mediated [3, 4, 21, 25, 36] the changes in the relationship of different spectral components might provide an insight into the task-related interplay of sympathetic and vagal mechanisms. We completed our investigations with the simultaneous use of another markers of sympathetic activity. In the field of stress research a lot of efforts have been made to use non-invasive indices of myocardial contractility [2, 12, 16, 35]. Such indices are systolic time intervals (STI)-s and several measures derivable from impedance cardiogram. For details in definition, derivation and significance of these indices as well as for information how useful they are in judging the presence of inotropic activation see References [1, 11, 14, 15, 17, 29]. An additional goal was to study the contribution of genetic factors to the control of HP oscillations reflected by spectral components of HPV.

MATERIALS AND METHODS

Subjects and design of the experiment

60 healthy male subjects ranging in age from 24 to 32 y (mean = 28.2 y) participated in the experimental session. 40 of them were twins -10 monozygotic (MZ) and 10 dizygotic (DZ) twin pairs.

Two stress situations were used: a mental arithmetic task -a situation considered to be an active coping task evoking mainly beta adrenergic activity (2, 16) and a cold pressor (CP) test.

Following 15 minute adaptation physiological variables were recorded. Order of presentation of tasks was counterbalanced across subjects so that one half of the subjects received arithmetics first another half last. In this paper results concerning arithmetics are presented, those related to CP test will be published elsewhere.

After 4 minute resting baseline period (B1) subjects in Group I got instructions

concerning arithmetic task (A). A 20-sec, anticipation period (when the word "attention" was displayed on the computer screen in front of the subjects) was followed by the test. The word "attention" was replaced by a 4-digit number which was on the screen for 5 sec. Subjects had to subtract serially 8 from this number as quickly as they could. Two minutes repeated subtractions were performed in mind in order to avoid any artefact due to speaking. A question mark appeared on the screen signalling the subjects to tell the result and keep on sitting still for 1 minute. A 15 minute pause followed the completion of this task. Prior to the next test (CP) a 4 minute baseline (B2) was recorded. The completion of the 3 minute CP test was followed by a final 4 minute baseline (B3). Only the order of presentation of tasks (A and CP) was different for Group II.

Psychological recording techniques and data processing

Heart period (HP). The R-wave of the electrocardiogram in each cardiac cycle was detected with voltage level device and HP (R to R interval) was timed to the nearest msec.

Impedance cardiogram has been recorded using impedance-cardiograph (Minnesota, Model 304 B S/N B-302). The mean thoracic impedance (Z_0) and the first derivative impedance cardiogram (dZ/dt) were recorded and sampled with 10 and 500 Hz respectively.

Respiration was measured by means of a sphygmomanometer cuff attached around the subject's lower rib cage. Changes in cuff pressure were recorded via a Beckman type 4-327-0121 Pressure Transducer and a 9853 DC coupler and sampled with 10 Hz.

Power spectral density of HP variance (HPV) has been estimated using autoregressive algorithms developed in our laboratory [14, 33, 34] providing automatic decomposition of HPV spectra into individual spectral components. Power of spectral components as well as their percental values (in percentage of the total power) were calculated. The ratio of two components (spectral component around 0.1 Hz and spectral component around the respiratory frequency) was calculated. This ratio of mid- and high-frequency components (MF/HF ratio) was suggested by Pagani and coworkers [25] as a marker of changes in sympatho-vagal balance.

Contractility-based indices such as R Z-interval and electromechanic systole (QS2) were beat by beat determined (on the basis of impedance cardiogram and ECG) using waveform recognition computer algorithms developed in our laboratory [12, 13, 31, 32].

RESULTS

HP, RZ, QS2, total power of HPW, spectral components of HPV as well as MF/HF ratio were analysed using multivariate analysis of variance (MANOVA). MANOVA with group (I or II) as the between-groups factor and test (B1, A) as within group factor was used to analyse physiological data. No significant differences involving group (Group main effect or Group X Test interaction) were obtained for either variable.

A significant test main effect was found for HP ($p < .01$), RZ ($p < .0001$), QS2 ($p < .001$), MF power ($p < .005$), HF power ($p < .02$) reflecting a decrease in the above variables from B1 to A. MF/HF ratio significantly increased from B1 to A ($p < .05$). Total

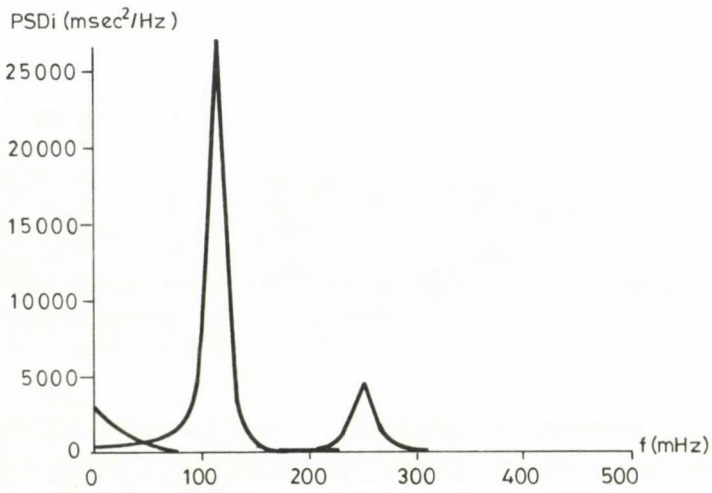


Fig. 1

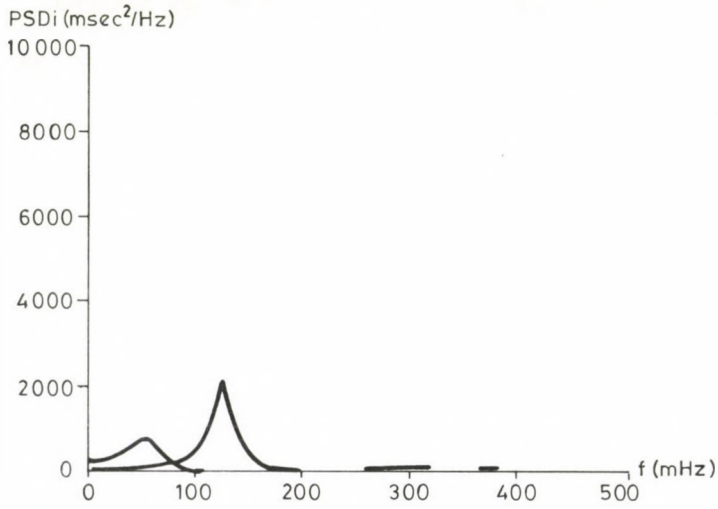


Fig. 2

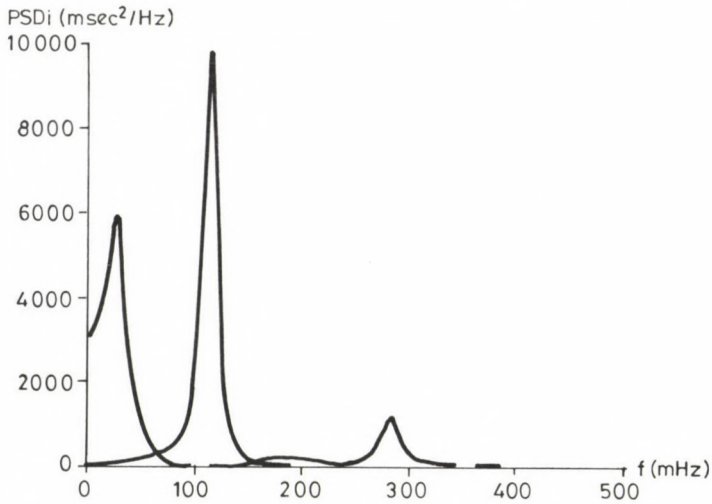


Fig. 3

Table 1

Mean scores of physiological variables and p values of difference between resting (B1) and test (A) values.

Measure	Baseline (B1) mean	Arithmetics (A) mean	B1 - A p value
HP	799.4	675.6	p<.01
QS2	358.3	326.1	p<.001
RZ	150	125	p<.0001
Total power of HPV	1824	1424	ns
LF power of HPV	528	720	ns
MF power of HPV	582	271	p<.005
HF power of HPV	426	201	p<.02
MF/HF ratio	2.18	3.25	p<.05

HP - heart period (msec); QS2 - electromechanic systole (msec); RZ - RZ-interval (msec); HPV - heart period variance (msec²); LF-power - spectral power of the low-frequency component (msec²); MF-power - spectral power of the mid-frequency component (msec²); HF-power - spectral power of the high-frequency component (msec²); MF/HF ratio - ratio of the two components computed separately for each subject.

Fig. 1-3: Power spectral density of heart period variance of one of the subjects in different conditions.

1: resting condition. 2: mental arithmetics. 3: period following the mental task. x-axis: frequency (mHz); y-axis: power.

Note: the vertical scale is not identical for different conditions.

power of HPV has a decreasing while power of low frequency component (LF) an increasing tendency from B1 to A (not significant). Mean scores of the above measures are presented in Table 1. In Fig. 1 individual HPV spectra are presented.

The intraclass correlations were calculated separately for MZ and DZ twin pairs for HP, HPV (total power), MF-power, HF-power, MF/HF ratio, QS2 and RZ intervals in resting condition (B1) and during mental arithmetic test (A). The significance of the intraclass correlations is given by the F-values from the corresponding ANOVA.

Table 2 presents those intraclass correlations calculated separately for MZ and DZ twin pairs which are significant for MZ twins and significantly greater in MZ twins compared to DZ twins (the difference between Fischer z transformed correlations is significant). The results show greater intraclass correlations in MZ twins compared to DZ twins for MF power in resting condition (B1).

The task condition in which mental arithmetic was required showed higher intraclass correlations for MZ twins compared to DZ twins for MF/HF ratio and RZ interval.

Table 2

Intraclass correlations and p values of difference between Fischer z transformed correlations.

Conditions	Intraclass correlation		Fischer z(MZ)-z(DZ) p value
	MZ twins	DZ twins	
Baseline: spectral power of mid-frequency component of HPV	0.722 ^{xx}	0.368	0.01
Arithmetics:			
MF/HF ratio	0.697 ^x	0.092	0.01
RZ-interval	0.757 ^{xx}	0.084	0.01
HP	0.46	0.39	0.01

^{xx}p<0.01

^xp<0.05

DISCUSSION

It was shown in experiments involving pharmacological manipulations and postural changes that respiratory frequency fluctuations in HP are solely vagally mediated [3, 21, 27], while MF oscillations are mediated jointly by the parasympathetic and sympathetic nerves [3, 4, 25, 27, 36]. Thus, during mental arithmetics vagal withdrawal might account for the dramatic reduction of both MF and HF components of HPV. Pagani and coworkers [25] proposed to use the ratio of spectral power of two components, namely: spectral component around 0.1 Hz and the respiratory component. This ratio was suggested to be a marker of changes in the sympatho-vagal balance. The significant task-related increase of MF/HF ratio computed separately for each individual might indicate an increase of sympathetic outflow to the heart. A considerable shortening of RZ interval is pointing to enhanced myocardial contractility hence to sympathetic activation. Probably central sympathetic activation is supported by peripheral mechanisms, namely: by a disinhibition of the norepinephrine release in the heart. It was shown [10, 24] that the release of norepinephrine from the atrial sympathetic nerve is presynaptically controlled (inhibited) by acetylcholine released from vagus nerve endings innervating the heart.

Comparison of concordance or discordance for a trait or disease between MZ respective DZ twins is a widespread method in human genetic research aiming at the degree of heritability of the trait in question. Intraclass correlations reflect the amount of within pair concordance. Assuming that each task and common environments have the same influence on both members of a MZ or DZ pair it can be concluded that higher correlations between MZ twins compared to DZ twins is due to genetic factors [26, 30].

When comparing correlations computed for MZ and for DZ twins highly significant correlations were obtained for the MF component of HPV in MZ but not in DZ twins in resting condition. The mid-frequency peak of HPV centered around 0.1 Hz can be regarded as baroreceptor response to blood pressure fluctuations in this frequency band [7]. Thus our findings indicate a substantial contribution of genetic control to mechanisms involved in the baroreflex.

The genetic control of stress-related interplay of autonomic outflows was revealed by obtaining significant intraclass correlations for the MF/HF ratio (proposed as a tool in the assessment of sympato-vagal balance [25] in MZ but not in DZ twins.

While RR interval does not differentiate between MZ and DZ twins, the contractility based measurement of the RZ interval can differentiate, being more sensitive variable in the assessment of genetic control.

REFERENCES

1. Ahmed, S.S., Levinson, G.E., Schwartz, C.J. and Ettinger, P.O. (1972) *Circulation*, 46, 559-571.
2. Allen, M.T., Obrist, P.A., Sherwood, A. and Crowell, M.D. (1987) *Psychophysiol.* 24, 648-656.
3. Akselrod, S., Gordon, D., Madwed, J.B., Snidman, N.C., Shannon, D.C. and Cohen, R.J. (1985) *Am. J. Physiol.* 249, 867-875.
4. Akselrod, S., Gordon, D., Ubel, F.A., Shannon, D.C., Berger, A.C. and Cohen, R.J. (1981) *Science*, 213, 220-222.
5. Baselli, G., Cerutti, I., Civardi, I., Lombardi, F., Malliani, A., Merri, M., Pagani, M. and Rizzo, G. (1987) *Int. J. Biomed. Computing*, 20, 51-70.
6. Bunnell, D. E. (1985) In: J.F. Orlebeke, G. Mulder and L.J.P. van Doornen (Eds.) *The psychophysiology of cardiovascular control*, pp. 221-235. New York: Plenum Press.
7. Hyndman, B.W., Kitney, R.I. and Sayers, B. McA. (1971) *Nature*, 233, 339-341.
8. Kalsbeek, J.W.H. (1971) In: W.T. Singleton, J.G. Fox and D. Withfield. *Measurement of man and work*. London: Taylor and Francis Ltd.
9. Kalsbeek, J.W.H. and Ettema, J.H. (1963) *Ergonomics*, 6, 306.
10. Kobayashi, O., Nagashima, H., Duncalf, D., Chaudhry, I.A., Hársing, L.G. Jr., Földes, F.F., Goldiner, P.L. and Vizi E.S. (1987) *J. Autonomic Nerv. System*, 18, 55-60.
11. Lamberts, R., Visser, K.R. and Zijlstra, W.G. (1984) Van Gorcum, Assen.
12. Láng, E., Szilágyi, N. and Ádám, G. (1989a) *Int. J. Psychophysiol.* 7, (Abstracts of the 4th Conference of the International Organization of Psychophysiology held in Prague, 1988), 287-288.
13. Láng, E., Szilágyi, N., Météneki, J., Czeizel, A. and Ádám, G. (1990) *Proceedings of the 5th Int. Cong. of Psychophysiology, Budapest, July 9-13, 1990.* p. 174.
14. Láng, E. and Szilágyi, N. (1991) *Acta Physiol. Hung.* 78, 241-260.
15. Lewis, R.P., Rittgers, S.E., Forester, W.F. and Bondoulas, H. (1977) *Circulation*, 56, 146-158.

16. Light, K.C. and Obrist, P.A. (1983) *Psychophysiol.*, 20, 301-312.
17. List, W.F., Gravenstein, J.S. and Spodick, D.H. (Eds.) (1980) *Systolic Time Intervals*. Springer-Verlag, Berlin-Heidelberg-New York.
18. Lombardi, F., Sandrone, G., Perprumer, I., Sala, R., Garimoldi, M., Cerutti, I., Baselli, G., Pagani, M. and Malliani, A. (1987) *The Am. J. Cardiol.* 60, 1239-1245.
19. Luczak, H., and Lauring, W. (1973) *Ergonomics*, 16, 85-94.
20. Mantysaari, M. (1984) *Scand. J. Clin. Lab. Invest.*, 44 (Supplement 170).
21. McCabe, P.M., Yongue, B.G., Ackles, P.K. and Porges, S.W. (1985) *Psychophysiol.*, 22, 195-203.
22. Mulder, G. and Mulder-Hajonides van der Meulen, W.R.E.H. (1973) *Ergonomics*, 16, 69-83.
23. Mulder, G., Mulder, L.J.M. and Veldman, J.B.P. (1985) In A. Steptoe, H. Ruddel and H. Neus (Eds.) *Clinical and methological issues in cardiovascular psychophysiology*, pp. 3-44. Berlin: Springer Verlag.
24. Muscholl, E. (1980) *Am. J. Physiol.* 239, H713-H720.
25. Pagani, M., Lombardi, F., Guzetti, S., Rimoldi, O., Furlan, R., Pizzinelli, P., Sandrone, G., Malfatto, G., Dell'Orto, S., Picalluga, E., Turiel, M., Baselli, G., Cerutti, S. and Malliani, A. (1986) *Circ. Res.*, 59, 178-193.
26. Plomin, R., DeFries, J.C. and McLearn, G.E. (1980) *Behavioral Genetics, a Primer*, W.H. Freeman and Co., San Francisco.
27. Pomeranz, B., Macaulay, R.J.B., Caudill, M.A., Kutz, I., Adam, D., Gordon, D., Kilborn, K.M., Barger, A.C., Shannon, D.C., Cohen, R.J. and Benson, H. (1985) *Am. J. Physiol.*, 248, 151-153.
28. Rohmert, W., Laurig, W., Philipp, U. and Luczak, H. (1973) *Ergonomics*, 16, 33-44.
29. Sayers, B. McA. (1973) *Ergonomics*, 16, 17-32.
30. Somsen, R.J.M., Boomsma, D.I., Orlebeke J.F. and van der Molen (1985) In: *Psychophysiology of Cardiovascular Control* (Orlebeke, J. F., Mulder, G. and van der Doornen, L. J. P., Eds.). Plenum Press, New York.
31. Szilágyi, N. and Láng, E. (1989) *Int. J. Psychophysiol.*, 7, (Abstracts of the 4th Conference of the International Organization of Psychophysiology held in Prague, 1988), 406-407.
32. Szilágyi, N., Láng, E. and Balázs, L. (1992) *Int. J. Psychophysiol.* In press.
33. Szilágyi, N. and Láng, E. (1991) 2nd European Congress of Psychophysiology (8-12 July, 1991. Budapest) 482.

34. Szilágyi, N., Láng, E. and Horváth, Gy. (1990) Proceedings of the 5th Int. Congr. of Psychophysiology, Budapest, July 9-13, 1990. p. 296.
35. Van Doornen, L.J.P. and de Geus, E.J.C. (1989) *Psychophysiol.* 26: 1728.
36. Weise, F., Baltrusch, K. and Heyddenreich, F. (1987) *J. Auton. Nerv. Syst.* 26, 223-230.

CORRELATION DIMENSION CHANGES OF THE EEG DURING THE WAKEFULNESS-SLEEP CYCLE

M. Molnár¹ and J.E. Skinner²

¹Institute for Psychology of the Hungarian Academy of Sciences, H-1394 Budapest VI,
Szondy u. 83-85. P.O. Box 398, Hungary and ²Baylor College of Medicine,
Department of Neurology, Houston

Summary: The mathematical tools of chaos theory make the quantification of a time series such as the electroencephalogram possible by calculating its correlation dimensions. In this study, the electroencephalogram was recorded from the vertex in cats during the wakefulness-sleep cycle and its correlation dimension was determined. For the estimation of the correlation dimension a new method, the point-correlation dimension was used. This method is more accurate than others currently used for tracking non-stationarities within the data. The point-correlation dimension was higher during the alert state than in slow wave sleep. It is suggested that during the alert state a different type of pacemaker activity takes over in the generation of the electroencephalogram.

INTRODUCTION

The recent development in non-linear mathematics allows the quantitative description of the complex behavior of systems. The new methods make it possible to differentiate between truly stochastic behavior and relatively low level of randomness. In the former case, the system's degree of freedom is very high; in the latter, it can be surprisingly low in which case the system shows characteristic features of deterministic chaos [7].

The central nervous system is one of the most complex systems known to man in the universe. Because of the non-linearity apparent in many aspects of its functions and its supposedly high degree of freedom, the application of chaos theory for the analysis of the electroencephalogram (EEG), a time-series this system is continuously generating, seems to be adequate and promising.

The complexity of a system can be quantified by determining its correlation dimension (D2). The value of D2 gives the number of independent variables (or degrees of freedom) which are active in the generation of the time series produced by the system [10]. The most widely used algorithm for the calculation of the D2 is that of Grassberger and Procaccia [5].

The value of D2 of the EEG decreases during slow wave sleep (SWS) compared to the alert state [2, 6]. In these studies, however, the EEG recorded in either one or another condition was analyzed by itself since the available algorithm [5] did not permit the analysis of non-stationarities and thus could not track the changes in the EEG such as which occur during the wakefulness-sleep cycle. These changes were analyzed in the present study by a new method, the "Point-D2", which is not biased by these difficulties and is more accurate than others currently being used in other laboratories for the calculation of D2 [8].

MATERIALS AND METHODS

Calculation of D2 by the Point-D2 (PD2) method

The correlation dimensions of a system is given by the following equation: $D2 = \log C(r,n)/\log r$, where $C(r,n)$ is the cumulative sum of rank ordered vector differences within a certain range of r , and n is the number of vector differences. When the vectors are constructed, one point of the time-series serves as a reference-point with respect to which the amplitudes of the digitized time-series are used as coordinates in the multidimensional state-space. Details of the procedure are outlined elsewhere (8,9). Mathematical stationarity is required in the above procedure which is hardly possible to achieve in biology.

The PD2-method does not use every vector difference, nor does it accept every reference point. Rather, those vector differences, where no convergence is seen in the $\log C(n,r) - \log r$ plot, or no saturation in the embedding dimension - slope plot, are not used during the calculation. In this way, unreally high D2 values or effects of non-stationarities will not erroneously modify the value of D2, which is designated as "PD2" in this study to indicate that this new procedure was used for its calculation (8).

Sleep experiments

3 adult cats of both sexes were used. Stainless steel electrodes (0.23 mm O.D.) were implanted in Nembutal anesthesia (40 mg/kg) into the peribulbar fat tissue to record the eye movements (EOG) and into the superficial neck muscles for the recording of the electromyogram (EMG). The stainless steel screw was placed in the midline 5 mm posterior to the bregma as a vertex electrode. The same type of stainless steel screw was driven into the bone covering the frontal sinuses in the midline which served as reference for the monopolar EEG-recording. The bioelectric signals were fed into the amplifiers (bandpass 0.1-1 kHz) via a long, flexible low-noise cable which did not interfere with the behavior of the animals. The EEG was digitized at 100 Hz and stored in an IBM 386 computer and simultaneously also on paper. Off-

line analysis was performed on a 486 IBM computer.

The experiments were begun after complete recovery following surgery. The animals were placed in a 2 x 0.7 m cage which was in an acoustically and electrically shielded chamber. Their behavior was monitored by a closed-loop television system.

RESULTS

The animals got accustomed to their cage within two or three days and spent considerable time sleeping there every day. Sleep stages were defined with the help of polygraphic recording of the EMG, EOG and EEG activities. A typical example of PD2 changes accompanying arousal from SWS caused by a loud acoustic stimulus is shown in Fig. 1. During SWS the peak value of PD2 was 1.4 (mean: 3.71, std: 5.69). The second highest value in the histogram of the PD2 values in SWS was peaking at 6.0. As the EEG became desynchronized as a result of the waking stimulus the PD2 values became much more coherent and stabilized at a significantly ($p < 0.001$, $t = 6.647$) higher value with a conspicuously lower standard deviation (peak: 5.6, mean: 6.22, std: 1.84).

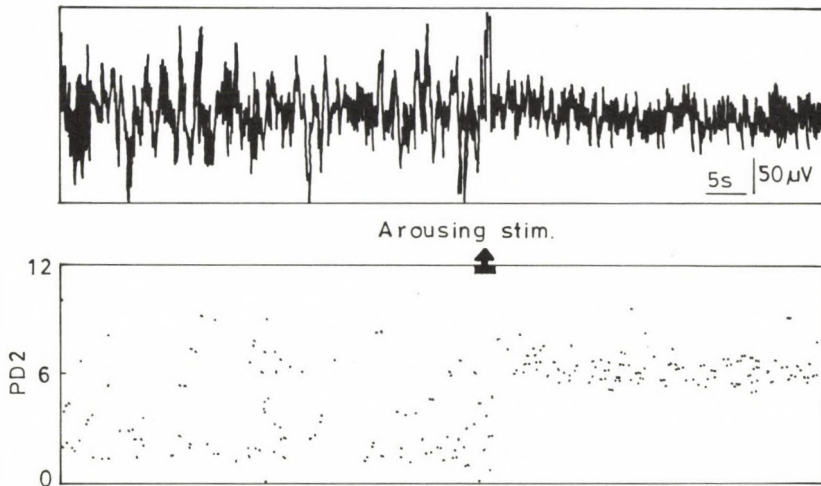


Fig. 1: The effect of arousal caused by a loud acoustic stimulus (Arousing stim.) on the EEG recorded from the vertex in a cat and on the PD2 calculated from the same epoch.

DISCUSSION

According to Andersen and Andersson [1] the pacemaker of cortical synchronous slow cortical activity is in the thalamus. We found that although the PD2 was definitely low in SWS, a distinct higher dimensional peak was also present. This finding indicates that during SWS at least two different generator systems -one having fewer, and the other higher degrees of freedom- are simultaneously active in the generation of the EEG. Although in the alert state the dimension of the system was significantly higher, it could still be determined. Destexhe and Babloyantz [4] suggest that in the absence of a pacemaker the D2 cannot be defined. Our finding, then, may indicate that some kind of a pacemaker activity is still present in the desynchronized EEG. The origin of this activity could be the ventral tegmental area [3].

ACKNOWLEDGEMENT

This publication is based on work sponsored by the Hungarian-U.S. Science and Technology Joint Fund in cooperation with the Hungarian Academy of Sciences and the Department of Health and Human Services.

REFERENCES

1. Andersen, P. and Andersson, S. A. In: Handbook of EEG and clinical Neurophysiology. (Reymond, A. ed.), pp. 91-118, Elsevier, Amsterdam.
2. Babloyantz, A. (1986) In: Dimensions and Entropies in Chaotic Systems (Mayer-Kress, G.; ed.) pp. 241-245. Springer, Berlin.
3. Buser, P. (1987) In: A Textbook of Clinical Neurophysiology (A. M. Halliday, S. R. Butler and R. Paul; eds.) pp. 595-621, J. Wiley & Sons, New York.
4. Destexhe, A. and Babloyantz, A. (1991) In: Self-Organization, Emerging Properties and Learning. (A. Babloyantz; ed.) pp. 1-24. Plenum Press, New York. ARW Series.
5. Grassberger, P. and Procaccia, I. (1983) Physical Review Letters, 50 (5), 346-349.
6. Roschke, J. and Basar, E. (1990) In: Chaos in Brain Function. (E. Basar; ed.) pp. 49-62. Springer, Berlin.
7. Schuster, H. G. (1988) Deterministic Chaos. VCH, Weinheim.
8. Skinner, J. E., Goldberger, A. L., Mayer-Kress, G. and Ideker, R. E. (1990) Biotechnology 8, 1018-1024.

9. Skinner, J. E., Molnár, M., Vybiral, T. and Mitra, M. (1992) *Integrative Physiological and Behavioral Science* 27, 43-57.
10. Takens, F. (1985) *Lecture Notes in Mathematics*, 1125, 99-106.

INCREASE OF STORAGE CAPACITY OF NEURAL NETWORKS BY PREPROCESSING USING CONVERGENCE AND DIVERGENCE

L. Orzó

Ist Department of Anatomy, Semmelweis University Medical School,
Neurobiology Unit, H-1450 Budapest, Tűzoltó u. 58, Hungary

Summary: The greatest practical limitation of the associative memory models, especially the Hopfield model [8] is the low storage capacity. It has been shown by Gardner [3], that the Hopfield type models storage limit is 2^*N , where N is the number of the processing elements or neurons. For biased patterns, on the other hand, it is much greater. But in general the input patterns are not biased. To approach to this problem and to increase the storage capacity of the model, the input patterns have to be diluted by some conversion method particularly which uses convergence and divergence in neuroanatomical sense. Based on this model these parameters can be estimated. As a consequence of this bias and the divergence, the storage capacity is increased. This preprocessing method doesn't lead to the loss of information and keeps the error correcting ability of the model.

INTRODUCTION

Recently there has been an upsurge of interest in models of neuronal networks [See Ref. 11: McCulloch and Pitts] especially which exhibit associative memory [See Ref. 19: Willshaw and Longuet-Higgins; 8, 9: Hopfield]. The detailed analysis of the model solved some emerging problems, such as the retrieval dynamics [1, 10], dilution of the synaptic strength (weight) matrix (3, 18), biased and hierarchical data storage [2, 4, 10], various learning rules [from 5 to 14], the memory capacity [5, 6, 12] and so on. The main limitation of practical application of the Hopfield model is the low storage capacity [11]. Considering the amount of the human memory capacity, it is necessary to raise the model's storage capability. Gardner has shown, that the model capacity limit is smaller than $2N$ (where N is the processing elements -neurons- and the stored patterns are random binary vectors with equal probability of 1 and -1. If there is

greater overlap between the patterns, namely they are biased patterns, the storage capacity is raised [7]. In general it is not indispensable to represent the information by an any-out-of-N code. The n-out-of-N is adequate by the informational theory point of view [17] (where n is a small, but not very small number compared to N) and it significantly increases the memory capacity [13, 19]. The other type of the capacity increment comes from the enhancing number of processing elements (divergence). There has to be some preprocessing method to solve the dilution of the primary input patterns to a greater storing pattern template in the same time. The conversation of information is here required.

MATERIALS AND METHODS

The conversion or remapping method makes a storing pattern from the input pattern. The input patterns are random m length vectors with binary entries, equal probability of -1 and 1. The stored patterns are N length vectors, with binary elements, but the probability of -1 (non selected) elements is $(N-n)/N$ and the 1 (selected) elements probability is n/N , that is the patterns are biased. The conversion is made so that each storing elements received input from k input patterns component and if these are bitwise the same as the prewired random binary weights, then their values are 1, that is active, otherwise it is -1. Such the number of the active bits of the storing pattern is $n=N/2^k$. It is really biased, if k is greater than one. Thus the storage capacity is increased by 2^k factor. The storage method is the wellknown Hebb rule for biased patterns:

$$J_{i,j} = \sum_{\mathbf{q}} (x_i^{\mathbf{q}} - \bar{x}_i) \times (x_j^{\mathbf{q}} - \bar{x}_j)$$

where the $x^{\mathbf{q}} = \{... x_i^{\mathbf{q}}...\}$ is the stored pattern and the $\bar{x} = \{...\bar{x}_i...\}$ means their average. If the conversion weights are prewired, these averages can be analytically computed. The first thesis is that there is no loss of information. The possible number of input patterns is 2^m . The possible storing patterns number is $(N!/(N-n)!n!)$. If the latter is much larger than the previous one, then the input patterns can be remapped in the storing patterns' configuration space. How can the input pattern be reconstructed from the stored pattern? $(1-k/m)^n$ is the probability, that each input neuron is one of the precursor of the selected stored pattern neuron ($n=N/2^k$). This is not great enough to estimate the whole input vector. The probability that the non selected storing neuron corresponding to some precursors incorrectly estimated from the conversion weights is $(1/2+1/k)$ or greater. There are $(N-n)$ such neuron, therefore if $1/k$ is greater than $\sqrt{1/((N-n) \times k/m)}$, (which is the case for small k, m and great N) then the state of the input pattern neurons can be estimated certainly. The non-selected neurons preserve the information of the input pattern. How can be maintained the error correcting ability of the model? The answer comes from the error increase through the operation. If the probability of the error in the input pattern is p then the error probability is $(1-(1-p)^k) \times 2$ in the storing pattern. If k is not too large then it does not amplify too quickly. If k is larger and the conversational weights are not binary vectors, then we have to use some threshold, which can be varied, for selection. Namely if a storing cell got greater weighted input than the threshold then it will be selected. In this case the error grows much faster, than the previous example. That is a small amount of error in the input pattern makes a larger part of the selection missed, because every elements such as

the erroneous ones of the input pattern take much greater place in the selection mechanism.

DISCUSSION

By this method the Hopfield model could become a practically useful associative memory model. The storage capacity of the input patterns is proportional to N^2/n , which is much greater than the original value which is proportional to m . Obviously it does not solve all the problems of the human memory, not yet the enormicity, but helps to understand the first steps of the information processing in a brain. The input patterns information is conserved. The error does not grow too fast, if the convergence parameter is low. So the convergence (k) is a number from 2 to 10. The divergence subsequently must be greater than k above two. This may be some type of practical rule in each step of information processing. The conversion (selectional) weights are capable to equalize or make hierarchy in the representation of the different input pattern distributions by some self-organizing method and ended by a fix wiring. Further question is, if there are some preprocessing or learning algorithms, which can use the original synaptic weights and so the initial inner hierarchical structure of the matrix (16) to enhance the memory capacity.

REFERENCES

1. Amit, D.J., Gutfreund, H. and Sompolinsky, H. (1987) *Ann. Phys.* 173, 30-67.
2. Cortes, C., Krogh, A. and Hertz, J.A. (1987) *J. Phys. A. Math. Gen.* 20, 4449-4455.
3. Derrida, B., Gardner, E. and Zippelius, A. (1987) *Europhys. Lett.* 3, 87.
4. Dotsenko, V.S. (1985) *J. Phys. C: Solid State Phys.* 18, L1017-1022.
5. Gardner, E. (1988) *J. Phys. A. Math. Gen.* 21, 257-270.
6. Gardner, E. and Derrida, B. (1988) *J. Phys. A. Math. Gen.* 21, 271-284.
7. Hebb, D.O. (1949) *The Organization of Behaviour* (New York: Wiley).
8. Hopfield, J.J. (1982) *Proc. Natl. Acad. Sci. USA* 79, 2554-2558.
9. Hopfield, J.J. (1983) *Nature* 304, 158-159.
10. Kanter, I. and Sompolinsky, H. (1986) *Phys. Rev. A.* 35, 380-392.
11. McCulloch, W.S. and Pitts, W.A. (1943) *Bull. Math. Biophys.* 5, 115.

12. Mezard, M. (1989) *J. Phys. A. Math. Gen.* 22, 2181-2190.
13. Palm, G. (1980) *Biological Cybernetics* 36, 19-31.
14. Parisi, G. (1986) *J. Phys. A. Math. Gen.* 19, L617-L620.
15. Rammal, R. (1986) *Rev. Mod. Phys.* 58, 765-788.
16. Toulouse, G., Dehaene, S. and Changeux, J.P. (1986) *Proc. Natl. Acad. Sci. USA* 83, 1695-1698.
17. Hecht-Nielsen, R. (1986) *Proc. Conf. on NN for Computing II*, 455-461.
18. Tsodyks, M.V. (1988) *Europhys. Lett.* 7, 203-208.
19. Willshaw, D.J. and Longuet-Higgins, H.C. (1969) *Nature* 222, 960-962.

CIRCULATORY AND RESPIRATORY EFFECTS OF CAPSAICIN AND RESINIFERATOXIN ON GUINEA PIGS

R. Pórszász and J. Szolcsányi

Department of Pharmacology, University Medical School,
H-7643 Pécs, P.O. Box 99, Hungary

Summary: The cardiorespiratory effects of capsaicin and its novel analogue resiniferatoxin (RTX) have been investigated in urethan anaesthetized guinea pigs. Intravenously administered capsaicin (5-20 $\mu\text{g}/\text{kg}$) failed to elicit the full pulmonary chemoreflex, but after a latency of 2 seconds caused a short period of tachypnea (6-9 sec) and hypotension without bradycardia. An initial tachypnea was observed in response to 1 $\mu\text{g}/\text{kg}$ intravenously administered RTX, which was followed by a slowly developing shallow breathing, accompanied by an increase in blood pressure after a transient hypotensive effect. RTX inhibited the reflex response evoked by capsaicin for about 10 minutes. After bilateral vagotomy neither tachypnea nor hypotension was observed in response to capsaicin. These results show that in the guinea pig the vagally mediated pulmonary chemoreflex evoked by capsaicin and inhibited by RTX is qualitatively different from that described on other mammalian species (cat, dog, rat, etc.).

INTRODUCTION

The classical pulmonary chemoreflex (Bezold-Jarisch reflex), evoked by stimulation of non-myelinated vagal afferent C fibers is a triad: bradycardia, fall in blood pressure and apnea. This triple response can be elicited with several compounds such as veratridine [3, 15, 16, 31], phenylbiguanide [3, 4, 9, 10, 16, 17, 30], capsaicin [2, 18, 19, 27], 5-HT [3, 14, 17] etc. These experiments have been made in cats, rats, rabbits and dogs. Capsaicin has a highly selective action on cutaneous polymodal nociceptors supplied by C or A delta fibers [3, 5, 7, 8, 11, 24, 25, 26, 28] and excites also selectively the pulmonary

chemosensitive receptors among other chemoceptive interoceptors. RTX resembles capsaicin in chemical structure, and evokes similar responses as capsaicin both in vivo and in vitro, but it is 3-4 orders of magnitude more potent than capsaicin [12, 20, 21, 22]. This novel capsaicin analogue acts selectively on primary sensory neurones in rats to produce ultrastructural alterations and CGRP, SP depletion from these neurones like capsaicin. Ligand binding studies on sensory ganglion cells have provided evidence for the existence of a common binding site for capsaicin and RTX [22, 23]. However there are species differences in cardiorespiratory effects of capsaicin and RTX. In the cat RTX can trigger the Bezold-Jarisch reflex and can achieve a desensitization to the capsaicin induced response [27]. In the rat desensitization with RTX to the capsaicin induced response was obtained without activation of the reflex [27, 29]. The aim of the present study was to get information about cardiorespiratory effects of capsaicin and RTX in the guinea pig.

MATERIALS AND METHODS

Recording of blood pressure and respiration in guinea pigs

Experiments were carried out on guinea pigs (510-860g) under urethan anaesthesia (1.0-1.2 g/kg i.p.). Blood pressure was measured in the cannulated left carotid artery with a Statham pressure transducer. The dp/dt values of the pressure curves were also recorded to indicate the changes in heart contractility. The respiratory movements were monitored by a low pressure transducer, connected to one side of an Y intratracheal cannula. All the recordings were made on a Beckman Dynograph Type RM. The heart rate was derived from the blood pressure by means of a heart rate coupler. For drug administration a polythene tube was introduced into the right jugular vein.

Drugs used

The following drugs were used: urethan (Reanal), capsaicin (Merck), resiniferatoxin (Chemsyn Science Laboratories, Lanexa, KS). Stock solutions of capsaicin (10 mg/ml) and resiniferatoxin (0.1 mg/ml) contained 10% ethanol, 10% Tween 80 and 80% 0.9% NaCl solution.

Statistics

Data are reported as mean \pm SE. The Mann-Whitney U test was used for statistical comparison of the data.

RESULTS

Experiments were made on 11 guinea pigs. Capsaicin (5-20 $\mu\text{g}/\text{kg}$) injected intravenously, slightly reduced the blood pressure and produced tachypnea after latency of two seconds (Fig. 1A), the rate of respiration after a dose of 5 $\mu\text{g}/\text{kg}$ increased from 144 to 192 per minute. After about 8 seconds the tachypnea ceased. Higher dose of capsaicin (20 $\mu\text{g}/\text{kg}$) caused the same effect. Intravenous injection of 1 $\mu\text{g}/\text{kg}$ RTX evoked a pressor effect following a transient hypotension (Fig. 1B). Bradycardia was absent, but an initial tachypnea was observed, which was followed by a slowly developing shallow breathing. Two minutes after RTX administration (Fig. 1C) 5 $\mu\text{g}/\text{kg}$ capsaicin evoked no tachypnea, instead bradypnea with longer latency (6-8 sec) appeared. The hypotensive effect of capsaicin was less pronounced than before RTX administration. 10 minutes after RTX injection (Fig. 1D), the same dose elicited a slight decrease in blood pressure with minimal increase in the respiration rate (from 70 to 108). This tachypnea suddenly ceased

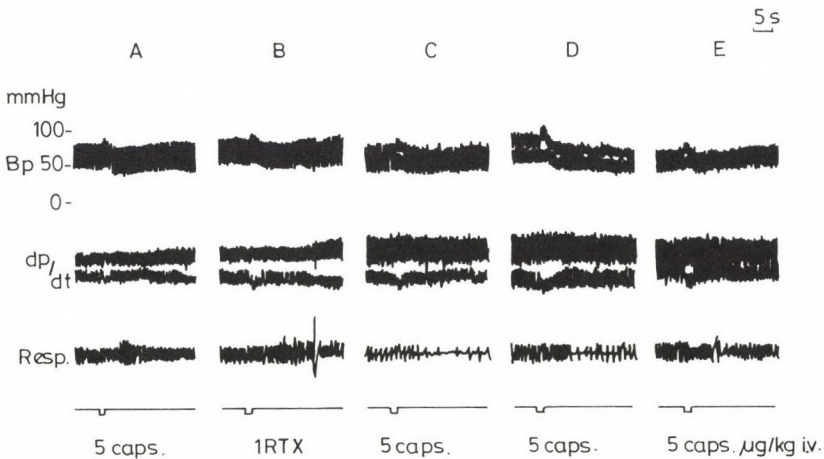


Fig. 1: Effect of intravenously applied capsaicin (caps) and resiniferatoxin (RTX) on blood pressure (BP), myocardial contractility (dp/dt) and respiration (Resp.) in guinea pigs with intact vagal nerves.

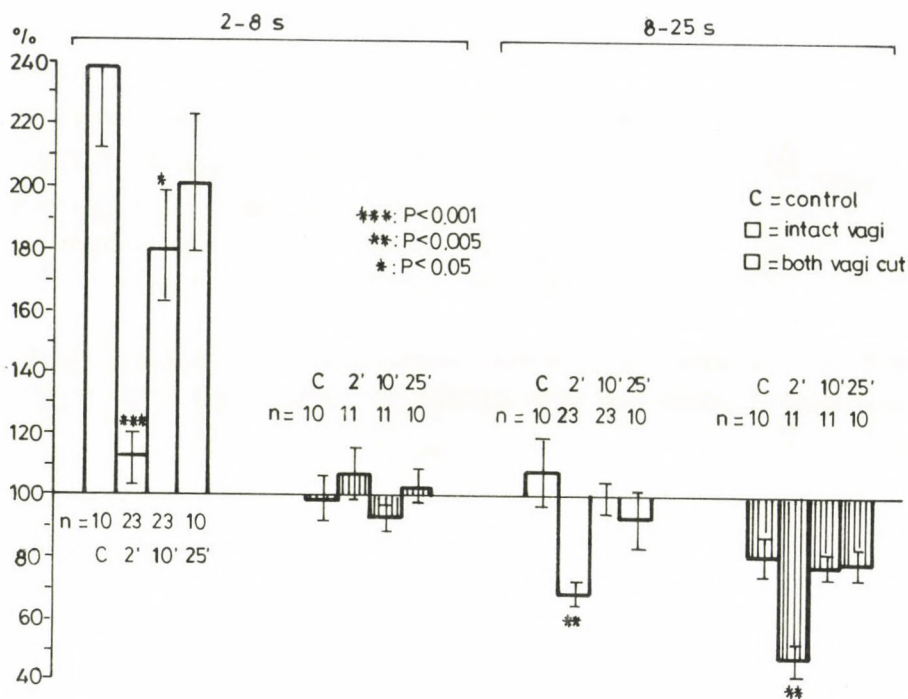


Fig. 2: Changes in rate of respiration in response to i.v. injection of 5 µg/kg capsaicin before (C) and after (2, 10, 25 minutes) RTX administration (1 µg/kg i.v.). Ordinate: ratio of respiration rate after and before drug administration.

in the 7-8th second and was followed by bradypnea with 43/min frequency. Recovery of the control responses appeared around 25-35 min after the RTX injection. Fig. 2 shows quantitative data obtained in this series of experiments. The inhibitory action of RTX on early (2-8 sec) tachypnoeic effect of capsaicin was statistically significant ($p < 0.05$) up to 10 minutes after RTX administration, with an almost complete abolition at the 2nd minute. 25 minutes after RTX injection no significant inhibition could be observed. The third group of columns shows that the late (from 8th second) bradypnoeic effect of capsaicin which was absent before RTX administration was the most expressed with capsaicin given 2 minutes after RTX injection. This effect subsides also 10 or 25 min after RTX administration. In guinea pigs undergone bilateral cervical vagotomy neither tachypnea, nor hypotension was observed in response to 5 µg/kg capsaicin (Fig. 3A). The late bradypnea

(from 8th second), which was seen in guinea pigs with intact vagi after RTX administration was also observed in vagotomized animals. Intravenous injection of RTX ($1 \mu\text{g}/\text{kg}$) produced a slowly developing pressor effect accompanied by an increase in the amplitude of respiratory movements (Fig. 3B). After RTX administration no changes in blood pressure, heart rate and myocardial contractility were observed in response to capsaicin ($5 \mu\text{g}/\text{kg}$). At the second minute injection of capsaicin evoked an apnea with a latency of 7 seconds, followed by bradypnea (Fig. 3C).

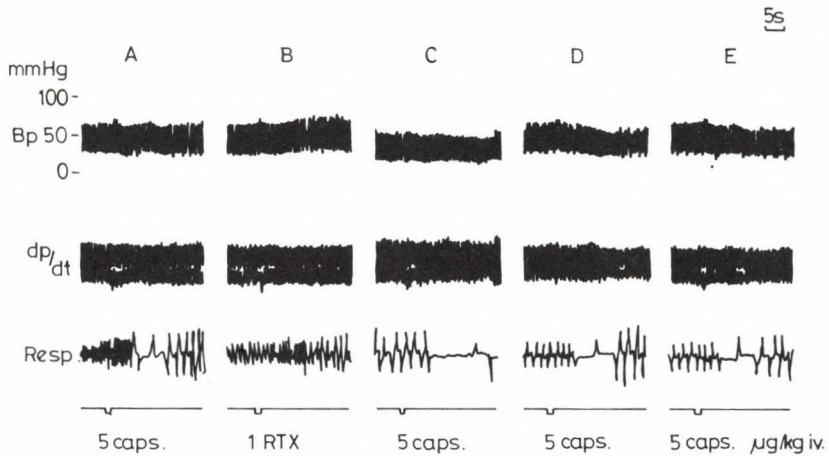


Fig. 3: Effect of intravenously applied capsaicin (caps) and resiniferatoxin (RTX) on blood pressure (BP), myocardial contractility (dp/dt) and respiration (Resp.) in guinea pigs after bilateral cervical vagotomy.

DISCUSSION

The present study revealed for the first time that in a species where capsaicin evokes nociceptive reactions does not evoke the Bezold-Jarisch reflex to intravenous injection. In contrast to the rat, rabbit, cat and dog, where the classical vagal reflex triad of bradycardia, hypotension and apnea was elicited [2, 3, 17, 18, 19], rapid breathing and

slight hypotension without bradycardia was observed in the guinea pig. This latter response is also due to a vagal reflex, since it is absent after bilateral vagotomy. The short latency of the tachypnoeic response corresponds to that observed for the apnea in other species and is well within the time period of pulmonary circulation. Consequently vagal receptors which are excited in the guinea pig by intravenous injection might be identical to the chemoceptive pulmonary J receptors described in other species. Mills and Widdicombe [13] suggested that in the guinea pig a vagal reflex is mainly responsible for the rapid shallow breathing due to histamine and partly responsible for the bronchoconstrictions and to anaphylaxis [1, 13]. Guinea pigs are more prone than other species to respond to antigens with symptoms resembling to asthmatic patients. It is interesting in this context that the pulmonary vagal reflex to capsaicin differs qualitatively from that observed in other mammalian species. Until recently, Bezold-Jarisch reflex was regarded as little more than a pharmacological curiosity. Some data indicate that under certain circumstances it might have a pathophysiological relevance. In postoperative pediatric surgical patients this reflex may provoke a lethal outcome because a relationship between this reflex and postoperative complications was described [6]. The blocking effect of RTX on the pulmonary reflex evoked by capsaicin in the cat and rat [23] was observed also in the guinea pig. In contrast to the former two species, this inhibitory action lasted only for a few minutes in the guinea pig. More experiments are needed to explain this unexpected findings as well as the mechanisms of late responses which were still present after bilateral vagotomy.

ACKNOWLEDGEMENT

This study was supported by OTKA and TKT.

REFERENCES

1. Bergren, D.R. and Sampson, S.R. (1982) *Resp. Physiol.* 47, 83-95.
2. Coleridge, H.M., Coleridge, J.C.G. and Kidd, C. (1964) *J. Physiol. (London)* 170, 272-285.
3. Coleridge, H.M. and Coleridge, J.C.G. (1986) In: *Handbook of Physiology, The Respiratory System vol.II., part I., /Cherniack, N.S. & Widdicombe, J.G.; eds/ pp. 395-429, American Physiological Society, Bethesda, MD, USA.*

4. Comroe, J.H. and Mortimer, L. (1964) *J. Pharmacol. Exp. Ther.* 146, 33-41.
5. Foster, R.W., Ramage, A.G. (1981) *Neuropharmac.* 20, 191-198.
6. Fullerton, D.A., Cyr, J.A.S. et al. (1991) *Ann. Thorac. Surg.* 52, 534-536.
7. Holzer, P. (1988) *Neurosci.* 24, 739-768.
8. Holzer, P. (1991) *Pharm. Rev.* 43, 143-203.
9. Jain, S., Subramanian, S., Julka, D.B., and Guz, A. (1972) *Clinical Science* 42, 163-177.
10. Kay, I.S. and Armstrong, D.J. (1990) *Exp. Physiol.* 75, 383-389.
11. Konietzny, F. and Hensel, H. (1983) *J. Therm. Biol.* 8, 213-215.
12. Maggi, C.A., Patacchini, R., Tramontana, M., Amann, R., Giuliani, S. and Santicioli, P. (1990) *Neurosci.* 37, 531-539.
13. Mills, J.E. and Widdicombe, J.G. (1970) *Br. J. Pharmacol.* 39, 724-731.
14. Mott, J.C. and Paintal, A.S. (1953) *Br. J. Pharmacol.* 8, 238-241.
15. Paintal, A.S. (1957) *J. Physiol.* 135, 486-510.
16. Paintal, A.S. (1969) *J. Physiol.* 203, 511-532.
17. Paintal, A.S. (1973) *Physiol. Rev.* 53, 159-228.
18. Pórszász, J., György, L. and Pórszász-Gibisz, K. (1955) *Acta Physiol. Acad. Sci. Hung.* 8, 61-76.
19. Pórszász, J., Such, Gy. and Pórszász-Gibisz, K. (1957) *Acta Physiol. Acad. Sci. Hung.* 12, 189-205.
20. Szállási, A. and Blumberg, P.M. (1989) *Neurosci.* 30, 515-520.
21. Szállási, A., Joó, F. and Blumberg, P.M. (1989) *Brain. Res.* 503, 68-72.
22. Szállási, A. and Blumberg, P.M. (1990) *Life Sci.* 47, 1399-1408.
23. Szállási, A., Szolcsányi, J., Szállási, Z. and Blumberg, P.M. (1991) *Naunyn-Schmiedeberg's Arch. Pharmacol.* 344, 551-556.
24. Szolcsányi, J. (1977) *J. Physiol. (Paris)* 73, 251-259.

25. Szolcsányi, J. (1984) In: *Antidromic Vasodilatation and Neurogenic Inflammation.* /Chahl, L.A., Szolcsányi, J., Lembeck, F.; eds/ pp. 27-55, Akadémiai Kiadó, Budapest.
26. Szolcsányi, J. (1987) *J. Physiol. (London)* 388, 9-23.
27. Szolcsányi, J., Szállási, A., Szállási, Z., Joó, F. and Blumberg, P.M. (1990) *J. Pharmacol. Exp. Ther.* 255, 923-928.
28. Szolcsányi, J. (1990) in *Chemical Senses, Vol 2: Irritation.* /Green, B.G., Manson, J.R., Kare, M.R.; eds/ pp. 141-169, Marcel-Dekker Inc., New York.
29. Szolcsányi, J., Barthó, L. and Pethő, G. (1991) *Acta Physiol. Hung.* 77, 293-304.
30. Trenchard, D., Russel, N.J.W. and Raybould, H.E. (1984) *Resp. Physiol.* 55, 63-79.

VARIOUS SIGNAL MOLECULES MODULATE VOLTAGE-ACTIVATED ION CURRENTS ON SNAIL NEURONS

A. Szűcs¹, G.B. Stefano², T.K. Hughes³ and K. S.-Rózsa¹

¹Balaton Limnological Research Institute of the Hungarian Academy of Sciences, H-8237 Tihany, Hungary; ²State University of New York, College at Old Westbury, Long Island, NY, USA and ³Department of Microbiology, University of Texas Medical Branch, Galveston, Texas, USA

Summary: The modulatory effects of interleukin-1 (IL-1), an immunotransmitter, and FMRFamide, a molluscan neuropeptide, were studied on identified neurons of *Helix pomatia* L. (Mollusca, Gastropoda) by using the method of two microelectrode voltage clamp. IL-1 and FMRFamide uniformly decreased the voltage-activated inward current (I_{Ca}), while the voltage-dependent outward potassium current ($I_{net K}$) increased. IL-1 and FMRFamide were shown to use the same cellular targets as used by the low molecular weight neurotransmitters.

Key words: Interleukin-1, FMRFamide, voltage-activated ion currents, voltage clamp, Helix neurons

INTRODUCTION

It is commonly accepted that various signal molecules, such as neurotransmitters, peptides and cytokines, function in close interaction in the nervous system. However, neither the functional link nor the membrane targets of their interactions is well understood, although various signal molecules can have multiple overlapping cell regulatory actions [1].

In the nervous system, various signal molecules may attenuate or augment each other's effects, interfering in this way with the transfer and analysis of information. The two classes of molecules which play a modulatory action in information processing are peptides and cytokines. The interaction of the endocrine and immune systems has been proved [2, 3, 4], but the mechanism of bidirectional interactions between the nervous and immune systems is still unknown.

The present experiments were undertaken to study whether an immunotransmitter, interleukin-1 (IL-1), and a molluscan neuropeptide (FMRFamide) have specific effects on the same nerve cells, using common or different ion channels as targets.

MATERIALS AND METHODS

The experiments were performed on identified neurons of the isolated subesophageal ganglia of *Helix pomatia* L. (Mollusca, Gastropoda) by using the method of two microelectrode voltage clamp. Current and voltage traces were registered and analyzed with an IBM-AT compatible computer equipped with a DMA Labmaster AD-DA converter, which digitized the traces at 10 kHz. Leakage currents were removed by a linear fitting procedure. To measure voltage-dependent inward or outward currents, voltage clamp pulses of various amplitudes were applied at holding potentials of from -40 to -80 mV, and stepped to test voltages between -80 and +30 mV. A family of currents were recorded before and following drug treatment and a resultant I-V relationship was characterized. The ion currents were separated according to their voltage activation and behavior to ion omission.

The effects of IL-1 and FMRFamide were compared on the same neurons. The drugs were applied to the cell surface by microperfusion. IL-1 was produced as an ultrapure consensus IL-1 (human) by Endogen Data Sheet Co., while FMRFamide was from Sigma.

The experiments were carried out at room temperature (20-22°C). Physiological saline had the following composition (in mM): NaCl-80, KCl-4, CaCl₂-7, MgCl₂-5, TrisHCl-5. The pH was adjusted to 7.4. To eliminate sodium current, Na-ions were substituted by TrisHCl, while potassium currents were isolated by using tetraethylammonium chloride, TEA-Cl (Sigma).

RESULTS

The modulatory effects of IL-1 and FMRFamide on the voltage-activated ion currents were compared on identified *Helix* neurons (RPa2, RPa3, LPa2 and LPa3). IL-1 and FMRFamide were shown to modify both the inward current carried by Ca-ions and the net outward potassium current on these neurons.

The effect of IL-1 on the behavior of the voltage-dependent outward current under control conditions and following IL-1 application to the surface of cell RPa3 is shown in Fig. 1. Here the net outward current was recorded in response to depolarizing currents from a holding potential of -60 mV. IL-1 (20 U/ml) increased the net outward potassium current from the beginning of the -30 mV command level (Fig. 1, right side). The net outward potassium current ($I_{\text{net } K}$) was uniformly increased following IL-1 treatment on all the investigated neurons. The effect of IL-1 on the outward current was partially reversible (Fig. 1, left side).

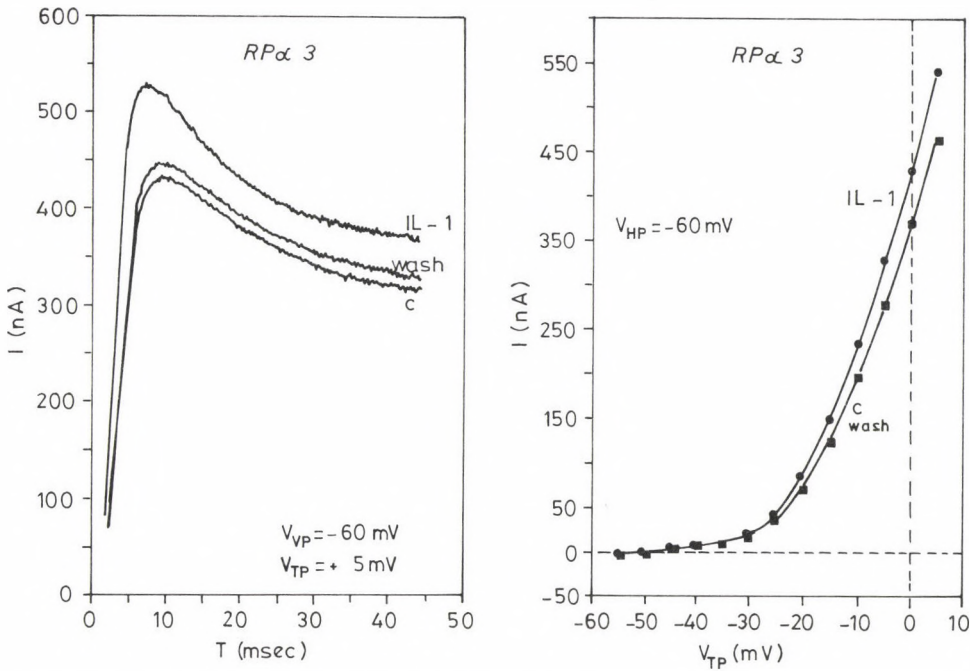


Fig. 1: Voltage-activated outward current recorded from neuron RPa3 before and following IL-1 application to the cell surface (left side) and after washing-out of IL-1. The cell was held at -60 mV in Na-free saline and the command potentials were stepped between -60 and +5 mV. The I-V characteristic of the effect of IL-1 is shown on the right side.

In contrast with the outward current, the voltage-activated inward current (I_{Ca}) was decreased by IL-1 treatment on the investigated neurons. This effect of IL-1 was more expressed in Na-free saline. The maximal decline in the peak amplitude of the inward current was observed during the depolarizing command to +15 mV from -60 mV holding potential. The effect of IL-1 on I_{Ca} was found to be voltage-dependent.

The modulatory effect of FMRFamide was very similar to that of IL-1. On neurons RPa2, RPa3, LPa2 and LPa3, the net outward potassium current was increased, while the inward current was diminished following application of FMRFamide (1 mM) to the cell surface. The modulatory effect of FMRFamide on the voltage-dependent inward current on cell LPa2 is demonstrated in Fig. 2. It can be seen in Fig. 2 that the effect of FMRFamide was reversible. The I-V characteristic of the effect of FMRFamide on the inward current revealed its voltage dependency. The decrease in I_{Ca} reached 30

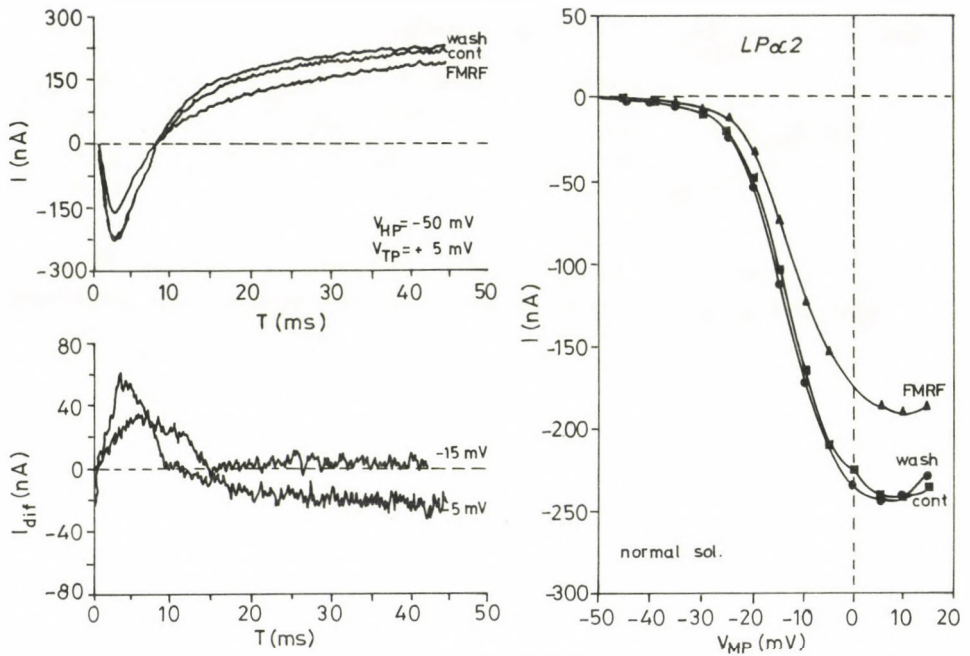


Fig. 2: Voltage-activated inward current recorded from neuron LP α 3 before and following treatment with FMRFamide and after its washing-out (left side, upper part). The I-V characteristic of the inward current in the control during and following FMRFamide application is seen in the right-side panel. The cell was held at -50 mV in Na-free saline and the command potentials were stepped between -50 and +5 mV. The FMRFamide effect was reversible. The inward current differences following FMRFamide treatment are shown in the lower part of the left panel. The current differences were obtained by subtraction of the control from the FMRFamide-modulated values.

percent of the original value. The differences in inward current curves recorded before and following FMRFamide application proved that the maximal decrease occurred within 10 msec (Fig. 2, left side, bottom). The modulatory effect of FMRFamide was more easily eliminated than that of IL-1 following washing-out.

The results emphasized that the immunotransmitter IL-1 and the molluscan neuropeptide FMRFamide alter the same voltage-activated outward and inward currents, but the intimate mechanism of this modulation remains to be discovered.

DISCUSSION

Many neurotransmitters and hormones are known to modulate voltage-activated calcium currents [5, 6]. In molluscs, dopamine has been shown to block the voltage-dependent calcium currents, while 5-hydroxytryptamine decreased the net outward current [7]. The depression of voltage-dependent calcium current by neurotransmitters and peptides is common in vertebrates, too, where noradrenaline, GABA and kappa-opiate agonists (dynorphin) have been shown to use the same mechanism [8, 9]. This regulatory mechanism was proved to be a result of modulation of the voltage dependence of channel activation [6]. The modulation of voltage dependence is a widespread mechanism whereby signal molecules regulate the activity of voltage-dependent channels.

Our results support the idea that the immunotransmitter IL-1 and the molluscan neuropeptide FMRFamide can affect the same population of voltage-activated calcium channels in neurons that are modulated by other signal molecules. Whether these molecules use a common or different mechanisms to modulate these calcium channels remains to be discovered. However, the voltage-activated ion channels can be regarded as target sites in the membrane where various signal molecules can interact with each other.

ACKNOWLEDGEMENT

This work was supported by OTKA National Science Grant No. 2756 (Hungary) to K.S.-Rózsa.

REFERENCES

1. Stefano, G.B. (1985) *Neurosci. Lett.* 56, 205-210.
2. Solomon, G.F. (1987) *J. Neurosci. Res.* 18, 1-9.
3. Blalock, J.E. (1989) *Physiol. Rev.* 69, 1-32.
4. Dunn, A.J. (1990) *Progr. Neuro-Endocrin.* 3, 26-34.
5. Reuter, H. (1983) *Nature* 301, 569-574.
6. Bean, B.P. (1989) *Nature* 340, 153-156.
7. Dunlap, K. and Fischbach, G.D. (1981) *J. Physiol.* 317, 519-535.
8. McDonald, R.L. and Werz, M.A. (1986) *J. Physiol.* 377, 237-249.
9. Deisz, R.A. and Lux, H.D. (1985) *Neurosci. Lett.* 56, 205-210.

5'-NUCLEOTIDASE POSITIVE MICROGLIA REACTION IN THE CENTRAL NERVOUS SYSTEM

L. Tóth¹, G.W. Kreutzberg², I. Bódi¹, R. Töpper²

¹Department of Anatomy, Albert Szent-Györgyi Medical University, H-6724 Szeged, Kossuth Lajos sgt. 40, Hungary and ²Department of Neuromorphology, MPI, Martinsried, Germany

Summary: Following peripheral nerve injury the proliferation of 5'-nucleotidase positive microglial cells has been noticed around projective motoneurons and autonomic preganglionic neurons of the central nervous system. Similar events were observed in the central arborization fields of the primary sensory fibers. Our results may suggest an important role of glial cells in the neuronal plasticity.

INTRODUCTION

The microglial cells are the resident macrophages of the CNS. There are several factors which may activate them: injuries of CNS, neurodegenerative processes, viral infections and the injuries of the peripheral nervous system. Morphological, genetical, functional classifications distinguish amoeboid, resting and reactive microglial cells. Apart from the histochemical methods, immunostaining, using monoclonal antibodies, against specific surface membrane antigens, help to identify the different types of microglial cells. In spite of these modern techniques the light- and electron microscopic visualization of the 5'-nucleotidase (5'-AMPase) - the characteristic ectoenzyme of the microglial cells - is still the most favourable method for revealing the presence of the proliferating microglia.

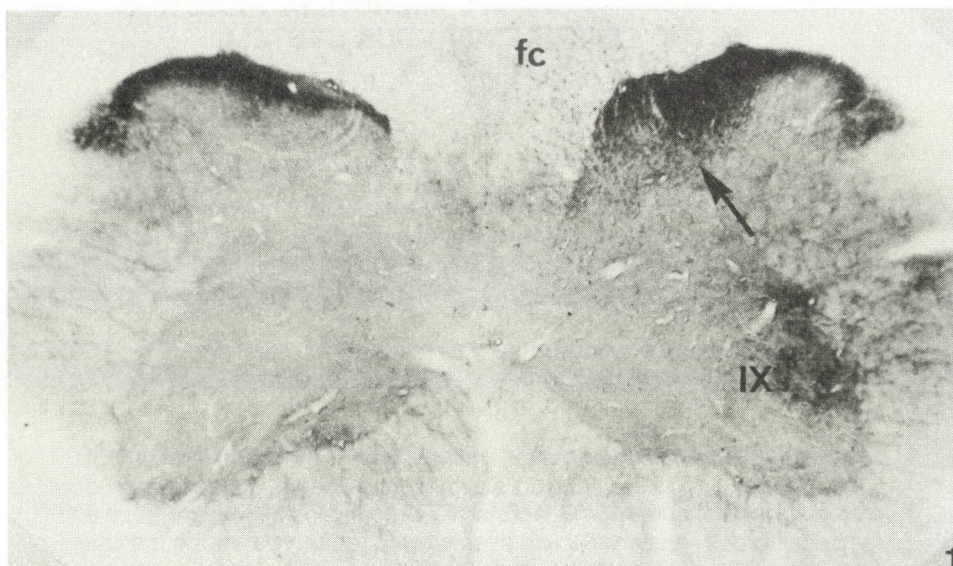


Fig. 1: Four days after brachial plexus transection 5'-AMPase positive microglia reaction can be seen in the substantia gelatinosa Rolandi and in deeper laminae of the dorsal horn (arrow), in the cuneate fascicle (fc) and in the motoneuron pool (IX) of the cervical spinal cord segment. X 30.



Fig. 2: 5'-AMPase positive microglial cells around the soma (arrows) of the spinal cord motoneurons (MN). Four days after lesion of brachial plexus. X 150.

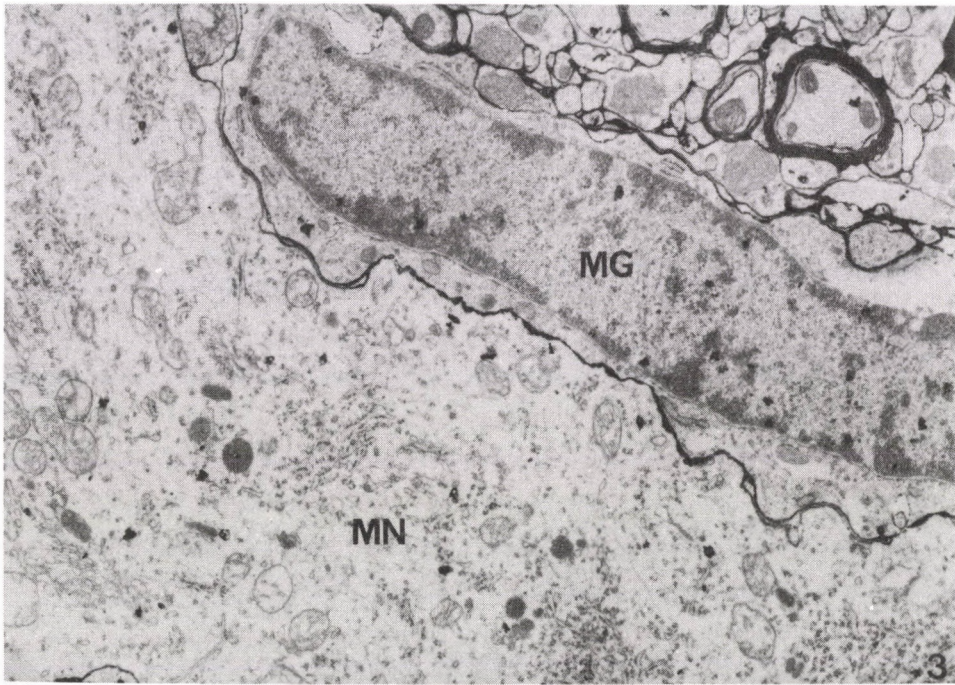


Fig. 3: Six days after trigeminal transection. The surface of a trigeminal motoneurons (MN) is covered by 5'-AMPase positive microglia cells (MG), which disconnect the axosomatic synapses (synaptic stripping). X 16000.

MATERIALS AND METHODS

The goal of our experiments by using Wachstein and Meisel's enzyme histochemical method [1] was to follow the microglial proliferation in the spinal cord (SC), brainstem, thalamus and cortex after the transection of peripheral nerves. For this purpose we transected the sciatic nerve, brachial plexus, trigeminal and vagus nerves of adult rats and we followed the appearance of 5'-nucleotidase positive glial reaction in the lumbar and cervical segments of SC and the motor nuclei of trigeminal and vagus nerves.

RESULTS

Perikaryal 5'-nucleotidase positive glial cells have been noticed in the motor nuclei of the transected peripheral nerve (Figs. 1, 2). Cytochemically [2] these cells proved to be microglial cells (Fig. 3).

Besides, 5'-nucleotidase-positive microglia cells could be noticed around the

soma of preganglionic neurons of the dorsal vagal nucleus following vagus transection [3].

It is known that the transection of the sciatic nerve and brachial plexus caused transganglionic degenerative atrophy in the central terminals of primary sensory fibres [4]. In the arborization zones of these sensory fibres, i.e. in the dorsal horn (Fig. 1), Clarke's nuclei, the gracile and cuneate nuclei (Fig. 4) 5'-nucleotidase positive reaction was also detected at the same time. In the latter these positive elements surrounding the soma of the neurons disconnected the axosomatic synapses. The same events could have been observed in the sensory and mesencephalic nuclei of trigeminal nerve. An additional interesting finding was that the glial cells in the contralateral thalamic nuclei such as VPL, VL, VM also displayed enzyme positivity after sciatic nerve transection. EM studies revealed that this enzyme positivity in the thalamus was due to the presence of reactive microglial cells. It is worth mentioning that the VPM as the subcortical relay centre of the trigeminal nerve did not show any glial reaction.

In addition, the parietal cortex also contained 5'-nucleotidase positive microglial reaction simultaneously with the other subcortical areas.

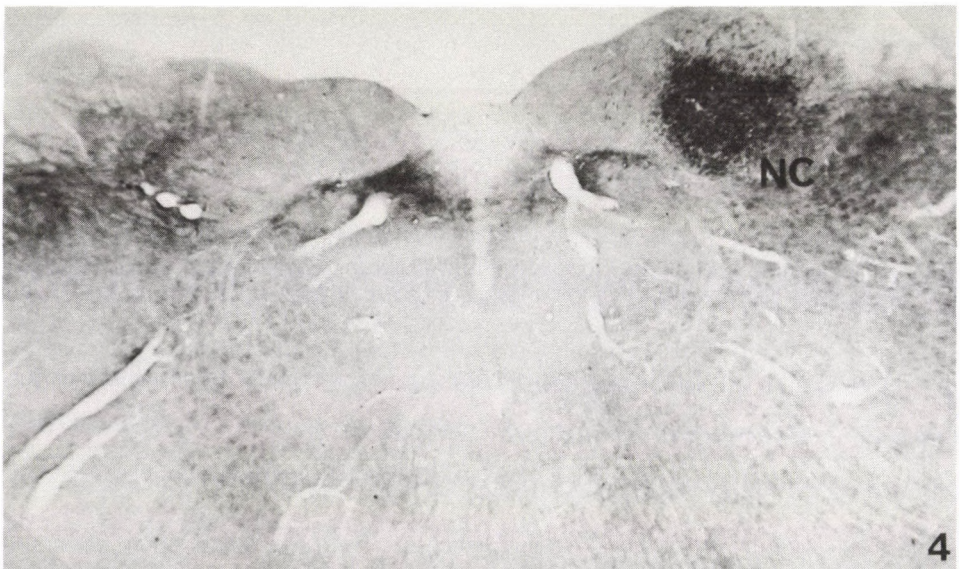


Fig. 4: Intensive enzyme positive microglial reaction is shown around neurons of the nucleus cuneatus (NC), 4 days following brachial plexus transection. X 35.

DISCUSSION

The results presented here may rise several questions:

1. What is the signal which may induce this microglia proliferation in the central arborization field of peripheral sensory nerves or in the nuclei of projective motor and autonomic preganglionic fibers following transecting of the corresponding peripheral nerves.

Making the problem more difficult these events are not taking place gradually from the lower to the highest level of the CNS but at the same time.

Excluding the possibility of transneuronal degeneration we supposed that the insufficient retrograde transport of trophic factors together with the missing action potential signal from the periphery may be responsible for the increasing 5'-nucleotidase positive microglia reaction.

2. Data from physiological experiments have suggested that there are modifications in the receptive field of the thalamus [5] or in the cortical barrells [6] after transection of the trigeminal and the sciatic nerves or any peripheral nerves, respectively. The 5'-nucleotidase positive structures seem to be sensitive markers for morphological analysis of functional changes.

3. The role of the glial cells in neuronal plasticity is not clear. The increasing 5'-nucleotidase positivity in glia cells may suggest an important role of adenosine in the modification of central receptive fields responding to the injury of peripheral nerves.

REFERENCES

1. Wachstein M. and Meisel E. (1957) *Amer. J. Clin. Path.* 27, 12-23.
2. Kreutzberg G.W. and Barron K.D. (1978) *J. Neurocytol.* 7, 601-610.
3. Tóth L., Bódi I. and Kreutzberg G.W. (1991) *Anat. Anz. Erg.* 172, 319.
4. Csillik B. and Knyihár E. (1975) *Z. mikr.-anat. Forsch.* 89, 1099-1103.
5. Pollin B., Albe-Fessard D. (1979) *Brain Res.* 173, 431-449.
6. Wall J.T. (1988) *TINS* 11, 549-557.

ON CELLULAR MECHANISM OF EPILEPTOGENESIS IN THE MIRROR FOCUS

B. Boda, M. Szenté and A. Baranyi

Attila József University, Department of Comparative Physiology
H-6726 Szeged, Középfasor 52, Hungary

Intracellular microelectrode recordings were made in the somatosensory cortex of anaesthetized rats. Electrophysiologically identified cells were studied in secondary epileptogenic foci (mirror focus) contralateral to a primary one induced by topical application of 3-aminopyridine. Firing activity patterns, excitatory and inhibitory postsynaptic potentials (EPSPs, IPSPs) and other membrane events were examined in the same cells under control circumstances, through the development of seizure activity, and in periods when seizure activity became well established. During development of the secondary epileptogenic focus paroxysmal output of the primary focus induced a sequence of pathological events (similar to those in the primary focus), in the synaptically related brain regions. Initially, a suppression of neuronal firing activity, increases in amplitude and duration of the late component of evoked IPSPs were observed without significant changes in EPSPs. After several ictal events regularly spiking neurons changed their firing patterns frequently and generated bursts of action potentials. Paroxysmal depolarization shifts (PDSs) appeared in clonic or interictal periods, taking their origin either from prolonged depolarizing afterpotentials of action potentials, bursts of action potentials or they were associated with the appearance of spikes of high threshold and long duration (probable Ca spikes). After repetitive seizure attacks high threshold spikes could be evoked by intracellular current injection. Due to ionic redistribution in the primary focus, ectopic action potential generation started to develop in the axon terminals of cells in the mirror focus. Since intracortical inhibitory mechanisms are less effective against antidromic, callosal invasion these nonsynaptic routes of propagation may contribute substantially to the establishment of secondary epileptogenic foci, particularly when they were combined with other abnormal firing patterns.

**AN ULTRASTRUCTURAL STUDY
ON THE VENTRAL NERVE CORD
OF EARTHWORM, LUMBRICUS TERRESTRIS L.**

M. Csoknya¹, I. Lengvári² and J. Hámori¹

¹Department of Zoology, Janus Pannonius University, H-7624 Pécs, Ifjúság u. 6, Hungary and ²Department of Anatomy, University Medical School, H-7643 Pécs, Szigeti u. 12, Hungary

Several attempts have been made to describe the ultrastructural characteristics of the ventral nerve cord of Oligochaets. Our purpose of such study was to relate ultrastructurally identified structures to those we have previously identified by light microscopy immunohistochemistry. The majority of nerve cells in the ventral cord is situated ventrally, and medio-laterally can be divided into three major groups. The perikarya of the middle group are large with a diameter of about 30-40 μm . They exhibit a large nucleus with a centrally located nucleolus, as well as rough endoplasmic reticulum and well developed Golgi apparatus. The cytoplasm of the cells contain both dense-core and dense granules. These perikarya probably corresponds to those which we previously stained with serotonin and NPY. The intermediate and lateral nerve cells exhibit only dense granules, and they are probably identical with peptidergic perikarya. Light microscopy immunohistology revealed the presence of substance P, calcitonin gene related peptide, proctolin, FMRF-amide and met-enkephalin in these cells.

EFFECT OF (-)DEPRENYL ON SEXUAL ACTIVITY AND LIFESPAN IN FEMALE RATS

J. Dalló and J. Knoll

Department of Pharmacology, Semmelweis University of Medicine,
H-1450 Budapest, P.O. Box 370, Hungary

Intact, sexually active (N=24) and inactive female rats (N=44) were selected and treated with (-)deprenyl in a dose of 0.25 mg/kg s.c. three times a week (on Monday, Wednesday and Friday); twelve sexually active and twenty-two inactive females treated with saline. Treatment started at the age of three months and lasted longevity.

The sexual activity and vaginal cycle of the females were checked twice a week (on Wednesday and on Saturday) in ovoid shaped boxes using sexually highly active males. Sexually active saline-treated female rats lived in average 96.33 weeks, whereas the inactive ones lived 128.59 weeks ($p < 0.05$).

The deprenyl treated sexually active females lived 84.58 weeks, whereas the inactive ones lived 125.75 weeks ($p < 0.05$). Thus, The relation between sexual activity and lifespan as well as the effect of deprenyl treatment on these parameters seems to be opposite as in male rats (Knoll, Yen, Dalló 1989).

**THE EFFECTS OF DIFFERENT DEAFFERENTATION
ON THE DISTRIBUTION OF NPY IMMUNOPOSITIVE FIBERS
IN THE FROG OPTIC TECTUM**

T. Kozicz and Gy. Lázár

Department of Anatomy, University Medical School,
H-7643 Pécs, Szigeti u. 12, Hungary

Mapping the immunopositive neuronal structures in the frog nervous system showed high concentration of NPY immunoreactive fiber terminals in the retinal recipient layers of the optic tectum, and large number of immunostained cells in the pretectal area and torus semicircularis. Eye removal and lesion studies have been performed to investigate the origin of the NPY positive fibers in the optic tectum.

Eye removal did not influence the NPY immunoreactivity in the contralateral optic tectum up to the 74th postoperative day. On the contrary NPY immunoreactivity markedly decreased in the retinal recipient layers by the 14th postoperative day ipsilateral to the pretectal lesion. A loose network of NPY immunoreactive fibers remained intact in layer 9 and the periventricular tectal layers. They may be either intratectal or toral of origin. Further studies are in progress to verify these possibilities.

It is concluded that the main source of NPY immunoreactivity in the outer tectal layers is the posterior thalamic nucleus in the pretectal region.

MONOAMINERGIC ELEMENTS IN THE NERVOUS SYSTEM OF LUMBRICUS TERRESTRIS L.

I. Lengvári¹, M. Csoknya², M. Szelier¹ and J. Hátori²

¹Department of Anatomy, University Medical School,
H-7643 Pécs, Szigeti u. 12, Hungary and ²Department of Zoology,
Janus Pannonius University, H-7624 Pécs, Ifjúság u. 6, Hungary

According to the light microscop immunohistochemistry, the main monoamine of the nervous system of *Lumbricus terrestris* is serotonin, since large number of serotonergic elements can be found each part of the central and peripheral nervous system. In the central ganglion a group of serotonergic cells situated dorsally and another one close to the origin of the circumpharyngeal connectives. In the ventral cord, large serotonergic perikarya compose the middle cell group, which includes the Retzius cells, too, however, smaller serotonin positive cells can be found ventrally in every part of the ventral cord. Serotonergic cells of the ventral cord give rise a very rich network in the central neuropil, and serotonergic fibers can be traced in each segmental nerve. In the periphery, there is a rich network of serotonergic fibers beneath the surface epithelium, within the body wall muscle fibers and in the subepithelial plexus of the gut.

The number of noradrenergic cells of the central ganglion is significantly smaller than that of the serotonergic cells, and they do not show any preference as far as their location is concerned. In the ventral cord, noradrenergic cells can exclusively be found in the lateral cell group, and axons of these cells form a well circumscribed network in the lateral aspect of the central neuropil. No adrenergic elements could have been detected in the periphery.

Both in the cerebral ganglion and in the ventral cord very few dopaminergic cells were detected, and they do not show any preference as far as their location is concerned.

**CONNECTIONS OF THE CEREBRAL GANGLION
IN LUMBRICUS TERRESTRIS L.
Preliminary study**

M. Szeliér¹, M. Csoknya², I. Lengvári¹ and J. Hátori²

¹Department of Anatomy University Medical School,
H-7643 Pécs, Szigeti u. 12, Hungary and ²Department of Zoology,
Janus Pannonius University, H-7624 Pécs, Ifjúság u. 6, Hungary

Cerebral ganglion of *Lumbricus terrestris* was retrogradely labelled with cobalt-lysine complex either from the circumpharyngeal connective or from the medial prostomial nerve. Filling the circumpharyngeal connective resulted in labelling of about 30% of the nerve cells in the cerebral ganglion on the ipsilateral side and of about 10% on the contralateral side. Labelled cells are mostly large, uni- or bipolar cells, which preferably located on the dorsal side of the ganglion. Labelled nerve cells were seen in the stomatogastric ganglia on both sides. Filled fibers of the contralateral circumpharyngeal connective could be traced on the ipsilateral side of the subpharyngeal ganglion, where they ran longitudinally and were situated either close to the giant axons or in the ventral neuropil. Many fibers of the contralateral connective reach directly the pharyngeal plexus.

Filling the medial prostomial nerve resulted in a very rich labelling of fibers in the central neuropil without labelling nerve cells of the cerebral ganglion. Labelled fibers were detected in both circumpharyngeal connectives.

**DEVELOPMENTAL DYNAMICS
OF PURKINJE-CELL DENDRITIC SPINES
IN THE RAT CEREBELLAR CORTEX**

J. Takács and J. Hátori

1st Department of Anatomy, Semmelweis Medical University
H-1450 Budapest, Tűzoltó u. 58, Hungary

Quantitative morphological changes of the developing Purkinje-cells have been studied from 6 days to 90 days PN in the IVth lobule of vermis in the cerebellum of rats. General volume density of dendritic spines increased rapidly from about 10 days PN and reached a peak by 21 days PN (1.2×10^9 Pu-spines/mm³) followed by a significant (about 35%) drop and a subsequent though less rapid growth until 48 days PN. When the number of spines was calculated per one Purkinje-cell, this number was observed to raise also rapidly from 10 days PN on and reached a peak by the 48 days PN (4.7×10^3 Pu-spines/Pu-cell) followed by a significant (about 43%) decrease until the 90 PN days. The temporary overproduction and the following normalization (decrease) of Purkinje dendritic spines in the developing cerebellar cortex is the morphological indicator of the dynamism of synaptogenetic and of synaptic stabilization process.

CONTENTS

Regular articles

- Protein kinase C subtypes in human T lymphocytes. *Christiansen, N.O. and Larsen, C.S.* 1
- EM waves standards effectiveness. *Diaz, S.B.* 7
- Kinetics of histone glycation. *Lakatos, Á. and Jobst, K.* 33
- Single-channel analysis of Pb^{2+} modified steady-state Na-conductance in snail neurons. *Osipenko, O.N. and Kiss, T.* 39

Proceedings

(Annual Meeting of the Neuroscience Section of Hungarian Physiological Society, Visegrad, January 23-25, 1992) 51

- György Ádám *Kukorelli, T.* 53

Papers

- Effect of electrophoretically applied neurochemicals on activity of extrapyramidal and limbic neurons in the rat. *Czurkó, A., Faludi, B., Vida, I., Niedetzky, Cs., Hajnal, A., Karádi, Z. and Lénárd, L.* 57
- Dynamic phenomena in the olfactory bulb. *Gröbner, T. and Érdi, P.* 61
- Hunger- and satiety-related changes of amygdaloid catecholamines: a microdialytic study in freely moving rats. *Hajnal, A., Ábrahám, I., Vida, I., Karádi, Z. and Lénárd, L.* 67
- Local and distant effects of amygdaloid kainate lesions in the rat: a silver impregnation study. *Hajnal, A., Czurkó, A., Karádi, Z. and Lénárd, L.* 71
- Drugs acting at calcium channels can influence the hypnotic anesthetic effect of dexmedetomidine. *Horváth, Gy., Kovács, M., Szikszay, M. and Benedek, Gy.* 75
- The mathematical analysis of spontaneous and induced potentials in neural cultures. *Jánossy, V., Krinizs, K., Lukács, B., Rácz, A., Gyévai, A. and Madarász, E.* 83
- Vimentin immunopositivity in the brain of the adult frog. *Kálmán, M.* 89
- Calretinin ontogenesis in the developing DRG of chicken. *Király, E. and Celio, M. R.* 95
- Regeneration of dorsal column pathways in peripheral bypass autografts implanted in the spinal cord of adult rats. *Knyihár-Csillik, E., Török, Á., Mohtasham, S. and Csillik, B.* 97

Theorems speaking for the asymmetry of all animal brains. <i>Lábos, E.</i>	105
Effects of mental load on the spectral components of heart period variability in twins. <i>Láng, E., Szilágyi, N., Métneki, J. and Weisz, J.</i>	111
Correlation dimension changes of the EEG during the wakefulness-sleep cycle. <i>Molnár, M. and Skinner, J.E.</i>	121
Increase of storage capacity of neural networks by preprocessing, using convergence and divergence. <i>Orzó, L.</i>	127
Circulatory and respiratory effects of capsaicin and resiniferatoxin on guinea pigs. <i>Pórszász, R. and Szolcsányi, J.</i>	131
Various signal molecules modulate voltage-activated ion currents on snail neurons. <i>Szűcs, A., Stefano, G.B., Hughes, T.K. and S.-Rózsa, K.</i>	139
5'-nucleotidase positive microglia reaction in the central nervous system. <i>Tóth, L., Kreutzberg, G.W., Bódi, I. and Töpper, R.</i>	145
Abstracts	
On cellular mechanism of epileptogenesis in the mirror focus. <i>Boda, B., Szente, M. and Baranyi, A.</i>	151
An ultrastructural study on the ventral nerve cord of earthworm, <i>Lumbricus terrestris</i> L. <i>Csoknya, M., Lengvári, I. and Hámori, J.</i>	152
Effect of (-)deprenyl on sexual activity and lifespan in female rats. <i>Dalló, J. and Knoll, J.</i>	153
The effects of different deafferentation on the distribution of NPY immunopositive fibers in the frog optic tectum. <i>Kozicz, T. and Lázár, Gy.</i>	154
Monoaminergic elements in the nervous system of <i>Lumbricus terrestris</i> L. <i>Lengvári, I., Csoknya, M., Szelier, M. and Hámori, J.</i>	155
Connections of the cerebral ganglion in <i>Lumbricus terrestris</i> L. Preliminary study. <i>Szelier, M., Csoknya, M., Lengvári, I. and Hámori, J.</i>	156
Developmental dynamics of Purkinje-cell dendritic spines in the rat cerebellar cortex. <i>Takács, J. and Hámori, J.</i>	157

AUTHOR INDEX

Ábrahám, I.	67
Baranyi, A.	151
Benedek, Gy.	75
Boda, B.	151
Bódi, I.	145
Celio, M. R.	95
Christiansen, N.O.	1
Csillik, B.	97
Csoknya, M.	152, 155, 156
Czurkó, A.	57, 71
Dalló, J.	153
Diaz, S.B.	7
Érdi, P.	61
Faludi, B.	57
Gröbler, T.	61
Gyévai, A.	83
Hajnal, A.	57, 67, 71
Hámori, J.	152, 155, 156, 157
Horváth, Gy.	75
Hughes, T.K.	139
Jánossy, V.	83
Jobst, K.	33
Kálmán, M.	89
Karádi, Z.	57, 67, 71
Király, E.	95
Kiss, T.	39
Knoll, J.	153

Knyihár-Csillik, E.	97
Kovács, M.	75
Kozicz, T.	154
Kreutzberg, G.W.	145
Krinizs, K.	83
Kukorelli, T.	53
Lábos, E.	105
Lakatos, Á.	33
Láng, E.	111
Larsen, C.S.	1
Lázár, Gy.	154
Lénárd, L.	57, 67, 71
Lengvári, I.	152, 155, 156
Lukács, B.	83
Madarász, E.	83
Métneki, J.	111
Mohtasham, S.	97
Molnár, M.	121
Niedetzky, Cs.	57
Orzó, L.	127
Osipenko, O.N.	39
Pórszász, R.	131
Rácz, A.	83
S.-Rózsa, K.	139
Skinner, J.E.	121
Stefano, G.B.	139
Szelier, M.	155, 156
Szente, M.	151
Szikszay, M.	75

Szilágyi, N.	111
Szolcsányi, J.	131
Szűcs, A.	139
Takács, J.	157
Töpper, R.	145
Török, Á.	97
Tóth, L.	145
Vida, I.	57, 67
Weisz, J.	111

PRINTED IN HUNGARY

Akadémiai Kiadó és Nyomda Vállalat, Budapest

A desirable plan for the organization of a paper is the following: Summary, Introduction, Materials and methods, Results, Discussion, References.

A clear and informative title is very important. Provide a short title (not to exceed 50 characters and spaces) to be used as a running head. Every paper must begin with a **Summary** (up to 200 words) presenting the important and pertinent facts described in the paper.

The **Introduction** should state the purpose of the investigation, but should not include an extensive review of the literature. The description of the **Materials and methods** should be brief, but adequate for repetition of the work. Refer to previously published procedures employed in the work. It is strongly recommended that author(s) should draw attention to any particular chemical or biological *hazards* that may occur in carrying out experiments described in the paper. Relevant safety precautions should be suggested. The **Results** may be presented in tables or figures. The **Discussion** should be concise and deal with the interpretation of the results. In some cases combining **Results and discussion** in a single section may give a clearer presentation.

References to the literature in the text should be by numbers in parentheses. In the reference list the items should be arranged in order of these serial numbers. For citation note the following examples:

1. Drust, D. S. and Martin, T. F. J. (1985) *Biochem. Biophys. Res. Commun.* 128, 531–537
2. Hoyer, S. (1980) in *Biochemistry of Dementia* (Roberts, P. J. ed.) pp. 252–257, J. Wiley and Sons, New York

Abbreviations and symbols defined in the IUPAC-IUB Document No. 1 (*Arch. Biochem. Biophys.* 115, 1–12, 1966) may be used without definition, but others are to be avoided. When necessary, *abbreviations must be defined in a footnote and typed single-spaced on a separate page*, rather than in the text. Abbreviations *must not* be used in the Summary. Enzyme names should not be abbreviated except when the substrate has an accepted abbreviation (e.g. ATPase). Use of Enzyme Commission (EC) code number is required when available. Styling of isotopes should follow the recommendations of the IUB Commission of Editors. The symbol of the isotope should be placed in brackets attached directly to the front of the name, e.g. [³²P] AMP. Isotope number should only be used as a (superior) prefix to the atomic symbol, not to an abbreviation.

Typing of manuscript

The accepted articles are reproduced directly from the submitted manuscript as camera ready copy, thus *no changes can be made in the manuscript after acceptance*. Therefore black silk or carbon typewriter ribbon should be used. For obvious reasons proofs are not required and cannot be supplied. Special care should be taken to ensure a sharp, clean impression of letters throughout the whole manuscript. It is strongly recommended to use an *electric typewriter*. Erasures or other corrections should be avoided. Spelling, word division and punctuation must be carefully controlled.

The title of the paper should be typed in capital letters near the top of the first page, with the name(s) an affiliation(s) of the author(s) just typed below. Manuscripts should be double-spaced; methods, references, abbreviations, footnotes and figure legends should be *single-spaced*. Typing area of the page must be as close as possible to 16 × 24 cm.

Each page should be numbered at the bottom in light blue pencil marks. On a separate sheet indicate a running title, not more than 6 key-words for subject indexing and the author to whom reprints are to be sent, including a telephone number if possible.

Illustrations and tables. Do not attempt to insert figures, figure legends or tables into the text. This will be done by the Publisher. Original drawings should be clearly labelled in black ink in a manner suitable for *direct reproduction*. Typewritten lettering is not acceptable. Figures will be reduced to fit within the area of the page. All letters, numbers and symbols should be drawn to be at least 2.5 mm high after reduction. Glossy photographs or drawings are acceptable provided they are sharp, clear prints with an even black density. Illustrations in colour cannot be accepted. Mathematical and chemical symbols that cannot be typed should be drawn carefully in black. Tables and illustrations should be submitted on separate sheets.

Fifty reprints will be supplied free of charge.

